NORSAR

NORSAR Scientific Report No. 1-2004

Semiannual Technical Summary

1 July - 31 December 2003

Frode Ringdal (ed.)

Kjeller, February 2004

REPORT DOCUMENTATION PAGE

Form Approved
OMB No. 0704-0188

1a. REPORT SECURITY CLASSIFICATION Unclassified		1b. RESTRICTIVE MARKINGS Not applicable
2a. SECURITY CLASSIFICATION AUTHORITY Not Applicable		3. DISTRIBUTION/AVAILABILITY OF REPORT Approved for public release; distribution unlimited
2b. DECLASSIFICATION/DOWNGRADING SCHEDULE		
4. PERFORMING ORGANIZATION REPORT NUMBER(S) Scientific Rep. 1-2004		5. MONITORING ORGANIZATION REPORT NUMBER(S) Scientific Rep. 1-2004

6a. NAME OF PERFORMING ORGANIZATION NORSAR	6b. OFFICE SYMBOL *(If applicable)*	7a. NAME OF MONITORING ORGANIZATION HQ/AFTAC/TTS
6c. ADDRESS *(City, State, and ZIP Code)* Post Box 53 NO-2027 Kjeller, Norway		7b. ADDRESS *(City, State, and ZIP Code)* Patrick AFB, FL 32925-6001

8a. NAME OF FUNDING/SPONSORING ORGANIZATION Defense Threat Reduction Agency/NTPO	8b. OFFICE SYMBOL *(If applicable)* DTRA/NTPO	9. PROCUREMENT INSTRUMENT IDENTIFICATION NUMBER Contract No. F08650-01-C-0055

8c. ADDRESS *(City, State, and ZIP Code)* 1515 Wilson Blvd., Suite 720 Arlington, VA 22209	10. SOURCE OF FUNDING NUMBERS			
	PROGRAM ELEMENT NO. R&D	PROJECT NO. NORSAR Phase 3	TASK NO. SOW Task 5.0	WORK UNIT ACCESSION NO. Sequence No. 004A2

11. TITLE *(Include Security Classification)*

Semiannual Technical Summary, 1 July - 31 December 2003 (Unclassified)

12. PERSONAL AUTHOR(S)

13a. TYPE OF REPORT Scientific Summary	13b. TIME COVERED FROM 1 Jul 03 TO 31 Dec 03	14. DATE OF REPORT *(Year, Month, Day)* 2004 Feb	15. PAGE COUNT 97

16. SUPPLEMENTARY NOTATION

17.	COSATI CODES		18. SUBJECT TERMS *(Continue on reverse if necessary and identify by block number)*
FIELD	GROUP	SUB-GROUP	NORSAR, Norwegian Seismic Array
8	11		

19. ABSTRACT *(Continue on reverse if necessary and identify by block number)*

This report describes the research activities carried out at NORSAR under Contract No. F08650-01-C-0055 for the period 1 July - 31 December 2003. In addition, it provides summary information on operation and maintenance (O&M) activities at the Norwegian National Data Center (NDC) during the same period. Research activities described in this report, as well as transmission of selected data to the United States NDC, are funded by the United States Government. The O&M activities, including operation of transmission links within Norway and to Vienna, Austria, are being funded jointly by the CTBTO/PTS and the Norwegian Government, with the understanding that the funding of O&M activities for primary IMS will gradually be transferred to the CTBTO/PTS. The O&M statistics presented in this report are included for the purpose of completeness, and in order to maintain consistency with earlier reporting practice.

(cont.)

20. DISTRIBUTION/AVAILABILITY OF ABSTRACT ☐ UNCLASSIFIED/UNLIMITED ☐ SAME AS RPT. ☐ DTIC USERS	21. ABSTRACT SECURITY CLASSIFICATION
22a. NAME OF RESPONSIBLE INDIVIDUAL TSgt Mark C. Gerick	22b. TELEPHONE *(Include Area Code)* (321) 494-3582	22c. OFFICE SYMBOL AFTAC/TTD

DD Form 1473, JUN 86

Previous editions are obsolete.

SECURITY CLASSIFICATION OF THIS PAGE

Abstract

The NOA Detection Processing system has been operated throughout the period with an uptime of 100%. A total of 2535 seismic events have been reported in the NOA monthly seismic bulletin from July through December 2003. On-line detection processing and data recording at the NDC of ARCES and FINES data have been conducted throughout the period. Data from the two small-aperture arrays at sites in Spitsbergen and Apatity, Kola Peninsula, as well as the Hagfors array in Sweden, have also been recorded and processed. Processing statistics for the arrays for the reporting period are given.

A summary of the activities at the Norwegian NDC and relating to field installations during the reporting period is provided in Section 4. Norway is now contributing primary station data from two seismic arrays: NOA (PS27) and ARCES (PS28) and one auxiliary seismic array SPITS (AS72). These data are being provided to the IDC via the global communications infrastructure (GCI). Continuous data from all three arrays are in addition being transmitted to the US NDC. The performance of the data transmission to the US NDC has been satisfactory during the reporting period.

Results from testing of seismometers for the ongoing Spitsbergen array refurbishment are presented in Section 4.4. Various seismometer configurations have been installed and operated on an experimental basis at the NORES array center site since mid-December 2003. This exercise has enabled us to compare in detail the recordings (at the same site and at the same time period) of several different seismometers. Based on this testing, we recommend that CMG-3T broadband seismometers with acceleration type response be installed when the array is refurbished.

Summaries of six scientific and technical contributions are presented in Chapter 6 of this report.

Section 6.1 discusses some aspects and potential improvements of the regional processing currently carried out at NORSAR for the European Arctic. In particular, the study addresses the question of automatic detection and association of phases for small seismic events in the Novaya Zemlya region, using the on-line Generalized Beamforming (GBF) process. It is noted that the number of false associations can be reduced by 90 per cent through relatively simple selection criteria. Furthermore, some possibilities for additional future improvements are discussed, including the development of a systematic automatic post-processing algorithm to be applied to event candidates produced by the GBF process currently in operation.

Section 6.2 is entitled "Source depths at regional distances: an example from the Western Barents Sea / Svalbard Region" and contains a detailed location analysis of an earthquake with a magnitude of mb 5.7 and Ms 5.1 (NEIC) which occurred in the Western Barents Sea, close to Hopen Island on 4 July 2003 at 07:16. The aim of this study was to relocate the event using classical and non-linear/probabilistic location procedures and to assess the reliability of the source depth determination. The paper concludes that classical event location procedures using travel times generally underestimate the uncertainty of source-depth determinations, in particular, in cases where the azimuthal coverage of observations is very uneven or nearby observations are missing. More realistic error estimates are yielded by using techniques like the Bootstrap method or Monte Carlo search.

Section 6.3 is a study of location accuracy for seismic events near the Spitsbergen archipelago. In cooperation with Kola Regional Seismological Centre (KRSC), we have relocated more than 200 earthquakes occurring during the first half of 2003 with epicenters in Spitsbergen and

adjacent areas. We have compared our location results with those published in the Reviewed NORSAR Regional Bulletin, which makes use of the same station network. Additionally, we compared both of these interactive location results to the automatic location provided by the on-line GBF procedure at NORSAR. We have found that the reviewed locations in our study compared to those routinely produced by the NORSAR analyst are usually close (within a few tens of kilometers), but there are occasional large deviations, in a few cases exceeding 100 km. The automatic GBF locations produced on-line at NORSAR are naturally less reliable than the analyst reviewed locations. Nevertheless they are quite consistent with the reviewed solutions, except for some large differences in location of smaller earthquakes, which are located using the SPITS array alone in the GBF procedure. Some possibilities for future enhancements of the event location procedures are discussed.

Section 6.4 is entitled "Ground Truth information from Khibiny mining explosions". KRSC has for the past 10 years provided to NORSAR ground truth information for selected mining explosions in the Kola Peninsula. Since 2001, the project has been expanded in scope, and is currently carried out jointly with Lawrence Livermore National Laboratory, in a DOE-funded project. In particular, we discuss two large explosions, one underground and one at the surface in the Rasvumchorr/Central mines in Khibiny on 16 November 2002. These explosions were only 300 m apart, so that differences in path effects at the more distant stations can be ignored. Nevertheless, the recorded signals at stations in our network (up to 400 km distance) were remarkably different: At lower frequencies (2-4 Hz), the underground explosion was stronger by a factor of 10 in amplitude, whereas above 10 Hz, the surface explosion had by far the stronger signals. The Mining Institute of the Kola Science Centre have made a video recording of the explosions on 16 November 2002. This video has been made available to us, and the paper presents selected snapshots of the explosions.

Section 6.5 is entitled: "Study of regional variations of the coda characteristics in the Barents Sea using small-aperture arrays". The paper investigates the characteristics of the coda for a large data set recorded by ARCES and SPITS. F-k decompositions have been used to calculate the time evolution of the parameters of propagation of the different phases that compose the coda. It is shown that for the arrays ARCES and SPITS, the characteristics of the coda are very similar for events located in northern Fennoscandia / Kola Peninsula region, close to Novaya Zemlya and close to Spitsbergen in the Barents Sea. The coda propagates mainly along the great circle paths between sources and arrays. The apparent velocities are typical of Pn phases for the Pn coda and Sn phases for the Sn coda. In this case, we infer mechanisms like multiple crustal reflections to explain our observations. The characteristics of the coda are very different for all the events located along the Mid-Atlantic ridge. For these events, strong differences are generally observed between the direction of propagation of the coda phases and the expected theoretical direction. This shows that the scattering is no longer confined to the great circle path, but that lateral structures are also involved into multipathing and diffraction processes.

Section 6.6 is a study entitled "ARCES recordings of events from the Khibiny and Olenegorsk mines". This paper is a report under a separate project sponsored by National Nuclear Security Administration, and is included in view of its relevance to our studies under the present contract. We have started to investigate in detail events from the Khibiny and the Olenegorsk mines in the Kola Peninsula. We show several panels of waveform plots from various mines in these mining complexes, using a semblance analysis technique applied to the ARCES waveform recordings. From these panels we see that some of the events show a relatively simple source signature, whereas others have longer duration and consist of several pulses, which could be an

effect of multiple seismic sources in combination with near-source scattering. Based on the overview gained from semblance analysis and visual inspection of ARCES data of 99 compact shots from the underground Rasvumchorr mine, we have found that the vast majority of these events are characterized by a single strong Pn pulse. For these events, it should be possible to detect and characterize the Pn, Pg, Sn and Lg phases at ARCES automatically. However, for about 25% of the events, there are multiple pulses in the Pn-Pg time window, indicating separate explosions with time delays ranging from 1 and up to several seconds. Consequently, automatic processing of these events will be a more difficult task.

AFTAC Project Authorization	:	T/0155/PKO
ARPA Order No.	:	4138 AMD # 53
Program Code No.	:	0F10
Name of Contractor	:	Stiftelsen NORSAR
Effective Date of Contract	:	1 Feb 2001 (T/0155/PKO)
Contract Expiration Date	:	31 December 2005
Project Manager	:	Frode Ringdal +47 63 80 59 00
Title of Work	:	The Norwegian Seismic Array (NORSAR) Phase 3
Amount of Contract	:	$ 3,383,445
Period Covered by Report	:	1 July - 31 December 2003

Table of Contents

1　Summary

This report describes the research activities carried out at NORSAR under Contract No. F08650-01-C-0055 for the period 1 July - 31 December 2003. In addition, it provides summary information on operation and maintenance (O&M) activities at the Norwegian National Data Center (NDC) during the same period. Research activities described in this report, as well as transmission of selected data to the United States NDC, are funded by the United States Government. The O&M activities, including operation of transmission links within Norway and to Vienna, Austria are being funded jointly by the CTBTO/PTS and the Norwegian Government, with the understanding that the funding of O&M activities for primary IMS stations will gradually be transferred to the CTBTO/PTS. The O&M statistics presented in this report are included for the purpose of completeness, and in order to maintain consistency with earlier reporting practice.

The seismic arrays operated by the Norwegian NDC comprise the Norwegian Seismic Array (NOA), the Arctic Regional Seismic Array (ARCES) and the Spitsbergen Regional Array (SPITS). This report also presents statistics for additional seismic stations which through cooperative agreements with institutions in the host countries provide continuous data to the NORSAR Data Processing Center (NDPC). These stations comprise the Finnish Regional Seismic Array (FINES), the Hagfors array in Sweden (HFS) and the regional seismic array in Apatity, Russia.

The NOA Detection Processing system has been operated throughout the period with an uptime of 100%. A total of 2535 seismic events have been reported in the NOA monthly seismic bulletin from July through December 2003. On-line detection processing and data recording at the NDC of ARCES and FINES data have been conducted throughout the period. Data from the two small-aperture arrays at sites in Spitsbergen and Apatity, Kola Peninsula, as well as the Hagfors array in Sweden, have also been recorded and processed. Processing statistics for the arrays for the reporting period are given.

A summary of the activities at the Norwegian NDC and relating to field installations during the reporting period is provided in Section 4. Norway is now contributing primary station data from two seismic arrays: NOA (PS27) and ARCES (PS28) and one auxiliary seismic array SPITS (AS72). These data are being provided to the IDC via the global communications infrastructure (GCI). Continuous data from all three arrays are in addition being transmitted to the US NDC. The performance of the data transmission to the US NDC has been satisfactory during the reporting period.

So far among the Norwegian stations, the NOA and the ARCES array (PS27 and PS28 respectively) and the radionuclide station at Spitsbergen (RN49) have been certified. Provided that adequate funding continues to be made available (from the PTS and the Norwegian Ministry of Foreign Affairs), we envisage continuing the provision of data from these and other Norwegian IMS-designated stations in accordance with current procedures.

Results from testing of seismometers for the ongoing Spitsbergen array refurbishment are presented in Section 4.4. Various seismometer configurations have been installed and operated on an experimental basis at the NORES array center site since mid-December 2003. This exercise has enabled us to compare in detail the recordings (at the same site and at the same time period) of the Teledyne 20171 SP seismometer (which is the type of SP seismometer installed in the NORSAR array), the Teledyne KS-54000 BB (posthole) seismometer (which forms the main

broadband component of the NORSAR array), the Guralp CMG-ESP seismometer and the Guralp CMG-3T seismometer. The latter two types of seismometers are candidates for installation in Spitsbergen. The CMG-3T seismometer has already been chosen for the broad-band sensors at Spitsbergen, but there is still a choice to be made between CMG-3T and CMG-ESP for the "short-period" component. The crucial point is whether the broadband seismometer can match the ESP seismometer at high frequencies.

The preliminary results of our tests have shown that the two Guralp seismometers have indistinguishable signal and noise recordings in various high-frequency filter bands (the highest filter band tested is 24-48 Hz, using an order 5 Butterworth bandpass filter). It therefore seems reasonable to use the CMG-3T seismometer for the entire array (SP and LP). Dr. Cansun M. Guralp, who visited NORSAR in December 2003, concurs with this assessment. An important question is whether to select an acceleration type seismometer or a velocity type seismometer. Acceleration response has the advantage of providing higher amplification at high frequencies, which is important for the Spitsbergen site, and we recommend that acceleration type seismometers be installed when the array is refurbished.

Summaries of six scientific and technical contributions are presented in Chapter 6 of this report.

Section 6.1 discusses some aspects and potential improvements of the regional processing currently carried out at NORSAR for the European Arctic. In particular, the study addresses the question of automatic detection and association of phases for small seismic events in the Novaya Zemlya region, using the on-line Generalized Beamforming (GBF) process. It is noted that the number of false associations can be reduced by 90 per cent through relatively simple selection criteria. Furthermore, some possibilities for additional future improvements are discussed, including the development of a systematic automatic post-processing algorithm to be applied to event candidates produced by the GBF process currently in operation.

As an initial step, we have implemented a script to apply the criteria discussed in this paper to the GBF on-line output, so as to produce an abbreviated list of event candidates to be analyzed interactively at NORSAR. This should ensure that future small seismic events in the Novaya Zemlya region will be included in the reviewed regional bulletin, while involving only a modest additional analyst effort.

Section 6.2 is entitled "Source depths at regional distances: an example from the Western Barents Sea / Svalbard Region" and contains a detailed location analysis of an earthquake with a magnitude of mb 5.7 and Ms 5.1 (NEIC) which occurred in the Western Barents Sea, close to Hopen Island on 4 July 2003 at 07:16. The aim of this study was to relocate the event using classical and non-linear/probabilistic location procedures and to assess the reliability of the source depth determination.

The paper concludes that classical event location procedures using travel times generally underestimate the uncertainty of source-depth determinations, in particular, in cases where the azimuthal coverage of observations is very uneven or nearby observations are missing. More realistic error estimates are yielded by using techniques like the Bootstrap method or Monte Carlo search.

However, one of the most important unknown factors for locating earthquakes is the velocity structure. Incorporating only a 5-percent uncertainty of the crustal velocities led to nearly

meaningless source depth estimates. The 90-percent confidence region extends over more than a hundred kilometers in depth, which can only be restricted with further seismological evidence like the occurrence of Lg or Rg. This result throws a somewhat negative light on studies which use source depths from catalogues. Improvements are conceivable with good station coverage in short distances and with detailed knowledge of the regional velocity distribution within the Earth.

Section 6.3 is a study of location accuracy for seismic events near the Spitsbergen archipelago. In cooperation with Kola Regional Seismological Centre (KRSC), we have relocated more than 200 earthquakes occurring during the first half of 2003 with epicenters in Spitsbergen and adjacent areas. We have compared our location results with those published in the Reviewed NORSAR Regional Bulletin, which makes use of the same station network. Additionally, we compared both of these interactive location results to the automatic location provided by the on-line GBF procedure at NORSAR.

The complex geology of the Spitsbergen archipelago and surrounding regions results in very complex seismograms. Multiple onsets of P and S waves are often observed, and can easily cause phase misinterpretations which strongly increase location errors. We have found that the reviewed locations in our study compared to those routinely produced by the NORSAR analyst are usually close (within a few tens of kilometers), but there are occasional large deviations, in a few cases exceeding 100 km. The automatic GBF locations produced on-line at NORSAR are naturally less reliable than the analyst reviewed locations. Nevertheless they are quite consistent with the reviewed solutions, except for some large differences in location of smaller earthquakes, which are located using the SPITS array alone in the GBF procedure.

Future work should focus on making more systematic use of array azimuth estimates for small events, perhaps by introducing fixed-frequency f-k analysis both in the automatic and interactive procedures. We suggest that more attention should also be given to high-frequency processing of data for phase identification and velocity/azimuth estimation purposes. Furthermore, the planned installation of several three-component seismometers in the refurbished SPITS array is expected to significantly improve the automatic S-wave detection capability, thereby improving the ability to locate small seismic events in the region.

Section 6.4 is entitled "Ground Truth information from Khibiny mining explosions". KRSC has for the past 10 years provided to NORSAR ground truth information for selected mining explosions in the Kola Peninsula. Since 2001, the project has been expanded in scope, and is currently carried out jointly with Lawrence Livermore National Laboratory, in a DOE-funded project. The Khibiny Massif forms a natural laboratory for examining the variations of mining explosion observations as a function of source type, since the mining explosions there are conducted in colocated underground and surface mines, with a variety of different shot geometries. In this paper we provide some examples of the type of ground truth collected, and illustrate some of the characteristic features observed from approximately colocated underground and surface explosions.

In particular, we discuss two large explosions, one underground and one at the surface in the Rasvumchorr/Central mines in Khibiny on 16 November 2002. These explosions were only 300 m apart, so that differences in path effects at the more distant stations can be ignored. Nevertheless, the recorded signals at stations in our network (up to 400 km distance) were remarkably different: At lower frequencies (2-4 Hz), the underground explosion was stronger by a

factor of 10 in amplitude, whereas above 10 Hz, the surface explosion had by far the stronger signals. The Mining Institute of the Kola Science Centre have made a video recording of the explosions on 16 November 2002. This video has been made available to us, and the paper presents selected snapshots of the explosions.

A particularly interesting type of underground explosions in the Khibiny Massif is the so-called compact explosions, which typically comprise 2-3 groups of charges of about 700 kg for each group, detonated with a small delay (typically 20 ms) between each group. The compact explosions are the closest approximation to single, well-tamped underground explosions that are currently available in the Khibiny area, and we compare ARCES recordings of one such (1 ton) explosion in the Rasvumchorr mine to the recordings of the two large explosions on 16 November 2002.

Section 6.5 is entitled: "Study of regional variations of the coda characteristics in the Barents Sea using small-aperture arrays". At regional distances, coda waves arriving after deterministic phases like Pn, Pg, Sn, or Lg are broadly attributed to seismic wave scattering phenomena associated with heterogeneities located within the crust. Therefore, the characteristics of the coda depend on the characteristics of the seismic source, but also on the properties of the medium of propagation. The analysis of phases composing the coda is then ideally suited for studying crustal structures. In this study, the objective has been to apply small-array analysis to obtain a better understanding of the propagation effects that affect the seismic wave field when it propagates through the Barents Sea region.

The paper investigates the characteristics of the coda for a large data set recorded by ARCES and SPITS. F-k decompositions have been used to calculate the time evolution of the parameters of propagation of the different phases that compose the coda.

It is shown that for the arrays ARCES and SPITS, the characteristics of the coda are very similar for events located in northern Fennoscandia / Kola Peninsula region, close to Novaya Zemlya and close to Spitsbergen in the Barents Sea. The coda propagates mainly along the great circle paths between sources and arrays. The apparent velocities are typical of Pn phases for the Pn coda and Sn phases for the Sn coda. In this case, we infer mechanisms like multiple crustal reflections to explain our observations. The characteristics of the coda are very different for all the events located along the Mid-Atlantic ridge. For these events, strong differences are generally observed between the direction of propagation of the coda phases and the expected theoretical direction. This shows that the scattering is no longer confined to the great circle path, but that lateral structures are also involved into multipathing and diffraction processes.

Section 6.6 is a study entitled "ARCES recordings of events from the Khibiny and Olenegorsk mines". This paper is a report under a separate project sponsored by National Nuclear Security Administration, and is included in view of its relevance to our studies under the present contract. The principal objective of the project is to develop and test a new advanced, automatic approach to seismic detection/location using array processing. The aim is to obtain significantly improved precision in location of low-magnitude events compared to current automatic approaches, combined with a low false alarm rate. We have started to investigate in detail events from the Khibiny and the Olenegorsk mines in the Kola Peninsula. Ground truth information and earlier studies of mining events from this region have revealed that a wide range of source types are present at these mines. The blasts in the open-pit mines are usually large ripple-fired explosions, often detonated in several groups with some seconds delay. So-called compact shots with yields between 1 and up to a few tons are also routinely detonated.

We show several panels of waveform plots from various mines in the Olenegorsk and Khibiny mining complexes, using a semblance analysis technique applied to the ARCES waveform recordings. From these panels we see that some of the events show a relatively simple source signature, whereas others have longer duration and consist of several pulses, which could be an effect of multiple seismic sources in combination with near-source scattering.

Based on the overview gained from semblance analysis and visual inspection of ARCES data of 99 compact shots from the underground Rasvumchorr mine, we have found that the vast majority of these events are characterized by a single strong Pn pulse. For these events, it should be possible to detect and characterize the Pn, Pg, Sn and Lg phases at ARCES automatically. However, for about 25% of the events, there are multiple pulses in the Pn-Pg time window, indicating separate explosions with time delays ranging from 1 and up to several seconds. Consequently, automatic processing of these events will be a more difficult task.

Frode Ringdal

2 Operation of International Monitoring System (IMS) Stations in Norway

2.1 PS27 — Primary Seismic Station NOA

The average recording time was 100%, the same as for the previous reporting period.

There were no outages of all subarrays at the same time.

Monthly uptimes for the NORSAR on-line data recording task, taking into account all factors (field installations, transmissions line, data center operation) affecting this task were as follows:

July	:	100%
August	:	100%
September	:	100%
October	:	100%
November	:	100%
June	:	100%

J. Torstveit

NOA Event Detection Operation

In Table 2.1.1 some monthly statistics of the Detection and Event Processor operation are given. The table lists the total number of detections (DPX) triggered by the on-line detector, the total number of detections processed by the automatic event processor (EPX) and the total number of events accepted after analyst review (teleseismic phases, core phases and total).

	Total DPX	Total EPX	Accepted Events		Sum	Daily
			P-phases	Core Phases			
Jul	7,178	960	420	60	480	15.5
Aug	7,777	765	239	93	332	10.7
Sep	9,716	1,533	397	58	455	15.2
Oct	11,013	1,067	424	66	490	15.8
Nov	11,727	1,003	388	42	430	14.3
Dec	11,952	908	300	48	348	11.2
	59,363	6,236	2,168	367	2,535	13.78

Table 2.1.1. *Detection and Event Processor statistics, 1 July - 31 December 2003.*

NOA detections

The number of detections (phases) reported by the NORSAR detector during day 182, 2003, through day 365, 2003, was 59,363, giving an average of 323 detections per processed day (184 days processed).

B. Paulsen
U. Baadshaug

2.2   PS28 — Primary Seismic Station ARCES

The average recording time was 99.65%, as compared to 100% for the previous reporting period.

Table 2.2.1 lists the time periods for the three outages in the reporting period.

Date	Time
03/08	04.53.10.000 - 20.19.30.000
03/08	20.20.20.000 - 20.20.40.000
07/08	04.59.00.000 - 05.06.00.000

Monthly uptimes for the ARCES on-line data recording task, taking into account all factors (field installations, transmission lines, data center operation) affecting this task were as follows:

Month		Uptime
July	:	100%
August	:	97.91%
September	:	100%
October	:	100%
November	:	100%
December	:	100%

J. Torstveit

Event Detection Operation

ARCES detections

The number of detections (phases) reported during day 182, 2003, through day 365, 2003, was 211,268, giving an average of 1148 detections per processed day (184 days processed).

Events automatically located by ARCES

During days 182, 2003, through 365, 2003, 8,581 local and regional events were located by ARCES, based on automatic association of P- and S-type arrivals. This gives an average of 46.6 events per processed day (184 days processed). 52% of these events are within 300 km, and 82% of these events are within 1000 km.

U. Baadshaug

2.3   AS72 — Auxiliary Seismic Station Spitsbergen

The average recording time was 98.84% as compared to 99.80% for the previous reporting period.

Table 2.3.1 lists the time periods of the main downtimes in the reporting period.

Day	Time
03/07	17.57.21.000 - 18.04.54.000
16/07	17.14.52.000 - 17.22.26.000
20/07	16.55.28.000 - 17.03.02.000
10/09	09.19.52.000 -
12/09	- 08.07.42.000
09/10	15.51.15.000 - 15.58.48.000
24/10	10.25.09.000 - 10.32.42.000
25/10	22.12.21.000 - 22.19.55.000
01/11	21.46.18.000 - 21.53.51.000
04/11	21.30.31.000 - 21.38.04.000
05/11	21.31.03.000 - 21.38.35.000
08/11	21.15.14.000 - 21.22.47.000
13/11	20.55.51.000 - 21.03.25.000
21/11	20.26.45.000 - 20.34.19.000
26/11	20.00.39.000 - 20.08.13.000
05/12	07.35.19.000 - 07.42.52.000
12/12	18.56.36.000 - 19.04.09.000
13/12	18.57.08.000 - 19.04.40.000
29/12	17.54.51.000 - 18.02.24.000

Table 2.3.1. *The main interruptions in recording of Spitsbergen data at NDPC, 1 July - 31 December 2003.*

Monthly uptimes for the Spitsbergen on-line data recording task, taking into account all factors (field installations, transmissions line, data center operation) affecting this task were as follows:

July	:	99.88%
August	:	100%
September	:	93.50%
October	:	99.94%
November	:	99.84%
December	:	99.88%

J. Torstveit

Event Detection Operation

Spitsbergen array detections

The number of detections (phases) reported from day 182, 2003, through day 365, 2003, was 445,777, giving an average of 2436 detections per processed day (183 days processed).

Events automatically located by the Spitsbergen array

During days 181, 2003, through 365, 2003, 54,526 local and regional events were located by the Spitsbergen array, based on automatic association of P- and S-type arrivals. This gives an average of 298.0 events per processed day (183 days processed). 66% of these events are within 300 km, and 85% of these events are within 1000 km.

U. Baadshaug

2.4   AS73 — Auxiliary Seismic Station at Jan Mayen

The IMS auxiliary seismic network includes a three-component station on the Norwegian island of Jan Mayen. The station location given in the protocol to the Comprehensive Nuclear-Test-Ban Treaty is 70.9°N, 8.7°W.

The University of Bergen has operated a seismic station at this location since 1970. A so-called Parent Network Station Assessment for AS73 was completed in April 2002. A vault at a new location (71.0°N, 8.5°W) was prepared in early 2003, after its location had been approved by the PrepCom. New equipment was installed in this vault in October 2003, as a cooperative effort bertween NORSAR and the CTBTO/PTS. Continuous data from this station are being transmitted to the NDC at Kjeller via a satellite link installed in April 2000. Data are also made available to the University of Bergen.

J. Fyen

2.5   IS37 — Infrasound Station at Karasjok

The IMS infrasound network will include a station at Karasjok in northern Norway. The coordinates given for this station are 69.5°N, 25.5°E. These coordinates coincide with those of the primary seismic station PS28.

A site survey for this station was carried out during June/July 1998 as a cooperative effort between the Provisional Technical Secretariat of the CTBTO and NORSAR. The site survey led to a recommendation on the exact location of the infrasound station. This location needs to be surveyed in detail. The next step will be to approach the local authorities to obtain the permission necessary to establish the station. Station installation is expected to take place in the year 2005.

S. Mykkeltveit

2.6   RN49 — Radionuclide Station on Spitsbergen

The IMS radionuclide network includes a station on the island of Spitsbergen. This station is also among those IMS radionuclide stations that will have a capability of monitoring for the presence of relevant noble gases upon entry into force of the CTBT.

A site survey for this station was carried out in August of 1999 by NORSAR, in cooperation with the Norwegian Radiation Protection Authority. The site survey report to the PTS contained a recommendation to establish this station at Platåberget, near Longyearbyen. The infrastructure for housing the station equipment was established in early 2001, and a noble gas detection system, based on the Swedish "SAUNA" design, was installed at this site in May 2001, as part of PrepCom's noble gas experiment. A particulate station ("ARAME" design) was installed at the same location in September 2001. A certification visit to the station took place in October 2002, and the particulate station was certified on 10 June 2003. The equipment at RN49 is being maintained and operated in accordance with a contract with the CTBTO/PTS.

S. Mykkeltveit

3 Contributing Regional Seismic Arrays

3.1 NORES

NORES has been out of operation since a thunderstorm destroyed the station electronics on 11 June 2002.

J. Torstveit

3.2 Hagfors (IMS Station AS101)

The average recording time was 96.89% as compared to 100% for the previous reporting period.

Table 3.2.1 lists the time period of the main outages in the reporting period.

Date	Time
02/09	14.16.20.000 - 14.23.50.000
17/09	00.00.10.000 -
22/09	- 07.58.50.000
22/09	08.28.50.000 - 08.57.00.000
30/10	11.28.10.000 - 16.53.20.000
30/10	17.16.40.000 - 17.33.30.000

Table 3.2.1. *The main interruptions in recording of Hagfors data at NDPC, 1 July - 31 December 2003.*

Monthly uptimes for the Hagfors on-line data recording task, taking into account all factors (field installations, transmissions line, data center operation) affecting this task were as follows:

Month		Uptime
July	:	99.99%
August	:	100%
September	:	82.14%
October	:	99.23%
November	:	100%
December	:	100%

J. Torstveit

Hagfors Event Detection Operation

Hagfors array detections

The number of detections (phases) reported from day 182, 2003, through day 365, 2003, was 126,372, giving an average of 687 detections per processed day (184 days processed).

Events automatically located by the Hagfors array

During days 182, 2003, through 365, 2003, 3703 local and regional events were located by the Hagfors array, based on automatic association of P- and S-type arrivals. This gives an average of 20.1 events per processed day (184 days processed). 62% of these events are within 300 km, and 85% of these events are within 1000 km.

U. Baadshaug

3.3 FINES (IMS station PS17)

The average recording time was 100% as it was for the previous reporting period.

There were 51 outages that lasted from 1 to 10 seconds in the period.

Monthly uptimes for the FINES on-line data recording task, taking into account all factors (field installations, transmissions line, data center operation) affecting this task were as follows:

July	:	100%
August	:	100%
September	:	100%
October	:	100%
November	:	100%
December	:	100%

J. Torstveit

FINES Event Detection Operation

FINES detections

The number of detections (phases) reported during day 182, 2003, through day 365, 2003, was 55,250, giving an average of 302 detections per processed day (183 days processed).

Events automatically located by FINES

During days 182, 2003, through 365, 2003, 2513 local and regional events were located by FINES, based on automatic association of P- and S-type arrivals. This gives an average of 13.7 events per processed day (183 days processed). 80% of these events are within 300 km, and 91% of these events are within 1000 km.

U. Baadshaug

3.4   Apatity

The average recording time was 97.71% in the reporting period compared to 99.62% during the previous period.

The main outages in the period are given in Table 3.4.1.

Date	Time
04/07	20.40.33.000 -
05/07	- 10.14.26.000
09/07	00.35.28.000 - 04.44.38.000
13/07	18.00.59.000 -
14/07	- 05.49.36.000
10/09	14.11.47.000 -
11/09	- 05.23.53.000
19/09	11.56.16.000 - 13.31.16.000
14/11	06.40.36.000 -
16/11	- 11.27.16.000

Table 3.4.1. *The main interruptions in recording of Apatity data at NDPC. 1 July - 31 December 2003.*

Monthly uptimes for the Apatity on-line data recording task, taking into account all factors (field installations, transmissions line, data center operation) affecting this task were as follows:

July	:	96.02%
August	:	99.99%
September	:	97.63%
October	:	99.98%
November	:	92.62%
December	:	100%

J. Torstveit

Apatity Event Detection Operation

Apatity array detections

The number of detections (phases) reported from day 182, 2003, through day 365, 2003, was 205,682, giving an average of 1124 detections per processed day (183 days processed).

As described in earlier reports, the data from the Apatity array is transferred by one-way (simplex) radio links to Apatity city. The transmission suffers from radio disturbances that occasionally result in a large number of small data gaps and spikes in the data. In order for the communication protocol to correct such errors by requesting retransmission of data, a two-way radio link would be needed (duplex radio).

However, it should be noted that noise from cultural activities and from the nearby lakes cause most of the unwanted detections. These unwanted detections are "filtered" in the signal processing, as they give seismic velocities that are outside accepted limits for regional and teleseismic phase velocities.

Events automatically located by the Apatity array

During days 182, 2003, through 365, 2003, 2787 local and regional events were located by the Apatity array, based on automatic association of P- and S-type arrivals. This gives an average of 15.2 events per processed day (183 days processed). 36% of these events are within 300 km, and 72% of these events are within 1000 km.

U. Baadshaug

3.5   Regional Monitoring System Operation and Analysis

The Regional Monitoring System (RMS) was installed at NORSAR in December 1989 and has been operated at NORSAR from 1 January 1990 for automatic processing of data from ARCES and NORES. A second version of RMS that accepts data from an arbitrary number of arrays and single 3-component stations was installed at NORSAR in October 1991, and regular operation of the system comprising analysis of data from the 4 arrays ARCES, NORES, FINES and GERES started on 15 October 1991. As opposed to the first version of RMS, the one in current operation also has the capability of locating events at teleseismic distances.

Data from the Apatity array was included on 14 December 1992, and from the Spitsbergen array on 12 January 1994. Detections from the Hagfors array were available to the analysts and could be added manually during analysis from 6 December 1994. After 2 February 1995, Hagfors detections were also used in the automatic phase association.

Since 24 April 1999, RMS has processed data from all the seven regional arrays ARCES, NORES, FINES, GERES (until January 2000), Apatity, Spitsbergen, and Hagfors. Starting 19 September 1999, waveforms and detections from the NORSAR array have also been available to the analyst.

Phase and event statistics

Table 3.5.1 gives a summary of phase detections and events declared by RMS. From top to bottom the table gives the total number of detections by the RMS, the number of detections that are associated with events automatically declared by the RMS, the number of detections that are not associated with any events, the number of events automatically declared by the RMS, and finally the total number of events worked on interactively (in accordance with criteria that vary over time; see below) and defined by the analyst.

New criteria for interactive event analysis were introduced from 1 January 1994. Since that date, only regional events in areas of special interest (e.g, Spitsbergen, since it is necessary to acquire new knowledge in this region) or other significant events (e.g, felt earthquakes and large industrial explosions) were thoroughly analyzed. Teleseismic events of special interest are also analyzed.

To further reduce the workload on the analysts and to focus on regional events in preparation for Gamma-data submission during GSETT-3, a new processing scheme was introduced on 2 February 1995. The GBF (Generalized Beamforming) program is used as a pre-processor to RMS, and only phases associated with selected events in northern Europe are considered in the automatic RMS phase association. All detections, however, are still available to the analysts and can be added manually during analysis.

	Jul 03	Aug 03	Sep 03	Oct 03	Nov 03	Dec 03	Total
Phase detections	192645	199361	184110	175425	158654	199536	1109731
- Associated phases	5439	5951	7556	7043	6374	6346	38709
- Unassociated phases	187206	193410	176554	168382	152280	193190	1071022
Events automatically declared by RMS	1106	1372	1649	1504	1364	1445	8440
No. of events defined by the analyst	113	43	73	46	91	72	438

Table 3.5.1. RMS phase detections and event summary 1 July - 31 December 2003.

U. Baadshaug
B. Paulsen

4   NDC and Field Activities

4.1   NDC Activitities

NORSAR functions as the Norwegian National Data Center (NDC) for CTBT verification. Six monitoring stations, comprising altogether 119 field instruments, will be located on Norwegian territory as part of the future IMS as described elsewhere in this report. The four seismic IMS stations are all in operation today, and three of them are currently providing data to the IDC on a regular basis. The radionuclide station at Spitsbergen was certified on 10 June 2003, whereas the infrasound station in northern Norway will need to be established within the next few years. Data recorded by the Norwegian stations is being transmitted in real time to the Norwegian NDC, and provided to the IDC through the Global Communications Infrastructure (GCI). Norway is connected to the GCI with a frame relay link to Vienna.

Operating the Norwegian IMS stations continues to require increased resources and additional personnel both at the NDC and in the field. The PTS has established new and strictly defined procedures as well as increased emphasis on regularity of data recording and timely data transmission to the IDC in Vienna. This has led to increased reporting activities and implementation of new procedures for the NDC operators. The NDC carries out all the technical tasks required in support of Norway's treaty obligations. NORSAR will also carry out assessments of events of special interest, and advise the Norwegian authorities in technical matters relating to treaty compliance.

Verification functions; information received from the IDC

After the CTBT enters into force, the IDC will provide data for a large number of events each day, but will not assess whether any of them are likely to be nuclear explosions. Such assessments will be the task of the States Parties, and it is important to develop the necessary national expertise in the participating countries. An important task for the Norwegian NDC will thus be to make independent assessments of events of particular interest to Norway, and to communicate the results of these analyses to the Norwegian Ministry of Foreign Affairs.

Monitoring the Arctic region

Norway will have monitoring stations of key importance for covering the Arctic, including Novaya Zemlya, and Norwegian experts have a unique competence in assessing events in this region. On several occasions in the past, seismic events near Novaya Zemlya have caused political concern, and NORSAR specialists have contributed to clarifying these issues.

International cooperation

After entry into force of the treaty, a number of countries are expected to establish national expertise to contribute to the treaty verification on a global basis. Norwegian experts have been in contact with experts from several countries with the aim of establishing bilateral or multilateral cooperation in this field. One interesting possibility for the future is to establish NORSAR as a regional center for European cooperation in the CTBT verification activities.

NORSAR event processing

The automatic routine processing of NORSAR events as described in NORSAR Sci. Rep. No. 2-93/94, has been running satisfactorily. The analyst tools for reviewing and updating the solutions have been continually modified to simplify operations and improve results. NORSAR is currently applying teleseismic detection and event processing using the large-aperture NORSAR array as well as regional monitoring using the network of small-aperture arrays in Fennoscandia and adjacent areas.

Communication topology

Norway has implemented an independent subnetwork, which connects the IMS stations AS72, AS73, PS28, and RN49 operated by NORSAR to the GCI at NOR_NDC. A contract has been concluded and VSAT antennas have been installed at each station in the network. Under the same contract, VSAT antennas for 6 of the PS27 subarrays have been installed for intra-array communication. The seventh subarray is connected to the central recording facility via a leased land line. The central recording facility for PS27 is connected directly to the GCI (Basic Topology). All the VSAT communication is functioning satisfactorily.

Jan Fyen

4.2   Status Report: Provision of data from Norwegian seismic IMS stations to the IDC

Introduction

This contribution is a report for the period July - December 2003 on activities associated with provision of data from Norwegian seismic IMS stations to the International Data Centre (IDC) in Vienna. This report represents an update of contributions that can be found in previous editions of NORSAR's Semiannual Technical Summary. (Note that these status reports previously were entitled "Status Report: Norway's participation in GSETT-3".) It is noted that as of 31 December 2003, two out of the three Norwegian seismic stations providing data to the IDC have been formally certified.

Norwegian IMS stations and communications arrangements

During the reporting interval 1 July - 31 December 2003, Norway has provided data to the IDC from the three seismic stations shown in Fig. 4.2.1. The NORSAR array (PS27, station code NOA) is a 60 km aperture teleseismic array, comprised of 7 subarrays, each containing six vertical short period sensors and a three-component broadband instrument. ARCES is a 25-element regional array with an aperture of 3 km, whereas the Spitsbergen array (station code SPITS) has 9 elements within a 1-km aperture. ARCES and SPITS both have a broadband three-component seismometer at the array center.

The intra-array communication for NOA utilizes a land line for subarray NC6 and VSAT links based on TDMA technology for the other 6 subarrays. The central recording facility for NOA is located at the Norwegian National Data Center (NOR_NDC).

Continuous ARCES data has been transmitted from the ARCES site to NOR_NDC using a 64 kbits/s VSAT satellite link, based on BOD technology.

Continuous SPITS data has been transmitted to NOR_NDC via a VSAT terminal located at Platåberget in Longyearbyen (which is the site of the IMS radionuclide monitoring station RN49 installed during 2001).

Seven-day station buffers have been established at the ARCES and SPITS sites and at all NOA subarray sites, as well as at NOR_NDC for ARCES, SPITS and NOA.

The NOA and ARCES arrays are primary stations in the IMS network, which implies that data from these stations is transmitted continuously to the receiving international data center. Since October 1999, this data has been transmitted (from NOR_NDC) via the Global Communications Infrastructure (GCI) to the IDC in Vienna. The SPITS array is an auxiliary station in the IMS, and the SPITS data have been available to the IDC throughout the reporting period on a request basis via use of the AutoDRM protocol (Kradolfer, 1993; Kradolfer, 1996). In addition, continuous data from all three arrays is transmitted to the US NDC.

Uptimes and data availability

Figs. 4.2.2 and 4.2.3 show the monthly uptimes for the Norwegian IMS primary stations ARCES and NOA, respectively, for the period 1 July - 31 December 2003, given as the hatched (taller) bars in these figures. These barplots reflect the percentage of the waveform data that is available in the NOR_NDC tape archives for these two arrays. The downtimes inferred from these figures thus represent the cumulative effect of field equipment outages, station site to NOR_NDC communication outage, and NOR_NDC data acquisition outages.

Figs. 4.2.2 and 4.2.3 also give the data availability for these two stations as reported by the IDC in the IDC Station Status reports. The main reason for the discrepancies between the NOR_NDC and IDC data availabilities as observed from these figures is the difference in the ways the two data centers report data availability for arrays: Whereas NOR_NDC reports an array station to be up and available if at least one channel produces useful data, the IDC uses weights where the reported availability (capability) is based on the number of actually operating channels.

Use of the AutoDRM protocol

NOR_NDC's AutoDRM has been operational since November 1995 (Mykkeltveit & Baadshaug, 1996). The monthly number of requests by the IDC for SPITS data for the period July - December 2003 is shown in Fig. 4.2.4.

NDC automatic processing and data analysis

These tasks have proceeded in accordance with the descriptions given in Mykkeltveit and Baadshaug (1996). For the period July - December 2003, NOR_NDC derived information on 423 supplementary events in northern Europe and submitted this information to the Finnish NDC as the NOR_NDC contribution to the joint Nordic Supplementary (Gamma) Bulletin, which in turn is forwarded to the IDC. These events are plotted in Fig. 4.2.5.

Data access for the station NIL at Nilore, Pakistan

NOR_NDC continued to provide access to the seismic station NIL at Nilore, Pakistan, through a VSAT satellite link between NOR_NDC and Pakistan's NDC in Nilore.

Current developments and future plans

NOR_NDC is continuing the efforts towards improving and hardening all critical data acquisition and data forwarding hardware and software components, so as to meet the requirements related to operation of IMS stations.

The NOA array was formally certified by the PTS on 28 July 2000, and a contract with the PTS in Vienna currently provides partial funding for operation and maintenance of this station. The ARCES array was formally certified by the PTS on 8 November 2001, and a contract with the PTS is in place which also provides for partial funding of the operation and maintenance of this station. Provided that adequate funding continues to be made available (from the PTS and the Norwegian Ministry of Foreign Affairs), we envisage continuing the provision of data from all Norwegian seismic IMS stations without interruption to the IDC in Vienna.

U. Baadshaug
S. Mykkeltveit
J. Fyen

References

Kradolfer, U. (1993): Automating the exchange of earthquake information. *EOS, Trans., AGU,* 74, 442.

Kradolfer, U. (1996): AutoDRM — The first five years, *Seism. Res. Lett.,* 67, 4, 30-33.

Mykkeltveit, S. & U. Baadshaug (1996): Norway's NDC: Experience from the first eighteen months of the full-scale phase of GSETT-3. *Semiann. Tech. Summ., 1 October 1995 - 31 March 1996,* NORSAR Sci. Rep. No. 2-95/96, Kjeller, Norway.
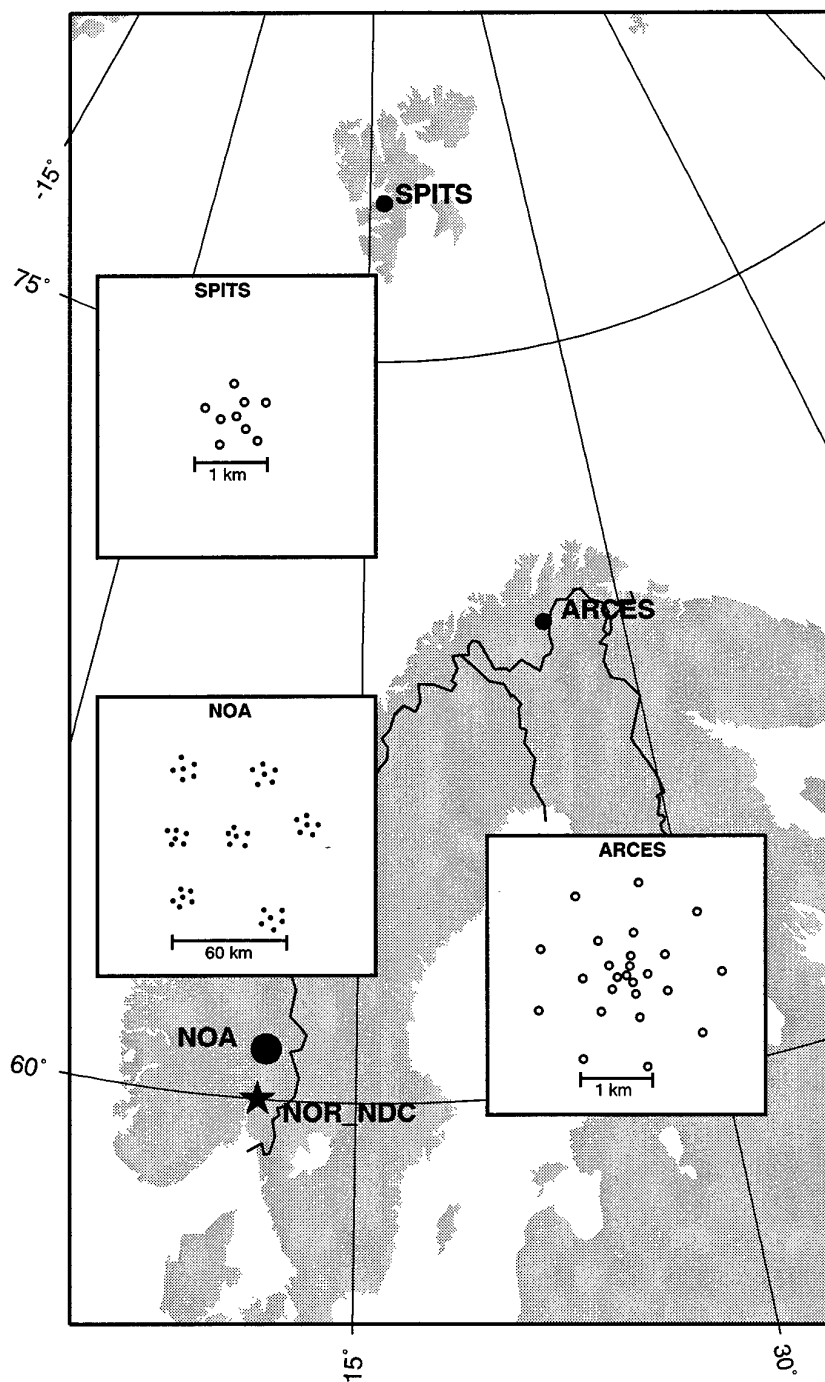
Fig. 4.2.1.　The figure shows the locations and configurations of the three Norwegian seismic IMS array stations that provided data to the IDC during the period July - December 2003. The data from these stations are transmitted continuously and in real time to the Norwegian NDC (NOR_NDC). The stations NOA and ARCES are primary IMS stations, whereas SPITS is an auxiliary IMS station.

ARCES data availability at NDC and IDC
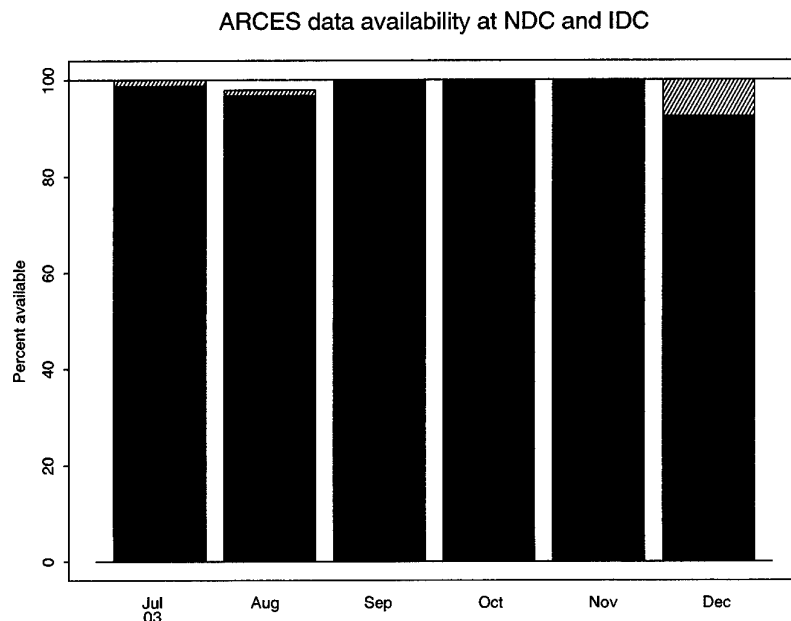
Fig. 4.2.2.   The figure shows the monthly availability of ARCES array data for the period July - December 2003 at NOR_NDC and the IDC. See the text for explanation of differences in definition of the term "data availability" between the two centers. The higher values (hatched bars) represent the NOR_NDC data availability.

NOA data availability at NDC and IDC
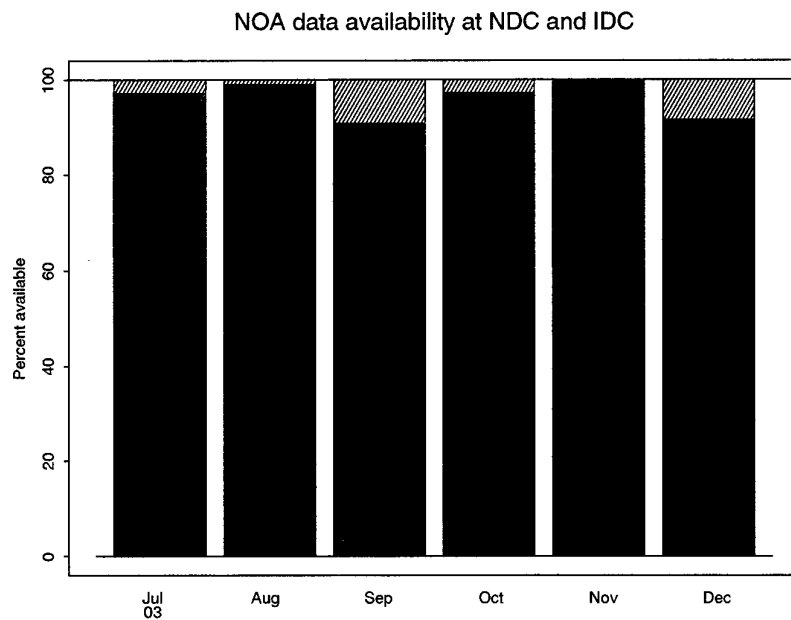
Fig. 4.2.3.   The figure shows the monthly availability of NORSAR array data for the period July - June 2003 at NOR_NDC and the IDC. See the text for explanation of differences in definition of the term "data availability" between the two centers. The higher values (hatched bars) represent the NOR_NDC data availability.

AutoDRM SPITS requests received by NOR_NDC from IDC
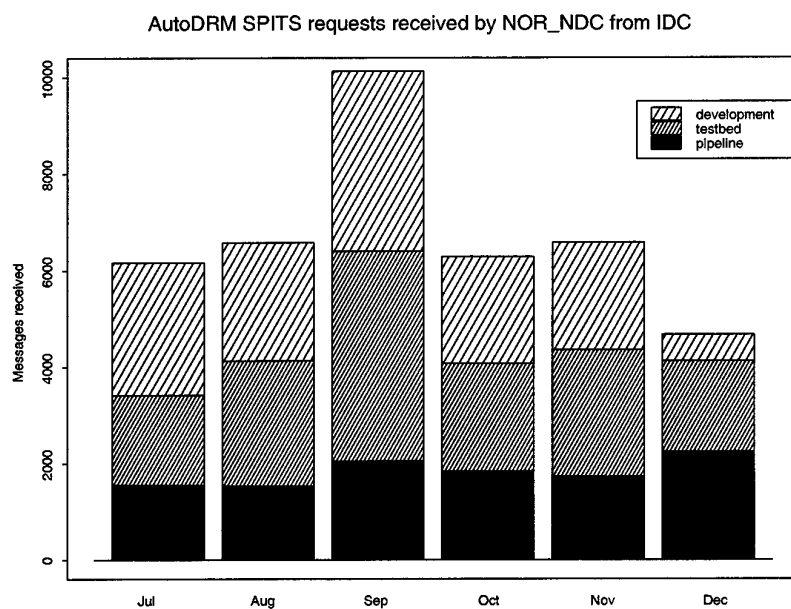
Fig. 4.2.4.   The figure shows the monthly number of requests received by NOR_NDC from the IDC for SPITS waveform segments during July - December 2003.

Reviewed Supplementary events
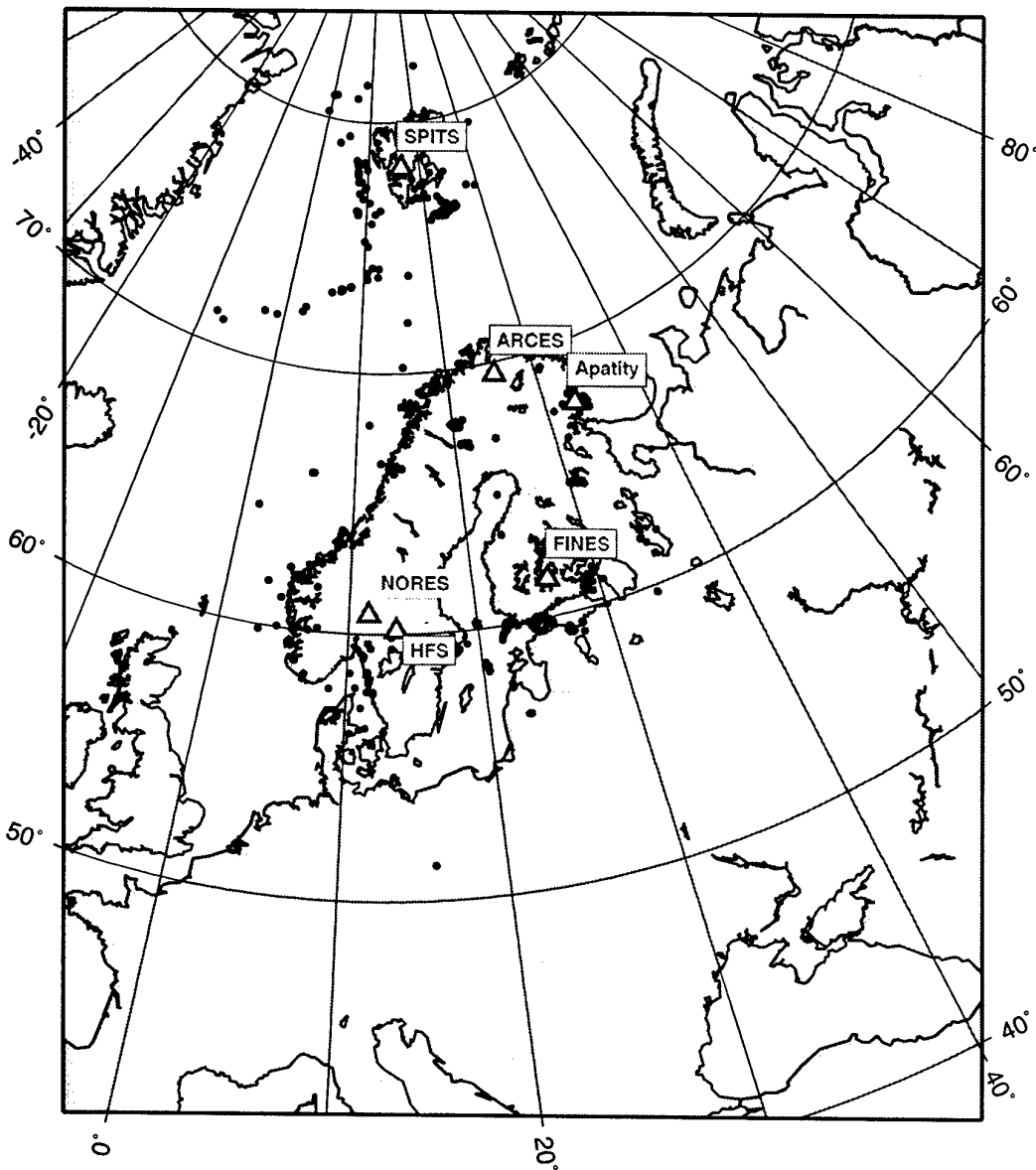
Fig. 4.2.5. The map shows the 423 events in and around Norway contributed by NOR_NDC during July - December 2003 as supplementary (Gamma) events to the IDC, as part of the Nordic supplementary data compiled by the Finnish NDC. The map also shows the seismic stations used in the data analysis to define these events.

4.3   Field Activities

The activities at the NORSAR Maintenance Center (NMC) at Hamar currently include work related to operation and maintenance of the following IMS seismic stations: the NOA teleseismic array (PS27), the ARCES array (PS28) and the Spitsbergen array (AS72). Some work has also been carried out in connection with the seismic station on Jan Mayen (AS73), the infrasound station at Karasjok (IS37) and the radionuclide station at Spitsbergen (RN49). NORSAR also acts as a consultant for the operation and maintenance of the Hagfors array in Sweden (AS101).

NORSAR carries out the field activities relating to IMS stations in a manner generally consistent with the requirements specified in the appropriate IMS Operational Manuals, which are currently being developed by Working Group B of the Preparatory Commission. For seismic stations these specifications are contained in the Operational Manual for Seismological Monitoring and the International Exchange of Seismological Data (CTBT/WGB/TL-11/2), currently available in a draft version.

All regular maintenance on the NORSAR field systems is conducted on a one-shift-per-day, five-day-per-week basis. The maintenance tasks include:

- Operating and maintaining the seismic sensors and the associated digitizers, authentication devices and other electronics components.
- Maintaining the power supply to the field sites as well as backup power supplies.
- Operating and maintaining the VSATs, the data acquisition systems and the intra-array data transmission systems.
- Assisting the NDC in evaluating the data quality and making the necessary changes in gain settings, frequency response and other operating characteristics as required.
- Carrying out preventive, routine and emergency maintenance to ensure that all field systems operate properly.
- Maintaining a computerized record of the utilization, status, and maintenance history of all site equipment.
- Providing appropriate security measures to protect against incidents such as intrusion, theft and vandalism at the field installations.

Details of the daily maintenance activities are kept locally. As part of its contract with CTBTO/ PTS NORSAR submits, when applicable, problem reports, outage notification reports and equipment status reports. The contents of these reports and the circumstances under which they will be submitted are specified in the draft Operational Manual.

P.W. Larsen
K.A. Løken

4.4   Selection of seismometers for Spitsbergen array refurbishment

In accordance with the current contract, NORSAR is refurbishing the Spitsbergen array to satisfy the IMS specifications. The refurbishment includes upgrading 5 of the array sites to comprise three-component seismometers instead of the current vertical sensors. Today, the Spitsbergen array configuration conforms to the minimum IMS requirement for a new seismic array, having 9 short-period vertical seismometers and one three-component broadband sensor.

The work reported here is a study to decide how to best upgrade the array with respect to the selection of seismometers. The array data acquisition system, including digitizers, authenticators, radio equipment and software has been ordered from Guralp. The type of digitizer used for this testing has been evaluated by Sandia, and their test results are documented in the report "Evaluation of the Guralp DM24-B1 Borehole digitizer" by Richard P. Kromer, Sandia National Laboratories, June 19, 2003.

In the fall of 1994, NORSAR installed the Guralp CMG-3ESP seismometers in the Spitsbergen array. These sensors have a flat velocity response from 0.1 Hz to 50 Hz with sensitivity 10000 V/m/s and comprise the "short-period" component of the array. At the same time, in site SPB4 of the array, we installed a Guralp CMG-3T broadband sensor (BB) above the ESP sensor and inside the same borehole. The CMG-3T has flat velocity response from 0.001 Hz to 50 Hz with sensitivity 10000 V/m/s.

In NORSAR Sci. Rep. No. 2-94/95, the complete system response of the current Spitsbergen array is described.

Throughout nearly 10 years of operation, we have had very good experience with the Guralp ESP seismometers, whereas we have had several problems with the BB sensor. After discussions with Dr. Cansun M. Guralp, we have come to the conclusion that the problems we have seen with the BB instrument result from a combination of problems with the sensor itself and the installation of the sensor above and within the same borehole as one of the short-period sensors.

For those periods when we have seen good data from this installation, we have also noted that the BB sensor provides recordings with a significantly lower signal-to-noise ratio as compared to the ESP sensors. This applies in particular to the frequency band from 2 Hz and above. Based on this observation, we have concluded that, with the current configuration, we would need to drill one more borehole for the purpose of re-installing a BB sensor in a borehole by itself, since the IMS specifications require at least one three-component BB sensor within the array.

However, as Cansun Guralp has pointed out, we should not expect to see any difference between the BB and the ESP sensor above 2 Hz, since they are basically identical in this band. Consequently, Guralp suggested to use CMG-3T sensors all over the array, as this would simplify the installation and maintenance. Moreover, since 1994, there has been improvements in the sensor electronics for both BB and ESP, so that it would be difficult to add more horizontal sensors with the same specifications as the old vertical ESP. We therefore decided that in any case it would be necessary to replace all the seismometers, so the question was whether to install ESPs plus one BB sensor, or BB sensors at all the sites.

Based on our previous problems with the BB sensor, we decided to test the newest versions of the ESP and BB sensors, and Guralp generously let us borrow two such sensors for test instal-

lation in subarray NC6 of PS27. This is the same location as the site A0 of the damaged NORES array.

From this test installation, we have now data for simultaneous recordings by:

NC602_vesp   Guralp CMG-ESPV (one component vertical installed 18 December 2003) and Guralp DM24 digitizer sampled at 100 Hz. The sensor response is flat to velocity from 0.1 Hz to 100 Hz. Sensitivity is 2*5000 V/m/s. Bit weight is 3.5 microvolts per count.

NC602_v3t   Guralp CMG-3TV (one component vertical installed 18 December 2003) and Guralp DM24 digitizer sampled at 100 Hz. The sensor response is flat to velocity from 0.01 Hz to 50 Hz. Sensitivity is 2*5000 V/m/s. Bit weight is 3.5 microvolts per count.

NC602_gs13   Geotech GS-13 (one component vertical installed 13 January 2004) and Guralp DM24 digitizer sampled at 100 Hz. The sensor response is flat to velocity from 1 Hz to DC. Sensitivity is 2000 V/m/s plus external amplifier factor 30.16. Bit weight is 3.5 microvolts per count.

NC602_bz,bn,be Guralp CMG-3T (three component installed 16 March 2000) and SHI AIM24BB digitizer sampled at 40 Hz. The sensor response is flat to velocity from 0.01 Hz to 50 Hz. Sensitivity is 2*2500 V/m/s. Bit weight is 3.8 microvolts per count.

NC602_bza,bna,bea   Teledyne KS54000 (three component installed 11 December 1995) and SHI AIM24BB digitizer sampled at 40 Hz. The sensor response is flat to acceleration from 0.01 Hz to 5 Hz (as per given theoretical response). Sensitivity is 2*5000 V/m/s/s. Bit weight is 3.8 microvolts per count.

NC602_sz   Teledyne 20171 (vertical component installed 29 October 1995) and SHI AIM24-1 digitizer sampled at 40 Hz. The sensor response is flat to velocity from 2 Hz to DC. Sensitivity is (637/0.7) V/m/s plus an external Brick amplifier of factor 39.8. Bit weight is 1.9 microvolts per count.

See Fig. 4.4.1 and Fig. 4.4.2 for illustration of these installations.
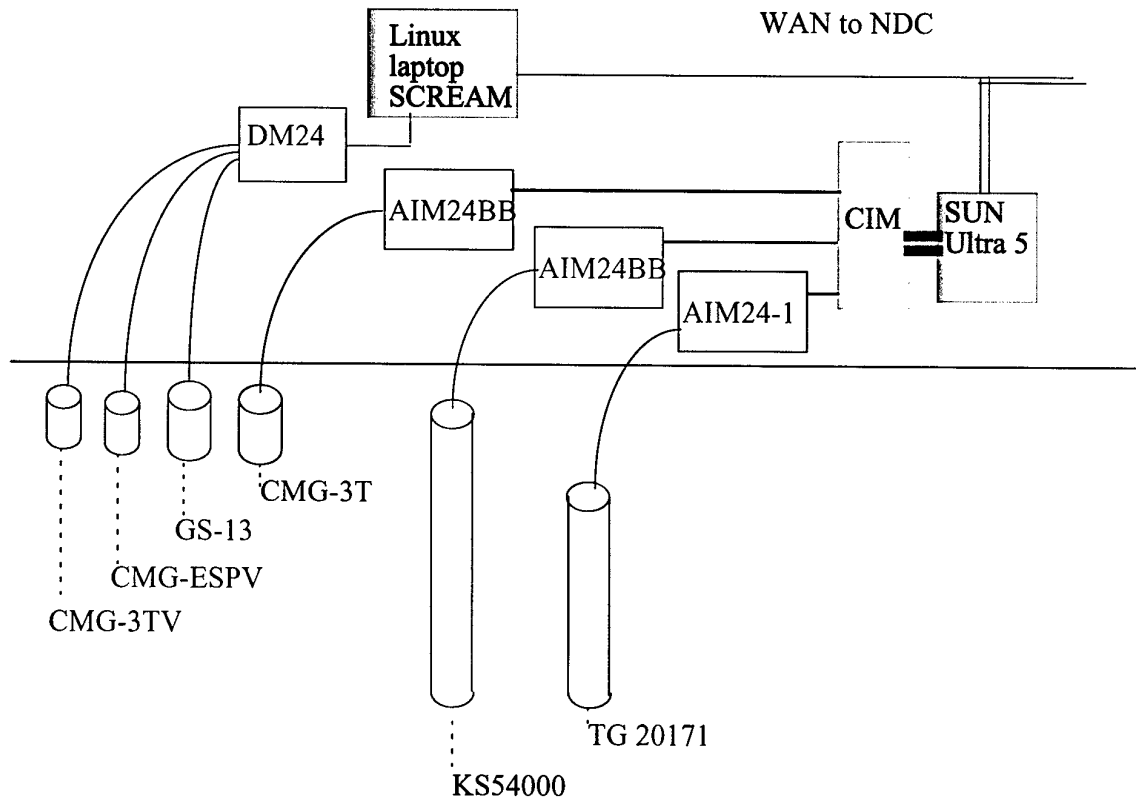
Fig. 4.4.1. *Schematic view of sensor test installation in Long Period Vault of subarray (LPV) NC6 of the PS27 - NOA array. See also Fig. 4.4.2 for a picture of the installation. The local area network in NC6 is connected to the NDC over a 64Kbit land line. The data sent to the IDC as NC602_b and NC602_sz components are marked in blue color. The red color marks equipment operated for the testing of sensors. All data is recorded continuously at the Norwegian NDC.*
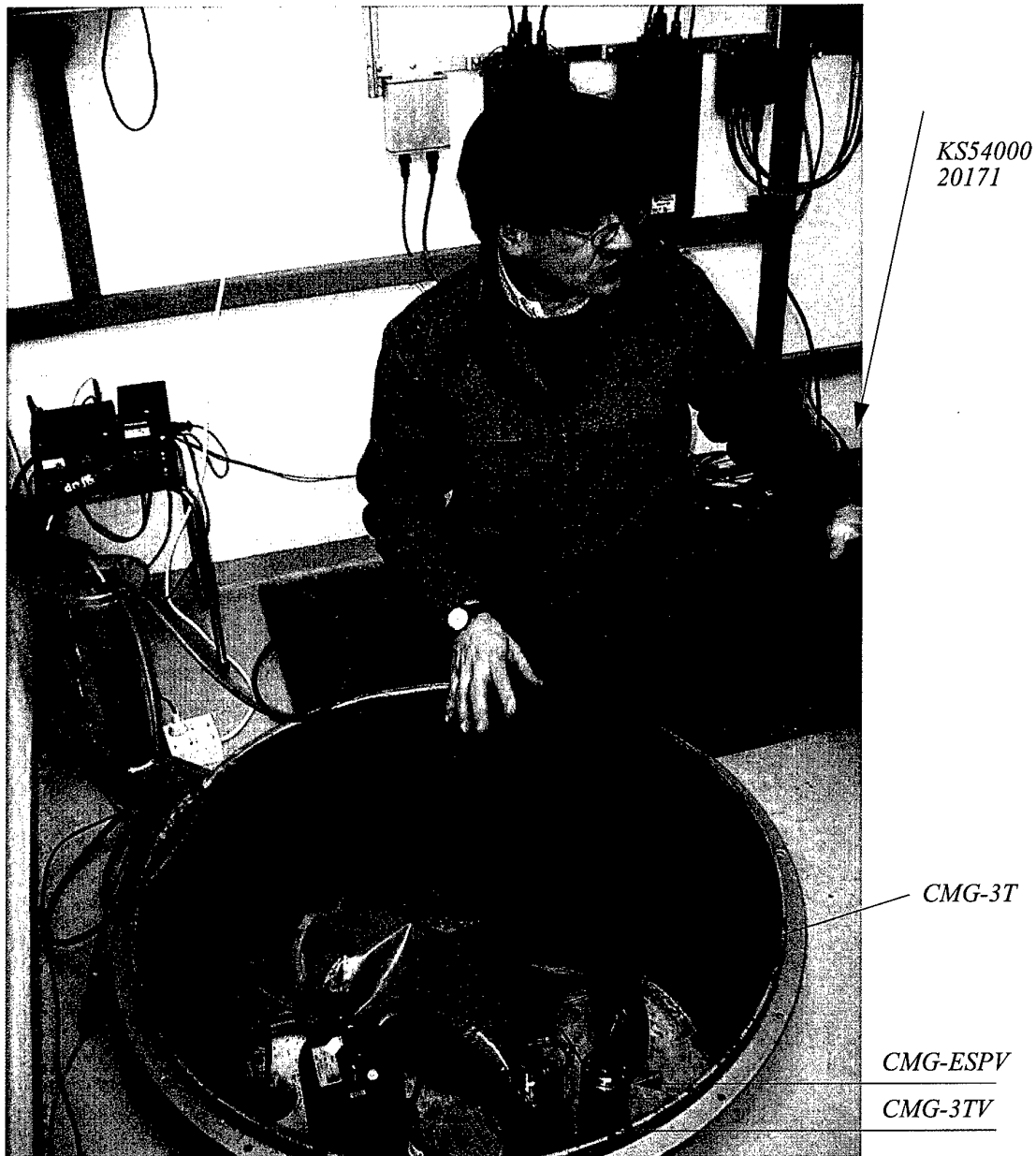
Fig. 4.4.2. *Installation of Guralp sensors by Dr. Cansun M. Guralp. The vault is the original sealed NOA vault which houses the NC602_b components (CMG-3T) of PS27, and we see the two new CMG-ESPV and CMG-3TV to the lower right of the vault. The sensors are borehole versions, and the coupling to bedrock is only through the sensors own (small) weight. The KS54000 and the 20171 sensors are in borehole in the rear right corner of the LPV, as indicated by one of the arrows.*

The aim of the testing was to determine whether the broadband sensors would give the same signal to noise ratios for high frequency signals as a "short-period" sensor. One simple way of doing this is to bandpass filter the data, and see if high frequency signals are equally visible on all sensors. Another issue we wanted to consider was whether any spikes in the data could be seen. No artificial spikes were seen during 30 days of automatic detector operation.

Fig. 4.4.3 shows an example of a local event where we have bandpass filtered the data from 8 to 16 Hz. The AIM24 digitizer runs at 40 Hz sampling, so the band limit is 16 Hz. The new sensors and DM24 digitizer have too low resolution for this very quiet site. However, there is no doubt that the signal to noise ratio we see for the new broadband sensor CMG-3TV is almost identical to that of the sensitive GS13 short period sensor.
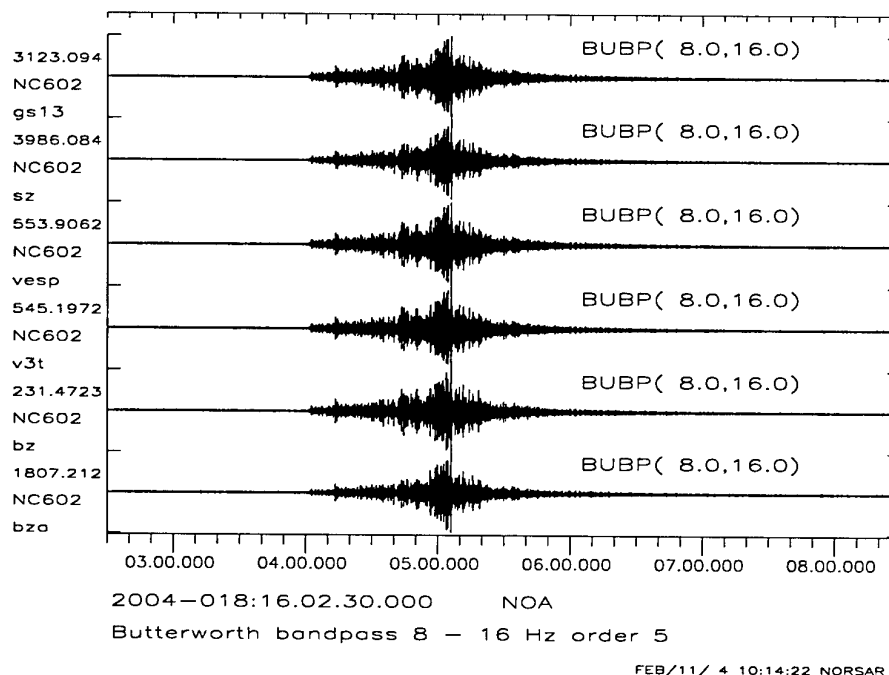
Fig. 4.4.3.   *The above figure shows from top to bottom, data observed in site NC602 for GS13, Teledyne 20171, Guralp CMG-ESPV, Guralp CMG-3TV, Guralp CMG-3T and KS54000. The data is filtered with a Butterworth bandpass filter of order 5 and band 8 - 16 Hz. The numbers annotated to the left side, is maximum amplitude in counts for the corresponding trace.*

Since the DM24 digitizer is run at 100 Hz, we can also inspect higher frequencies. Fig. 4.4.4 shows the three sensors GS13, CMG-ESPV and CMG-3TV filtered in the band 24 - 48 Hz. Note that for broadband sensors, we use higher order filters. This is because, in some filter bands from 2 Hz and above, the conventional 3rd order filters are not sharp enough to produce the best signal to noise ratio. From this figure we can see clearly that the SNR is essentially identical for all of the three sensors considered.
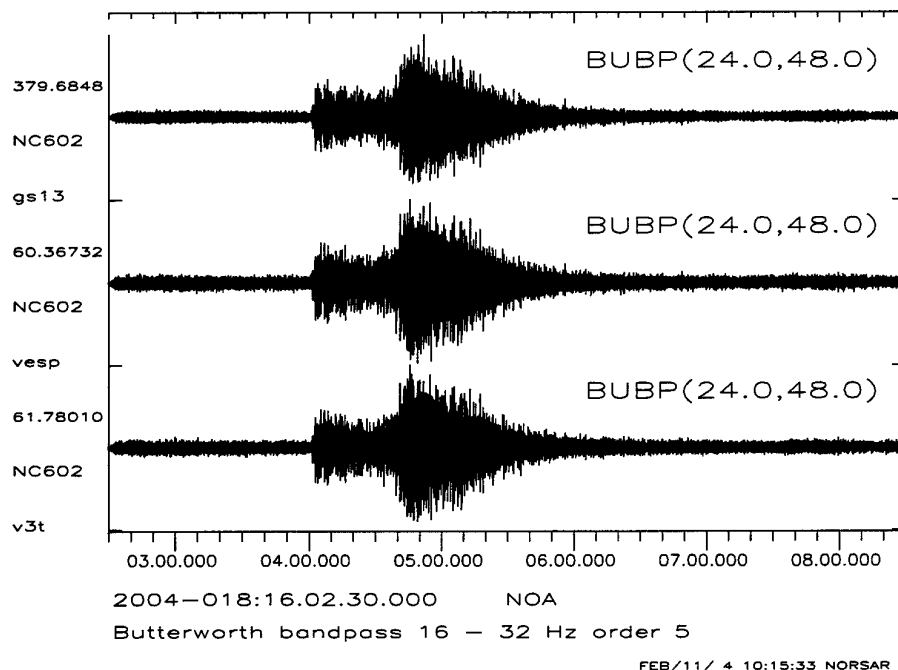
Fig. 4.4.4. *The above figure shows from top to bottom, data observed in site NC602 for Teledyne GS13, Guralp CMG-ESPV and Guralp CMG-3TV. The data is filtered with a Butterworth bandpass filter of order 5 and the filter band is 24 - 48 Hz. The numbers annotated to the left side represent maximum amplitude in counts for the corresponding trace.*

The conclusion from several observations, including power density measurements is clear: the broadband sensor will be the best choice for all frequency bands.

The noise level on Spitsbergen is maybe lower than the new low noise model at frequencies above 2 Hz. But for lower frequencies, the noise level increases to a level even above the high noise model. This is a challenge for the digital system. Using a highly sensitive velocity sensor to record the high frequency signals can result in a situation where strong surface waves at long periods will be clipped. On the other hand, if we use acceleration sensors, high frequency signals from local events of high magnitude may be clipped. It has also sometimes been argued that acceleration response may give higher instrument noise at high frequencies. This is according to Guralp not the situation for their instruments. Use of acceleration response implies that local noise sources (at high frequencies) are amplified. Such noise sources do not disappear with velocity sensors, and therefore this issue should not be considered when choosing velocity or acceleration response. Such high-frequency noise could be handled through correct processing of the velocity or acceleration data.

In consideration of the fact that the noise level on Spitsbergen has an extreme dynamic range over the entire observing broad frequency band, we conclude that all the seismometers of the upgraded Spitsbergen array should have acceleration response.

J. Fyen

5 Documentation Developed

Asming, V., E.O. Kremenetskaya & F. Ringdal (2004): Locating seismic events near the Spitsbergen archipelago, **In**: NORSAR Sci. Rep. 1-2004, 1 July - 31 December 2003, Kjeller, Norway.

Bungum, H., C. Lindholm & A. Dahle (2003): Long period ground motions for large European earthquakes, 1905-1992, and comparisons with stochastic predictions, J. Seism., 7, 377-396.

Engen, Ø., O. Eldholm & H. Bungum (2003): The Arctic plate boundary, J. Geophys. Res. 108 (B2).

Farahbod, A.M., C. Lindholm, M. Mokhtari & H. Bungum (2003): Aftershock analysis for the 1997 Ghaen-Birjand (Arkedul) earthquake, J. Seism. Earthq. Eng., 5(2), 1-10.

Fyen, J. & K. Iranpour (2003): Near real time data at NORSAR for CTBT monitoring. ORFEUS Electronic Newsletter, Vol 5, no 2, Sep 03.

Harris, D.B., F. Ringdal, E.O. Kremenetskaya, S. Mykkeltveit, J. Schweitzer, T. Hauk, V. Asming & J. Lewis (2003): Ground-truth collection for mining explosions in Northern Fennoscandia and Russia. Proc. 25th Seismic Research Review in Nuclear Explosions Monitoring, Tucson, Sep 2003.

Kozyrev, S., E.O. Kremenetskaya, V. Asming, F. Ringdal & T. Kværna (2004): Ground Truth information from Khibiny mining explosions. **In**: NORSAR Sci. Rep. 1-2004, 1 July - 31 December 2003, Kjeller, Norway.

Kværna, T. (2004): ARCES recordings of events from the Khibiny and Olenegorsk mines, **In**: NORSAR Sci. Rep. 1-2004, 1 July - 31 December 2003, Kjeller, Norway.

Kværna, T., E. Hicks, J. Schweitzer & F. Ringdal (2003): Regional seismic Threshold Monitoring. Proc. 25th Seismic Research Review in Nuclear Explosions Monitoring, Tucson, Sep 2003.

Ringdal, F. (Ed.): Semiannual Technical Summary, 1 January - 30 June 2003, NORSAR Sci. Rep. 2-2003, Kjeller, Norway.

Ringdal, F. & T. Kværna (2004): Some aspects of regional array processing at NORSAR, **In**: NORSAR Sci. Rep. 1-2004, 1 July - 31 December 2003, Kjeller, Norway.

Ringdal, F., T. Kværna, E.O. Kremenetskaya, V. Asming, S. Mykkeltveit, S. Gibbons & J. Schweitzer (2003): Research in regional seismic monitoring. Proc. 25th Seismic Research Review in Nuclear Explosions Monitoring, Tucson, Sep 2003.

Roth, M. & H. Bungum (2003): Waveform modeling of the August 17, 1999, Kola peninsula earthquake, Bull. Seis. Soc. Am., 93, 1559-1572.

Schissele, E. & J. Schweitzer (2004): Study of regional variations of the coda characteristics in the Barents Sea using small-aperture arrays, **In**: NORSAR Sci. Rep. 1-2004, 1 July - 31 December 2003, Kjeller, Norway.

Stange, S. & J. Schweitzer (2004): Source depths at regional distances: an example from the
Western Barents Sea / Svalbard region, **In**: NORSAR Sci. Rep. 1-2004, 1 July - 31
December 2003, Kjeller, Norway.

Stevens, J., N. Rimer, H. Xu, G. Baker, J. Murphy, B. Barker, C. Lindholm, F. Ringdal, S.
Gibbons, T. Kværna & I. Kitov (2003): Analysis and simulation of cavity-decoupled
chemical explosions, Proc. Seismic Research Review in Nuclear Explosions Monitor-
ing, Tucson, Sep 2003.

6 Summary of Technical Reports / Papers Published

6.1 Some aspects of regional array processing at NORSAR

Introduction

NORSAR has for a number of years carried out processing and analysis of seismic events in the European Arctic, using the regional array network in Fennoscandia and NW Russia. In this paper we describe some aspects and potential improvements of this processing, with emphasis on the Novaya Zemlya region.

The regional processing system at the NORSAR Data Center is illustrated in Figure 6.1.1 and comprises the following steps:

- Automatic single array processing, using a suite of bandpass filters in parallel and a beam deployment that covers both P and S type phases for the region of interest.

- An STA/LTA detector applied independently to each beam, with broadband f-k analysis for each detected phase in order to estimate azimuth and phase velocity.

- Single-array phase association for initial location of seismic events, and also for the purpose of chaining together phases belonging to the same event, so as to prepare for the subsequent multiarray processing.

- Multi-array event detection, using the Generalized Beamforming (GBF) approach (Ringdal and Kværna, 1989) to associate phases from all stations in the regional network and thereby provide automatic network locations for events in all of northern Europe. The resulting automatic event list is made available on the Internet (www.norsar.no).

- Interactive analysis of selected events, resulting in a reviewed regional seismic bulletin, which includes hypocentral information, magnitudes and selected waveform plots. This reviewed bulletin is also available on the Internet.

Recent enhancements

In previous Semiannual Technical Summaries, we have described a number of enhancements made to the regional processing at NORSAR over the years. For example, Kværna et. al. (1999) have provided an overview of such enhancements as of May 1999. Among the more recent developments after that time, we mention in particular:

- Development of an experimental site-specific GBF algorithm, with application to Lop Nor and Novaya Zemlya (Kværna et. al., 2002a,2003)

- Development of experimental site-specific threshold monitoring technique, with application to Novaya Zemlya (Kværna et. al., 2002b) and Lop Nor, (Lindholm et. al., 2002)

- Automatic optimized single-array detection and location, with application to selected mining sites in the Kola Peninsula (Gibbons et. al., 2003). This project is in an initial phase.

- Improved detector recipes and detection algoritm for the ARCES array (Schweitzer, 2003).

Experience over the past several years has demonstrated that the automated event list generated by the GBF procedure is nearly "complete", in the sense that it provides an exhaustive search

of all possible detected phase combinations that could correspond to real events. The reviewed bulletin is more selective, since our current resources do not allow a complete analysis of all real seismic events that are associated through the automatic algorithms. An important topic of current research is to develop methods to enable the analyst to easily select events from areas of particular interest, and focus on these events in the interactive analysis.

Network processing

The initial grid system for GBF processing at NORSAR is shown in Figure 6.1.2, which also includes the locations of the small-aperture arrays available to the regional processing. This fig-Figure 6.3 illustrates a finer "beampacking" grid which is used to refine the locations provided by the initial GBF grid. Currently, the five arrays ARCES, SPITS, HFS, APA and FINES are used for routine regional processing at NORSAR.

The initial grid GBF system provides a number of possible event locations. For each grid point, the detection logs of the different arrays are searched for signals matching the predicted travel time, azimuth and slowness of phases originating at the grid point. When a given number of matching phases are found, initial event hypotheses are formed. A denser grid system (the beampacking grid) is then constructed around the grid point providing the largest number of matching phases, and the data are reprocessed for a shorter time interval around the initial origin time.

The basis for the processing is the detection logs from the individual arrays. These logs can be quite extensive, with the number of phase detections ranging from several hundred to more than one thousand per day. When these detection logs are processed by the GBF algorithm, the result is a list of typically about 200 candidate events for each day. Only a small subset of these events are analyzed interactively.

Monitoring the Novaya Zemlya region

The philosophy behind the automatic process at NORSAR is to ensure, as far as possible, that no real detectable event is lost. The penalty is that a number of false associations are generated. This problem is most significant for regions at large distances from the arrays, such as the Novaya Zemlya region. We describe below some initial steps undertaken to eliminate many of these false associations.

It is well known that the most sensitive arrays for seismic events in the Novaya Zemlya region are ARCES and SPITS. Our initial step to reduce the number of false associations is therefore to require detection by one or both of these two arrays, using a combination of the following criteria:

1.   Pn and Sn detections by SPITS

2.   Pn and Sn detections by ARCES

3.   Pn detections by both SPITS and ARCES

In addition, we have experimented with additional constraints on Pn phase velocities for the two arrays, in order to eliminate obvious teleseismic or near-regional phases. Reasonable constraints,based on observational evidence, are:

- For ARCES: Pn velocity between 8-12 km/s

- For SPITS: Pn velocity between 7-10 km/s

Furthermore, we have considered the effects of constraining the acceptable difference in estimated azimuth for the P and S phase, by removing single-station events that have an azimuth difference (P-S) exceeding 15 degrees.

Table 6.1.1 gives an overview of the number of GBF event candidates located in the region surrounding Novaya Zemlya for the years 2002 and 2003. The geographical limits are 70-78 degrees North, 50-70 degrees East. The counts using the current on-line GBF algorithm as well as the counts requiring detection by ARCES and SPITS, and counts imposing additional constraints are given.

The criteria specified in the table are conservative in the sense that they should not eliminate any potential real seismic events occurring in this region. Nevertheless, we see from the table that the number of event candidates is reduced by about 90 per cent when applying the final (strongest) test.

We note that the significant reduction in false detections when imposing the azimuth constraint is due to a too wide azimuth window currently applied in the GBF processing. The GBF algorithm allows phases to be associated with the same event if they deviate less than 30 degrees from the grid point toward which the generalized beam is steered. This implies that P and S phases associated to a given event could (in extreme cases) differ by up to 60 degrees, which is clearly excessive. There is therefore a good argument for adding a more restrictive azimuth test in the second step of the on-line GBF process.

Examples of recent low-magnitude events

Table 6.1.2 lists small events in the Novaya Zemlya region, located outside the test site and detected over the years by the NORSAR regional processing. Recordings of the two most recent events are illustrated in Figures 6.1.4 through 6.1.6. The first two figures show a magnitude 3.0 event on 23 February 2002, as recorded by SPITS and ARCES respectively. In each figure, two filtered (4-8 Hz) array beams are displayed, corresponding to Pn and Sn velocities and directed towards the epicenter. Both arrays have high SNR for the P-phase, and the S-phase is clearly detected, with a particularly good SNR on the S-beams. A typical feature (also seen for other events) is that ARCES has a much stronger S-phase than SPITS. In fact, detection of S-phases using the SPITS array is often problematic, and improvements here is a topic of current research. With the planned refurbishment of SPITS, several 3-component sites will be included in the array, and this should improve the detection potential for S-phases in the future.

The second event (magnitude 2.5) occurred on 8 October 2003, and Figure 6.1.6 shows the SPITS Pn and Sn beams for this event. The waveforms have similar characteristics to those observed for the 23 February 2002 event. This event illustrates the importance of including in the detection criteria single-station detections (P and S phases detected at the same array) as well as events detected at both arrays. In fact, there was no automatic detection of this event at ARCES. However, by inspecting the ARCES waveforms visually, P and S onsets could be found, and were included in the reviewed event location (Table 6.1.2).

Discussion

Although the criteria listed above succeed in reducing the number of false associations significantly, there is still room for considerable improvement. A promising approach is to use fixed-frequency filter bands for the broad-band f-k estimation, as initially suggested by Kværna and Ringdal (1986). In this way, one can hope to obtain more stable azimuth estimates, thereby enabling a much lower tolerance than 15 degrees for the difference in P and S azimuths. We will continue our work on reducing the false alarm rate in the automatic GBF lists, while retaining as many as possible of the real seismic events. Furthermore, the automatic detector algorithms could be further improved, and work towards this end is continuing.

This analysis has reconfirmed our previous estimates of the detection capability of the regional network in northern Europe, indicating that the network is capable of detecting seismic events at Novaya Zemlya down to about magnitude 2.5 (Ringdal, 1997). Our preliminary results on reducing the number of false associations in the GBF process are promising, but a more systematic post-processing algorithm to address this problem needs to be developed.

As an initial step, we have implemented a script to apply the criteria discussed in this paper to the GBF on-line output, so as to produce an abbreviated list of event candidates to be analyzed interactively at NORSAR. This should ensure that future small seismic events in the Novaya Zemlya region will be included in the reviewed regional bulletin, while involving only a modest additional analyst effort.

F. Ringdal
T. Kværna

References

Gibbons, S., T. Kværna and F. Ringdal (2003): Single array analysis and processing of events from the Kovdor mine, Kola, NW Russia. *Semiannual Technical Summary 1 July - 31 December 2002*, NORSAR Sci. Rep. 1-2003, Kjeller, Norway.

Kværna, T. and F. Ringdal (1986): Stability of various f-k estimation techniques. *Semiannual Technical Summary 1 April - 30 September 1986*, NORSAR Sci. Rep. 1-86/87, Kjeller, Norway.

Kværna, T., J. Schweitzer, L. Taylor and F. Ringdal (1999): Monitoring of the European Arctic using Regional Generalized Beamforming. *Semiannual Technical Summary 1 October 1998 - 31 March 1999*, NORSAR Sci. Rep. 2-98/99, Kjeller, Norway.

Kværna, T., E. Hicks and F. Ringdal (2002a): Site-Specific Generalized Beamforming (SSGBF) applied to the Lop Nor test site. *Semiannual Technical Summary 1 January - 30 June 2002*, NORSAR Sci. Rep. 2-2002, Kjeller, Norway.

Kværna, T., F. Ringdal, J. Schweitzer, and L. Taylor (2002b): Optimized Seismic Threshold Monitoring – Part 1: Regional Processing. *Pure Appl. Geophys.*, 159, 969-987.

Kværna, T., E. Hicks and F. Ringdal (2003): Site-Specific GBF monitoring of the Novaya Zemlya test site. *Semiannual Technical Summary 1 July - 31 December 2002*, NOR-SAR Sci. Rep. 1-2003, Kjeller, Norway.

Lindholm, C., T. Kværna and J. Schweitzer (2002): Site-Specific Threshold Monitoring (SSTM) applied to the Lop Nor test site, *Semiannual Technical Summary, 1 July 2001 - 31 December 2001*, NORSAR Sci. Rep. 1-2002, Norway.

Marshall, P.D., R.C. Stewart and R.C. Lilwall (1989): The seismic disturbance on 1986 August 1 near Novaya Zemlya: a source of concern? *Geophys. J.*, 98, 565-573.

Ringdal, F., 1997. Study of low-magnitude seismic events near the Novaya Zemlya nuclear test site. *Bull. Seism. Soc. Am.*, **87**, 1563-1575

Ringdal, F. and T. Kværna (1989). A multichannel processing approach to real time network detection, phase association and threshold monitoring, *Bull. Seism. Soc. Am.*, **79**, 1927-1940.

Schweitzer, J. (2003): Upgrading the ARCES (PS 28) on-line data processing system. *Semiannual Technical Summary 1 July - 31 December 2002*, NORSAR Sci. Rep. 1-2003, Kjeller, Norway.

Table 6.1.1 GBF event candidates 70-78 deg N, 50-70 deg E

Detection criterion	ARCES Pn velocity	SPITS Pn velocity	Az. diff.	SNR Pn (1 station)	Total 2002	Total 2003	Sum
All GBF	All	All	All	All	683	950	1733
1 or 2 or 3	All	All	All	All	294	382	676
1 or 2 or 3	8-12 km/s	7-10 km/s	All	All	177	211	388
1 or 2 or 3	8-12 km/s	7-10 km/s	<15 deg	All	66	81	147

Table 6.1.2: List of seismic events in or near Novaya Zemlya (1980-2003) located outside the test site

Date/time	Location	m_b	Comment
01.08.86/ 13.56.38	72.945 N, 56.549 E	4.3	Located by Marshall et.al. (1989)
31.12.92/ 09.29.24	73.600 N 55.200 E	2.7	Located by NORSAR
23.02.95/ 21.50.00	71.856 N, 55.685 E	2.5	Located by NORSAR
13.06.95/ 19.22.38	75.170 N, 56.740 E	3.5	Located by NORSAR
13.01.96/ 17.17.23	75.240 N, 56.660 E	2.4	Approximately co-located with preceding event
16.08.97/ 02.11.00	72.510 N, 57.550 E	3.5	Located by NORSAR
16.08.97/ 06.19.10	72.510 N, 57.550 E	2.6	Co-located with preceding event
23.02.02/ 01.21.14	74.047 N, 57.671 E	3.0	Located by NORSAR
08.10.03/ 23.07.10	75.645N, 63.345E	2.5	Located by NORSAR

Overview - NORSAR Regional Processing
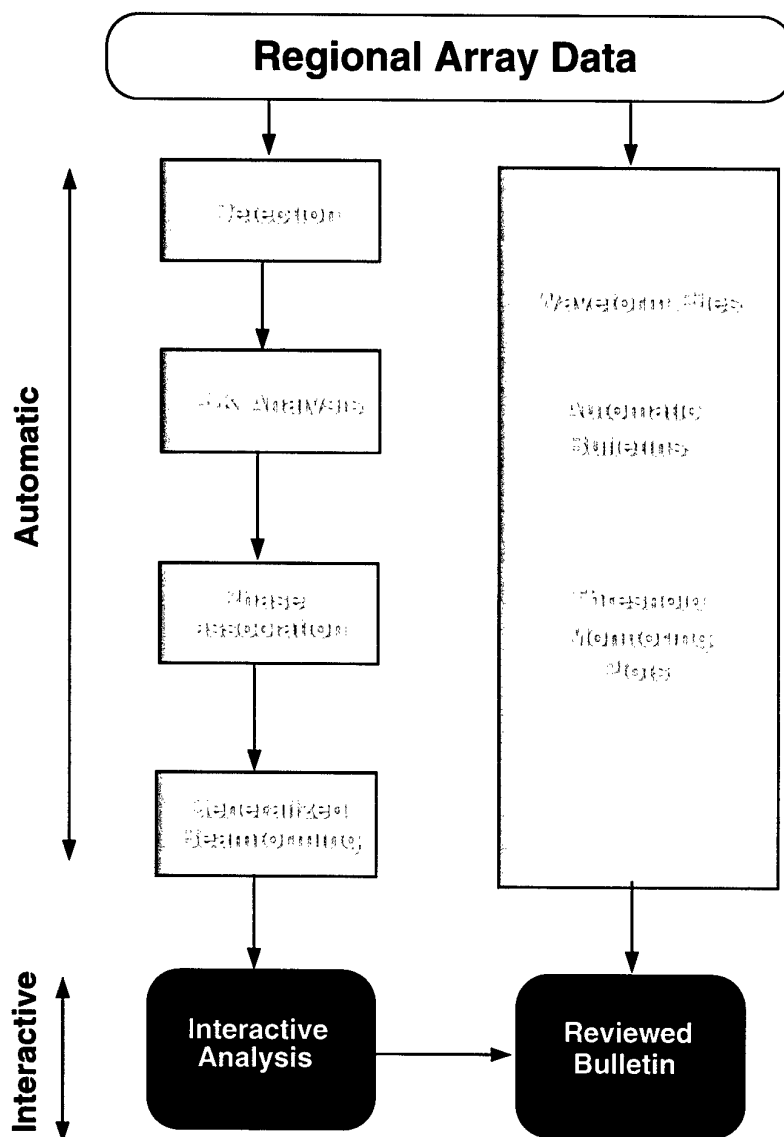
Fig. 6.1.1. *Overview of the regional processing at NORSAR.*
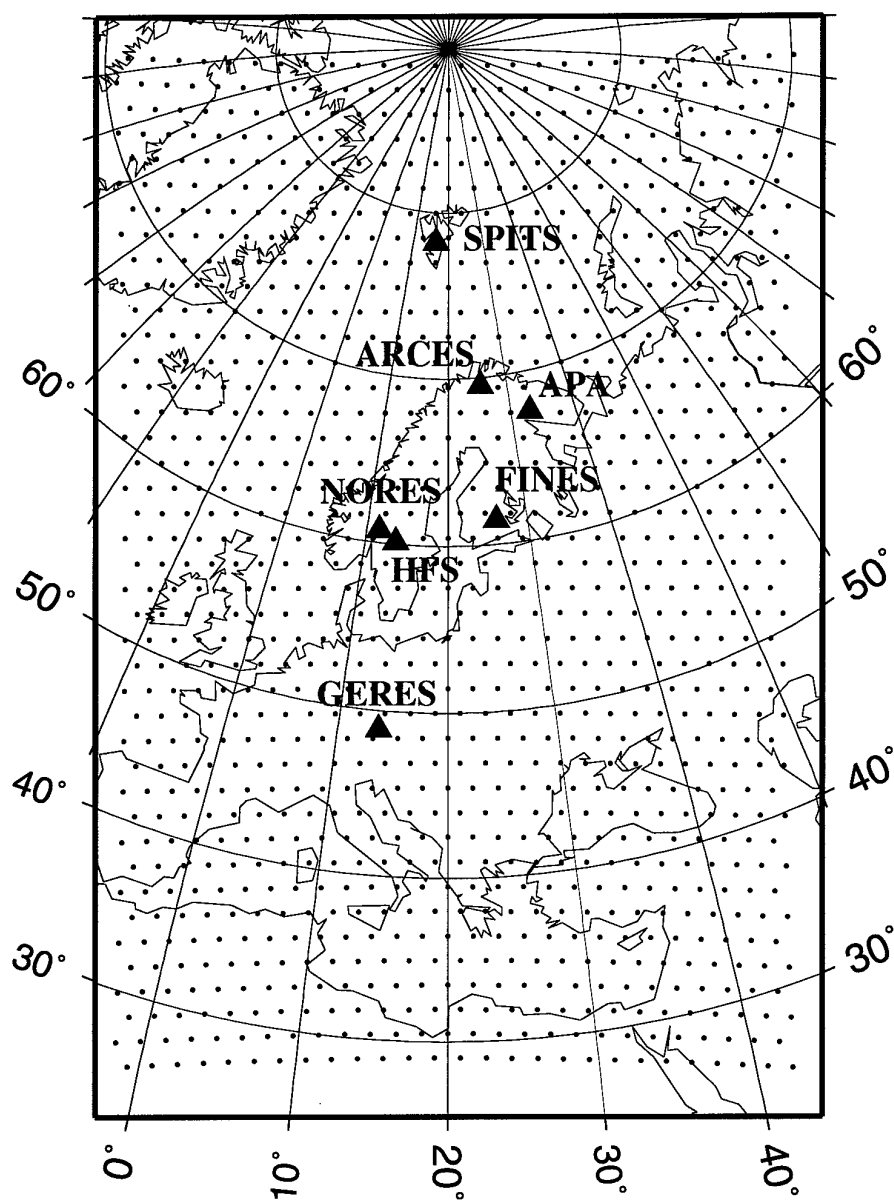
Fig. 6.1.2. *This map shows the array stations in the regional network and the initial grid system used by the GBF. Currently, the stations SPITS, ARCES, APA, FINES and HFS are used in the routine NORSAR regional processing. The distance between the grid nodes is 1.5 degrees.*
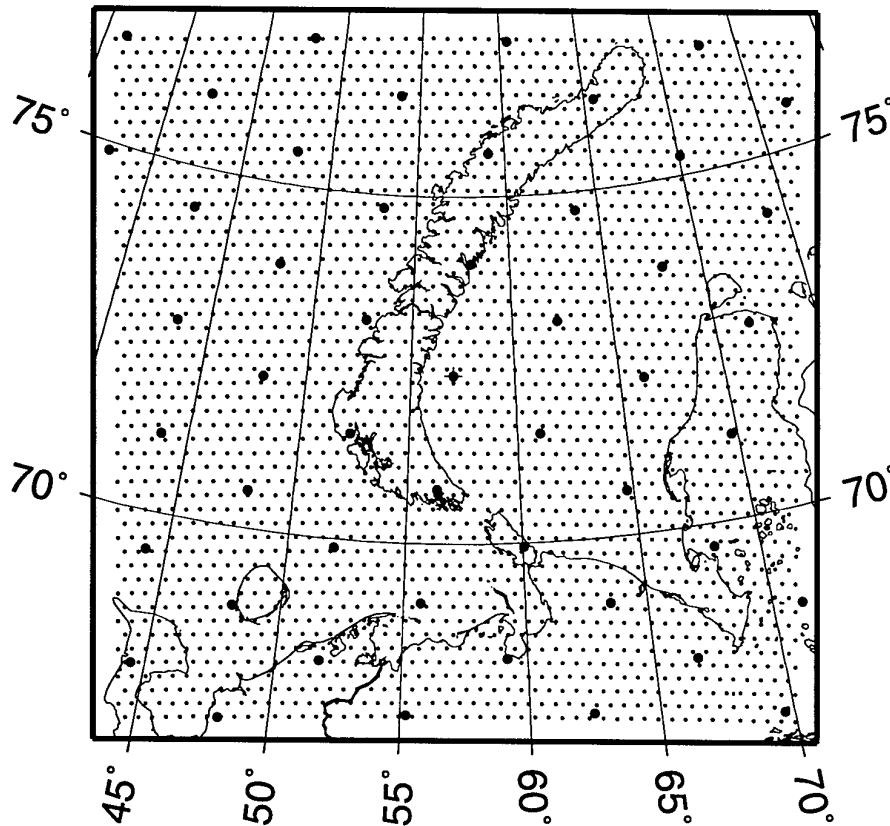
Fig. 6.1.3. *Example of a map of the "beampacking" grid system used by the NORSAR GBF, in this case constructed around an initial event location in the Kara Sea. This dense grid is used to refine locations provided by the initial grid (shown here as large dots). The distance between the grid nodes is 0.2 degrees.*

Novaya Zemlya 23 February 2002 - Spitsbergen array
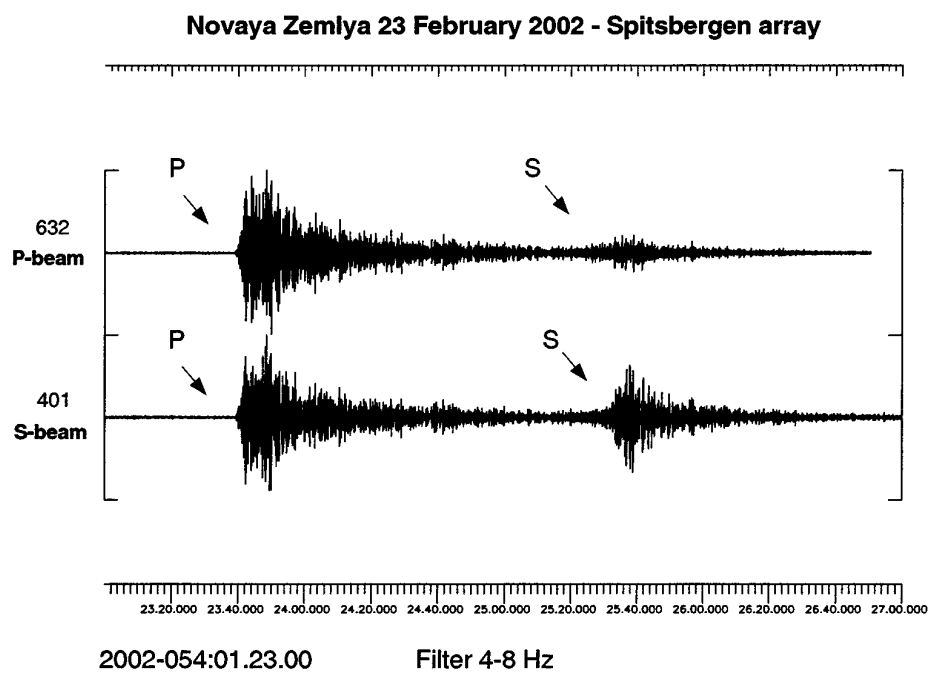
Fig. *6.1.4.* Spitsbergen P and S beams for the Novaya Zemlya event on 23 February 2002

Novaya Zemlya 23 February 2002 - ARCES array
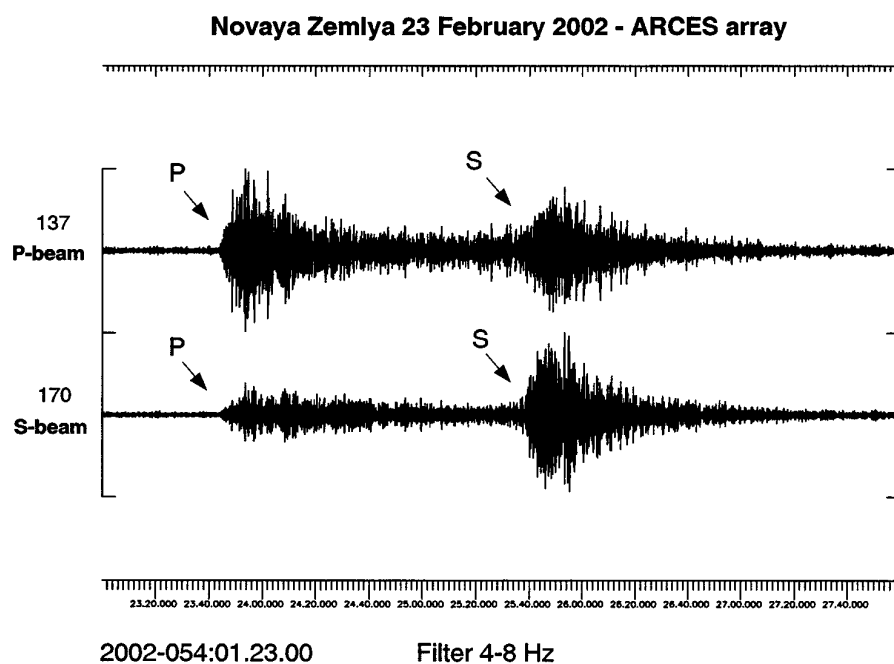
Fig. *6.1.5.ARCES* P and S beams for the Novaya Zemlya event on 23 February 2002

Novaya Zemlya 8 October 2003 - Spitsbergen array

2003-281:23.09.10   Filter 4-8 Hz
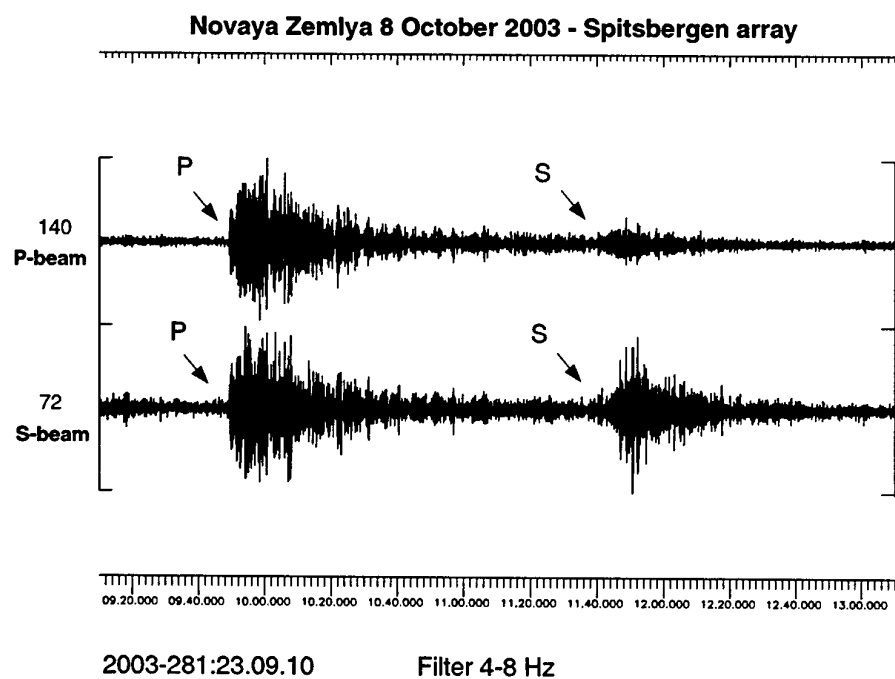
Fig. 6.1.6. Spitsbergen P and S beams for the Novaya Zemlya event on 8 October 2003

6.2   Source depths at regional distances: an example from the Western Barents Sea / Svalbard Region

6.2.1   Introduction

On 4 July 2003 at 07:16 an earthquake with a magnitude of mb 5.7 and Ms 5.1 (NEIC) occurred in the Flinn-Engdahl-Region Western Barents Sea, close to Hopen Island (see Figs. 6.2.1 and 6.2.2), which belongs to the Svalbard Archipelago (Norway). The analyst reviewed onset readings and an estimated hypocenter (event number 5487) are published on the web-page of the Norwegian National Data Center at NORSAR. An inspection of seismograms recorded at the stations and arrays (Fig. 6.2.1) collected at NORSAR revealed indications for a hypocenter within the crust, for instance due to the clear development of Lg waves.

The depth of the Mohorovicic discontinuity (Moho) in the Svalbard platform area is about 32 km (Faleide, 2000). Moho depths at the recording sites in Fennoscandia reach down below 40 km or even below 50 km beneath Finland. The 1D velocity model for routine analysis at NOR-SAR has a Moho depth of 41 km. The source depth of the event under consideration was deter-mined to 45 km by the routine location procedure, hence, below the Moho.

The aim of this study was to relocate the event using classical and non-linear/probabilistic loca-tion procedures and to determine the reliability of the source depth determination. Because of the more principal character of this study the analyst reviewed onset parameters were used unchanged and no extra data were collected from additional stations, which may also have observed this event.

6.2.2   Classical location procedure

The results of the routine processing at NORSAR can be found in the bulletin of the Norwegian National Data Center (http://www.norsar.no/NDC/bulletins/regional/2003/07/5487.html). Seis-mogram records range from the Spitsbergen array at a distance of around 270 km to the Hag-fors array at a distance of more than 1800 km. Located at 76.25° N and 22.75° E the epicenter uncertainty was given as an error ellipse with a major half axis of 50 km (strike 70°) and a minor half axis of 12 km (see the blue solution in Fig. 6.2.2). A hypocentral depth error is not given by the routine analysis programme package. The solution given in the bulletin of the NEIC (weekly listings) moves the event 19 km to the north-east to an epicenter at 76.37° N and 23.28° E with a fixed depth of 10 km.

A relocation of the event was performed with the linearized inversion program HYPOSAT (Schweitzer, 2001), introducing a-priori time errors for P-picks of 1 s and for S-picks of 1.7 s. As shown by Hicks *et al.* (2004), the velocity model BAREY (Schweitzer & Kennett, 2002) is more appropriate for locating seismic events in the Barents Sea than the Fennoscandia model used in the routine analysi. Therefore, this model was used throughout this study to relocate the event. The resulting error ellipse (90-percent confidence level) was nearly circular with half axes of 12 km (strike 31°) and 11 km, respectively (see the green solution in Fig. 6.2.2). Com-pared to the routine location the epicenter shifted towards North East and the new estimated source depth was calculated to 33 ±13 km.

6.2.3 Event location with the neighbourhood algorithm (NA)

The neighbourhood algorithm (Sambridge, 1999a; b) was applied for the inversion and confidence estimate of the location procedure. Localization with NA has already been implemented for instance by Sambridge & Kennett (2001) and the good convergence has been shown. The basic idea is a clever search of the parameter space invoking Voronoi cells and some measure of misfit, for instance X^2 (Chi squared, *e.g.*, Press *et al.*, 1986). This places the NA in a non-linear context comparable to genetic algorithms, simulated annealing and others. An important feature of the NA-sampler is its agility and the possibility to steer the convergence towards a misfit minimum by controlling the balance between exploration and exploitation of the parameter space. If convergence is achieved the solution of the non-linear location search is found as hypocenter coordinates (see also Schweitzer & Kennett, 2002).

In a second step, the sampling of the parameter space is used to compute a Bayesian estimate of the posterior probability-density distribution (PPD) of the location result (Sambridge, 1999b). In the case described here, the parameter space has three dimensions: latitude, longitude and depth of the hypocenter. The source time was found to converge to a stable value in the sampling process when the mean time residual of all phase readings was forced to vanish. Hence, the source time was not introduced as a free parameter of its own.

The initially sampled subregion of the parameter space, ranged 100 km in each coordinate direction. The convergence of the iteration process to a solution was very fast and reached the hypocenter marked in red in Figs. 6.2.2 and 6.2.3.

To illustrate and evaluate the complete (3-dimensional) PPD, 2D-marginals were computed (Sambridge, 1999b). These marginals are projections of the PPD onto two dimensions, for instance longitude-latitude or latitude-depth, from which confidence levels can be calculated. In Fig. 6.2.2 the contour of the 90-percent confidence level of the longitude-latitude marginal is directly comparable to the 90-percent error ellipses of the classical location procedures. Finally, the maximum of the 2D-marginal - that is the region of highest probability - can be compared to the result of the non-linear search. With only three free parameters the discrepancy of the epicenter in the presented example was found to be very small (Fig. 6.2.2). Other than the HYPOSAT result, the 90-percent confidence region shows an elongation similar to that of the routine error ellipse without reaching its size. Explanations for these discrepancies remain yet speculative.

Schweitzer & Kennett (2002) compared the classical and the NA location procedure in case of an event in the Kara Sea and found a satisfying consistency of the epicenters. On the other hand, the strong influence of applying the "right" Earth model became evident.

Another probabilistic approach (Lomax & Curtis, 2001) was utilized by Husen *et al.* (2003) to evaluate structure and hypocenters in Switzerland.

6.2.4 Source depth estimates

Fig. 6.2.3 comprises the available source depth estimates for the event in a vertical section with view from the East (latitude versus depth). The routine analysis depth of 45 km is depicted as a blue dot, the HYPOSAT determination is shown in green at 33 km with its 13 km-error bar, and the NA estimated depth is shown as a red dot. The 2D-marginal from the NA-procedure is shaded in gray with the 90-percent confidence contour depicted. The 90-percent region reaches from 20 to 60 km depth. Below the Moho the probability density broadens in latitude. The

probability for the hypocenter to be situated above or below the Moho is nearly even. In classical terms an uncertainty of more than 20 km should be assigned to the source depth.

At smaller epicentral distances as well as for teleseismic events additional information can be used to improve source depth estimates. Reflections from the Moho (PmP, SmS) or depth phases (pP, sP) provide useful constraints. Unfortunately, at regional distances, only full waveform inversion could improve the generally poor depth resolution, but only if the velocity model is really well known. Here we can only use the appearance of strong Lg waves as indication for a crustal event, which will make both hypocenter estimates (NA and HYPOSAT) more similar.

6.2.5　Earth model variations

The NA was used to evaluate the influence of our deficient knowledge of the Earth – that is the uncertainties in the velocity structure – on the error estimation of hypocenter determinations. The principles of the NA are not effected by the degrees of freedom, although the sampling and integration have to be performed in a higher-dimensional parameter space. Of course, it does not make sense to allow for model variations in regions where there is no resolution (*e.g.*, no ray-path coverage). This might only lead to instability when evaluating the Bayesian estimate of the PPD.

For the example studied here deviations of ±5 percent for P and S wave velocities in the crust were permitted for start model BAREY. Layer depths and mantle velocities were kept constant. Even with these relative moderate deviations, the resulting confidence region turned out to be huge (Fig. 6.2.4). The 90-percent contour of the latitude-depth marginal now comprises nearly the entire sampled parameter space-subregion ($100 \times 100 \text{ km}^2$). Essentially, the specification of a source depth became nearly meaningless. The only statement could read: probably not deeper than 100 km.

6.2.6　Conclusion

Classical event location procedures using travel times mainly underestimate the uncertainty of source-depth determinations, in particular, in such cases for which the azimuthal coverage of observations is very uneven or nearby observations are missing. More realistic error estimates are yielded by using techniques like the Bootstrap or Monte Carlo search. A complete picture can only be derived from a thoroughly computed PPD. For the presented example the confidence regions are at most in the same order of magnitude as the classical error bars or ellipses.

But, one of the most important unknowns for locating earthquakes is the velocity structure. Incorporating only a 5-percent uncertainty of the crustal velocities led to nearly meaningless source depth estimates. The 90-percent confidence region extends over more than a hundred kilometers in depth, which can only be restricted with further seismological evidence like the occurrence of Lg or Rg. However, it has to be concluded that this result throws a rather negative light on studies which use source depths from catalogues. Improvements are conceivable with good station coverage at short distances and an excellent knowledge of the velocity distribution within the Earth.

Acknowledgements

Stefan Stange, Landeserdbebendienst Baden-Württemberg, Freiburg, Germany

Johannes Schweitzer

References

Faleide, J. I. (2000). Crustal structure of the Barents Sea – important constraints for regional seismic velocity and travel-time models. NORSAR Sci. Rep. **2-1999/2000**, 119-129.

Hicks, E. C., T. Kværna, S. Mykkeltveit, J. Schweitzer & F. Ringdal (2004). Travel-times and attenuation relations for regional phases in the Barents Sea region. Pure appl. Geophys. **161**, 1-19.

Husen, St., E. Kissling, N. Deichmann, St. Wiemer, D. Girardini & M. Baer (2003). Probabilistic earthquake location in complex three-dimensional velocity models: Application to Switzerland. J. Geophys. Res. **108(B2)**, 5, 1-20.

Lomax, A. & A. Curtis (2001). Fast, probabilistic earthquake location in 3D models using Oct-Tree Importance sampling. Geophys. Res. Abstr. **3**, 2001.

Press, W. H., B. P. Flannery, S. A. Teukolsky & W. T. Vetterling (1986). *Numerical Recipes*, Cambridge University Press, New York, 993 pp.

Sambridge, M. S. (1999a). Geophysical inversion with a neighbourhood algorithm – I. Searching the parameter space. Geophys. J. Int. **138**, 479-494.

Sambridge, M. S. (1999b). Geophysical inversion with a neighbourhood algorithm – II. Appraising the ensemble. Geophys. J. Int. **138**, 727-746.

Sambridge, M. S. & B. L. N. Kennett (2001). Seismic Event Location: Nonlinear Inversion Using a Neighbourhood Algorithm. Pure appl. Geophys. **158**, 241-257.

Schweitzer, J. (2001). HYPOSAT – An enhanced routine to locate seismic events. Pure appl. Geophys. **158**, 227-289.

Schweitzer, J. & B. L. N. Kennett (2002). Comparison of location procedures – The Kara Sea event of 16 August 1997. NORSAR Sci. Rep. **1-2002**, 97-114.

Wessel, P. & W. H. F. Smith (1991). Free software helps map and display data. EOS Trans. Amer. Geophys. U. **72(41)**, 441, 445-446.
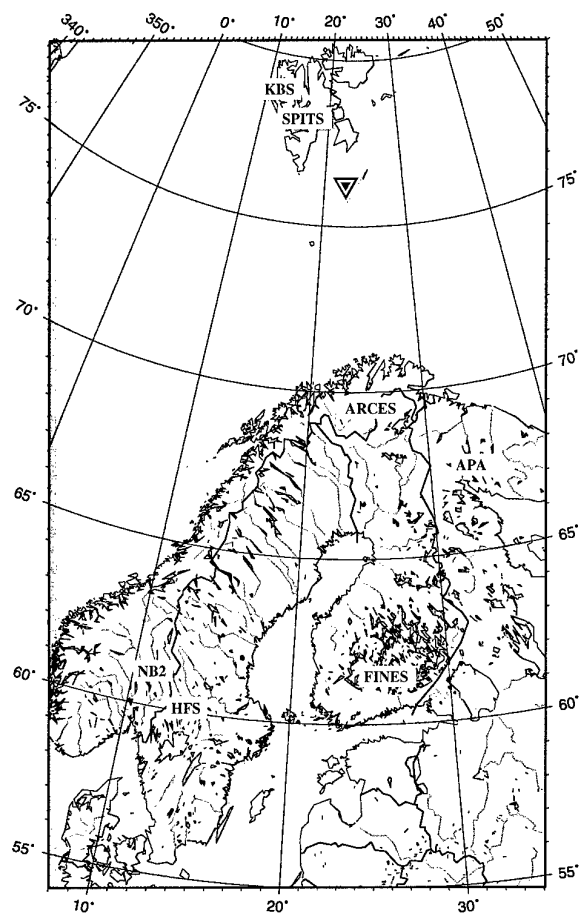
Fig. 6.2.1. *Map of the 4 July 2003 event (inverted triangle) with recording arrays and stations.*
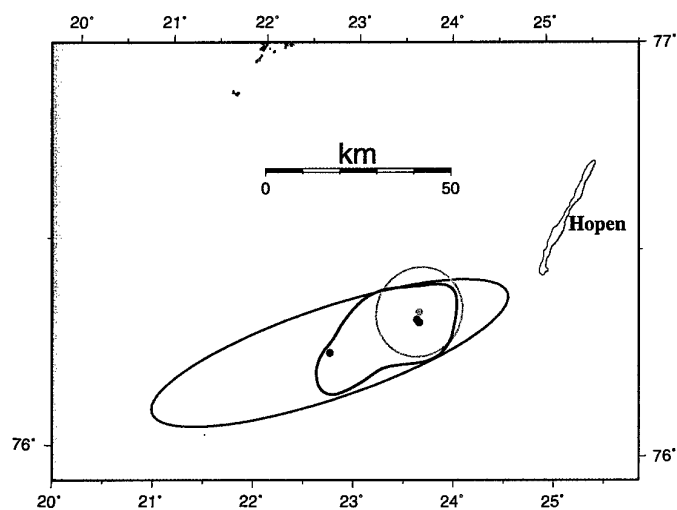
Fig. 6.2.2. *Epicenter map of the routine location (blue with error ellipse), the HYPOSAT location (green with error ellipse) and the NA location (red and black with 90-percent confidence region).*
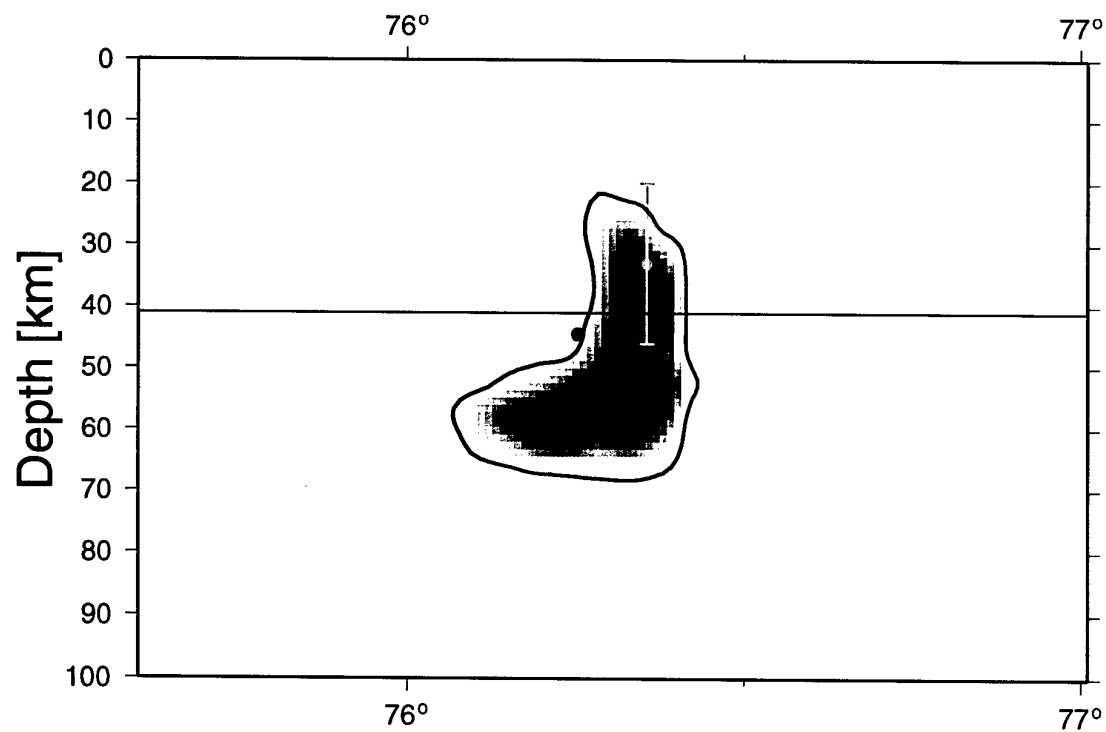
Fig. 6.2.3. *Latitude-depth section of the PPD-marginal (gray shading) and the 90-percent confidence contour. Green: HYPOSAT location with error bar. Blue: routine location. Red: NA location. The horizontal line indicates the Moho.*
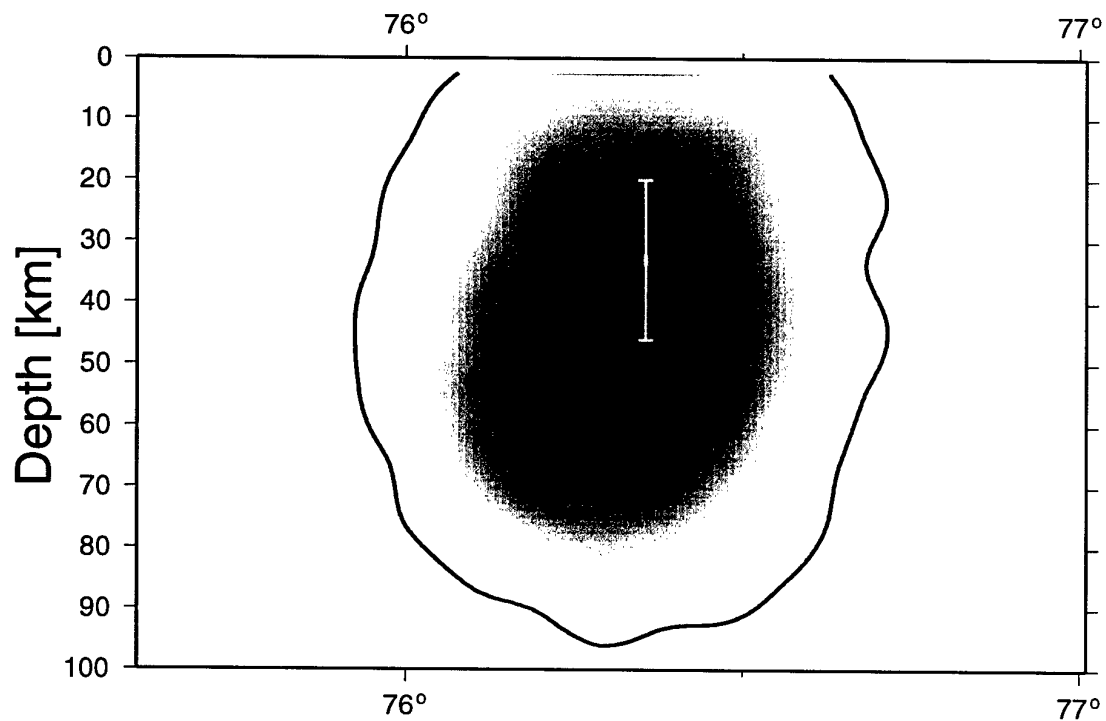
Fig. 6.2.4. *Same as Fig. 6.2.3 for the PPD-marginal computed including velocity model-variations.*

6.3   Locating seismic events near the Spitsbergen archipelago

Introduction

The work described in this paper is a part of KRSC - NORSAR cooperative activity aimed at a detailed study of seismicity in the Spitsbergen region. Part of the motivation for the study is to improve the quality and availability of well-located reference events ("ground truth data") for location calibration purposes, and to improve automatic and interactive event location accuracy.

Spitsbergen and the adjacent areas are parts of a geologically complex region with moderate to high seismicity. The main seismicity in the area is associated with the North-Atlantic Ridge, and especially the Knipovich Ridge situated at a distance less than 400 km from the archipelago (Sundvor and Eldholm, 1979, Bungum et. al., 1982, Mitchell et. al., 1990). In addition, some coal mines are located in the area of Spitsbergen, causing occasional induced seismicity. In this study we describe some of our observations of unusual features of seismic events and seismic wave propagation in the area and illustrate some problems in event location by comparing various earthquake bulletins.

Seismicity of the Spitsbergen region

The local earthquake activity on Spitsbergen and in adjacent seas is significant. Larger earthquakes are reported by the Norwegian National Seismic Network, and are routinely included in international seismic bulletins. However, until recently there has not existed any systematic and detailed monitoring of the smaller seismic events that often occur in mining areas.

Studies related to the earthquake activity on Svalbard and in adjacent seas have been presented in several previous NORSAR Semiannual Technical Summaries, e.g. Asming et. al. (1998, 2002), Kremenetskaya et al. (2001b), Kværna et. al. (2003). Active earthquake zones are found on Heerland and on Nordaustlandet. In addition, there is significant earthquake activity on the Mid-Atlantic Ridge about 100-200 km west of Vest-Spitsbergen.The Western Barents Sea south of Svalbard also exhibits frequent earthquake activity, and on 4 July 2003, a m_b of 5.4 earthquake with several aftershocks occurred in this region.

A general picture of seismic activity in Spitsbergen and adjacent areas still remains unclear due to several reasons such as small number of stations registering most part of local earthquakes, unknown travel time model for the region, and complex pattern of seismic waves arrivals due to complexity of the conductive medium.

Relocating Spitsbergen earthquakes

We made an attempt to relocate manually a set of earthquakes occurred in Spitsbergen during the first half of 2003. Our goal was to clear up spatial distribution of the events to try to find some characteristic features.

We selected more than 200 events which were strong enough to be registered by at least two stations: Kings Bay (KBS) and the Spitsbergen array (SPITS). For some of them ARCES data were also used. We used the SPITS0 travel time model (Asming et. al., 2002) which is reproduced in Table 6.3.1. This is a one-dimensional model which differs from our basic BARENTS model (Kremenetskaya et. al., 2001a) by including a top layer with low velocities representing

sediments. During the data analysis we noticed several specific features of the waveforms which cause difficulties in the event location procedure. One of them is multiple arrivals of P and S waves. The situation is typical for events occurring in the North-East land and to the south and south-east of Spitsbergen.

Table 6.3.1. Velocity model SPITS0

Depth (km)	Vp (km/s)	Vs (km/s)
0-2	4.54	2.52
2-10	6.20	3.44
10-30	6.70	3.72
30-55	8.10	4.50
55-210	8.23	4.57
>210	Same as IASPEI 91	

The complexity of the geological structure and underwater topography causes difficulties in location and interpretation of seismic events. We will present some examples in the next section.

Examples of recordings

Figure 6.3.1 shows a recording by the broad-band station KBS of a relatively strong earthquake in the North-East land during 2003 (ML=2.2). Two arrivals of both P-waves (P1, P2) and S-waves (S1,S2) are seen, the amplitudes of the first arrivals are much smaller than for the second arrivals. The same situation is seen for other earthquakes in this area. In general, the first arrival of S (S1) can be found only for the strongest events. For smaller events this arrival is masked by the P-wave coda. For still weaker events even the phase P1 becomes undetectable. Thus, typical mistakes when locating such events are to make wrong association of P and S phases, e.g. P1-S2 and P2-S2 instead of P1-S1. This can lead to distance errors of typically 50 km for events from this region.

We can correct this problem if we assume that the pattern of P and S phases are consistent for all events in this particular region. For example, if two P-phases and one S-phase are detected (the most common situation), we can assume that the S-phase is S2, and infer the approximate arrival of the first S-phase. In this way, it is usually possible for the analyst to find the S1 phase and use it in the location procedure. An alternative would be to develop a set of travel time curves for the P2 and S2 phases as well as for P1 and S1, but this approach has not been attempted. In any case, picking the correct phase arrival times for such complicated recordings is difficult, and the analyst needs to take into account detailed region-specific information on the waveform characteristics in order to make the correct pick.

A second example of an earthquake in the same area is shown in Figure 6.3.2. The same pattern of P and S phases is observed (P1, P2, S1, S2), but in addition there is also evidence of a possi-

ble Lg phase. Again, the interpretation and phase picking of such traces are quite difficult even for an experienced analyst.

For earthquakes occurring in the mid-Atlantic ridge zone, multiple arrivals are likewise observed. As an example, Figure 6.3.3 shows SPITS recording of a small earthquake in this area. In this case, three phases with estimated P-type velocity are observed, followed by a single S-phase. Here it is possible to use the phase velocity measurements by the array to identify the phases, but for single (3-component) stations, the seismogram interpretation will be ambiguous. For example, the phase P3 may easily be interpreted as Sn and the S-phase could then be interpreted as Lg.

To some extent, the phase picking is simplified if a network of seismic stations at different azimuths is available. In the case of Spitsbergen, many of the larger events (magnitude 2 and above) are observed by the ARCES array, and this helps remove ambiguities in the phase picking. Nevertheless, most small earthquakes are detected only by SPITS and (in some cases) by the nearby KBS station, and the events must therefore be located without the benefit of network observations.

While array velocity estimates are helpful in phase identification, we must also note that the estimated phase velocities for events near Spitsbergen often show significant anomalies. For example, many events in the rift zone have almost identical phase velocities for P and S phases. A possible explanation could be P to S conversion near the SPITS array. For other azimuths, the P and S phase velocities are close to normal.

A location experiment

As earlier mentioned, we have relocated more than 200 earthquakes occurring during the first half of 2003 with epicenters in Spitsbergen and adjacent areas. All of these events were detected by at least two stations (usually KBS and SPITS, sometimes with addition of ARCES and other distant stations). We compared our location results with those published in the Reviewed NORSAR Regional Bulletin, which makes use of the same station network. Additionally, we compared both of these interactive location results to the automatic location provided by the on-line GBF procedure at NORSAR.

We note that the GBF procedure uses only the regional arrays in the on-line process; therefore, the KBS station is not included in the GBF processing. However, since GBF accepts epicenters with only single-array detections (P and S), all of the events in the data set (a total of 207) had GBF solutions. We would of course expect the reviewed solutions to be more accurate than the automatic solutions, especially since KBS is not included in the automatic process, but it is nevertheless instructive to compare these procedures. We also note that the NORSAR Reviewed bulletin contained 75 of the 207 events, so the database for comparing this bulletin to KRSC and GBF was more limited.

Most of the earthquakes in this database are very small, usually in the magnitude range 1.0-2.0, and sometimes below 1.0. Clearly, obtaining accurate locations of such small events using a sparse network of stations is difficult, and one can expect significant uncertainties, as will be illustrated in the following.

The results of the location experiment are summarized on the maps in Figures 6.3.4 through 6.3.6, with histograms of the location differences shown in Figure 6.3.7. Our comments to these results are summarized as follows:

Comparing reviewed location results (NORSAR vs. KRSC)

From Figure 6.3.4 we note that the two sets of analyst reviewed locations (NORSAR and KRSC) in general are quite consistent. However, we note a systematic shift in the locations of groups of events, with the KRSC locations generally being shifted in westerly directions compared to those of the NORSAR analyst. Mostly, the location differences are small (a few tens of kilometers), but for a few events the difference exceeds 100 km, and in one case it is more than 200 km. The smaller differences can be attributed, at least in part, to the different velocity models used at KRSC and NORSAR (KRSC uses the SPITS0 model, whereas NORSAR uses a general Fennoscandian model). The cases with large differences are a direct consequence of the difficulties in phase interpretations discussed earlier, and demonstrates that locations of small earthquakes in this region can be associated with significant uncertainties.

Comparing automatic and reviewed location results

Figure 6.3.5 compares the NORSAR analyst reviewed locations to those generated by the automatic GBF procedure. We note that the analyst reviewed locations are more systematically located in the known seismic areas (the mid-Atlantic ridge and some concentrated earthquake zones in the North-East Land and South of the Spitsbergen archipelago). Nevertheless, the automatic GBF locations are typically quite good for this data set, which comprises the larger events in the database.

Figure 6.3.6 compares the KRSC reviewed locations to those generated by the automatic GBF procedure. Again, we note that the reviewed locations are more systematically located in the known seismic areas, but in this case the shifts in locations relative to the automatic procedure are larger than was observed for Figure 6.3.5. Part of the reason is that this data set contains many more small events than that presented in the previous figure, and these small events are usually less accurately located by the automatic procedure (using single-array locations only). In addition, the KRSC procedure, as earlier described, attempts to resolve ambiguities in cases of multiple phase detections, and this can have a significant effect on the resulting locations.

Conclusions

The geology of the Spitsbergen archipelago and surrounding regions is complex, and results in very complex seismograms from some areas. Multiple onsets of P and S waves can strongly increase location errors. Such onsets are not uncommon for Spitsbergen earthquakes.

By studying a set of more than 200 earthquakes in this region, we have shown that analyst reviewed locations (as processed by different analysts) can have occasional large deviations, in several cases exceeding 100 km.

The automatic GBF locations produced on-line at NORSAR are usually quite consistent with the analyst reviewed solutions, but the differences in locations can be large for the smaller earthquakes, which are located using the SPITS array alone in the GBF procedure.

Future work should focus on making more systematic use of array azimuth estimates for small events, perhaps by introducing fixed-frequency f-k analysis (Kværna and Ringdal, 1986) both in the automatic and interactive procedures. With the upgrade of the SPITS array in the near future, attention should also be given to high-frequency processing of data for phase identification and velocity/azimuth estimation purposes. Furthermore, the planned installation of several three-component seismometers in the upgraded SPITS array is expected to significantly improve the automatic S-wave detection capability, thereby improving the ability to locate small seismic events in the region.

Vladimir Asming, KRSC
Elena Kremenetskaya, KRSC
Frode Ringdal

References

Asming, V., E. Kremenetskaya and F. Ringdal (1998): Monitoring seismic events in the Barents/Kara Sea region, *Semiannual Tech. Summ., 1 October 1997 - 31 March 1998,* NORSAR Sci. Rep. 2-97/98, Kjeller, Norway.

Asming, V., E. Kremenetskaya, S. Baranov and F. Ringdal (2002): Monitoring the seismicity of the Spitsbergen archipelago, *Semiannual Tech. Summ., 1 July - 31 December 2001,* NORSAR Sci. Rep. 1-2002, Kjeller, Norway.

Bungum, H, B.J. Mitchell and Y. Kristoffersen (1982): Concentrated earthquake zones in Svalbard, Tectonophysics, 82, 175-188.

Kremenetskaya, E., V. Asming and F. Ringdal (2001a): Seismic location calibration of the European Arctic. *Pure and Applied Geophysics,* 158 No. 1-2, 117-128

Kremenetskaya E., S. Baranov, Y. Filatov, V. Asming and F. Ringdal (2001b): Study of seismic activity near Brontosaurs mines (Spitsbergen). *Semiannual Tech. Summ., 1 October 2000 - 30 June 2001,* NORSAR Sci. Rep. 1-2001, Kjeller, Norway.

Kværna, T. and F. Ringdal (1986): Stability of various f-k estimation techniques. *Semiannual Technical Summary 1 April - 30 September 1986,* NORSAR Sci. Rep. 1-86/87, Kjeller, Norway.

Kværna, T., J. Schweitzer, L. Taylor and F. Ringdal (1999): Monitoring of the European Arctic using Regional Generalized Beamforming. *Semiannual Technical Summary 1 October 1998 - 31 March 1999,* NORSAR Sci. Rep. 2-98/99, Kjeller, Norway.

Kværna, T., J. Schweitzer, F. Ringdal, V Asming and E. Kremenetskaya (2003): Seismic events associated with the Brontosaurs mining accident on 7 June 2003. *Semiannual Tech. Summ., 1 January - 30 June 2003,* NORSAR Sci. Rep. 2-2003, Kjeller, Norway.

Mitchell, B.J., H. Bungum, W.W. Chan and P.B. Mitchell(1990): Seismicity and present-day tectonics of the Svalbard region. Geophys. J. Int., 102, 139-149.

Ringdal, F. and T. Kværna (1989). A multi-channel processing approach to real time network detection, phase association, and threshold monitoring. Bull. Seism. Soc. Am. **79**, No. 6, pp. 1927-1940.

Sundvor E. and O. Eldholm (1979): The western and northern margin off Svalbard. *Tectono-physics*, 59, 239-250.
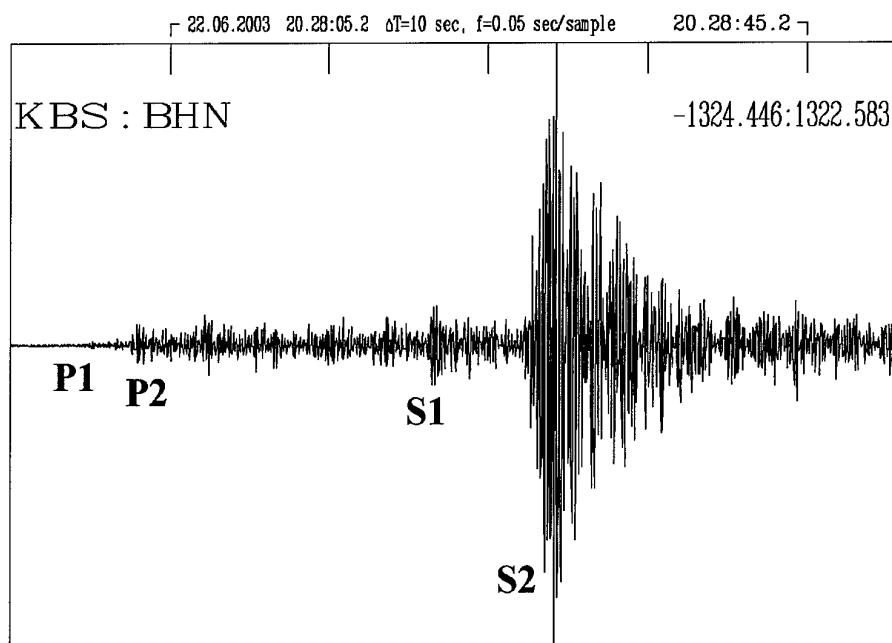
Fig. 6.3.1. KBS (broad-band N/S) recordings of earthquake in the North-East land. The trace has been high-pass filtered above 4 Hz.
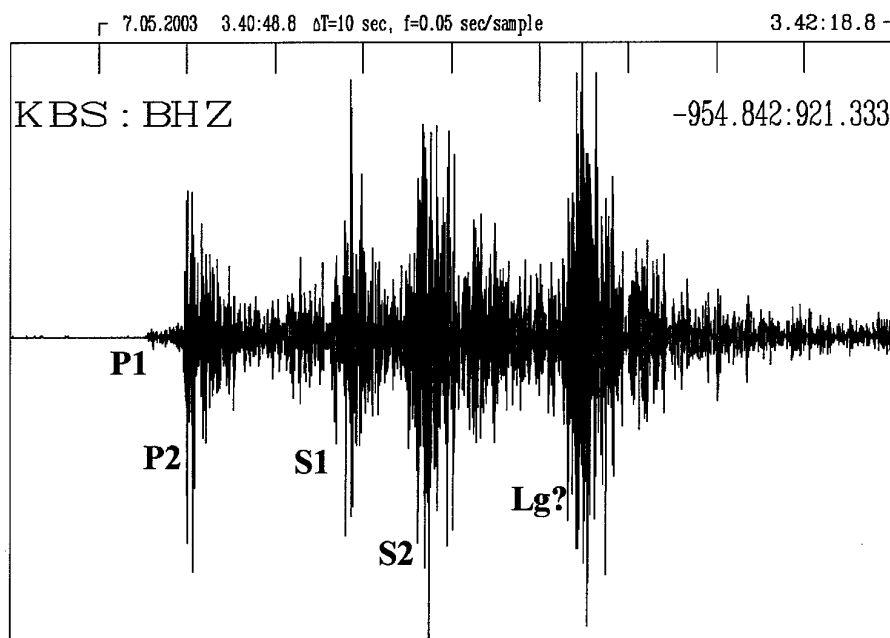
Fig. 6.3.2. KBS (broad-band vertical) recordings of earthquake in the North-East land. The trace has been high-pass filtered above 4 Hz.
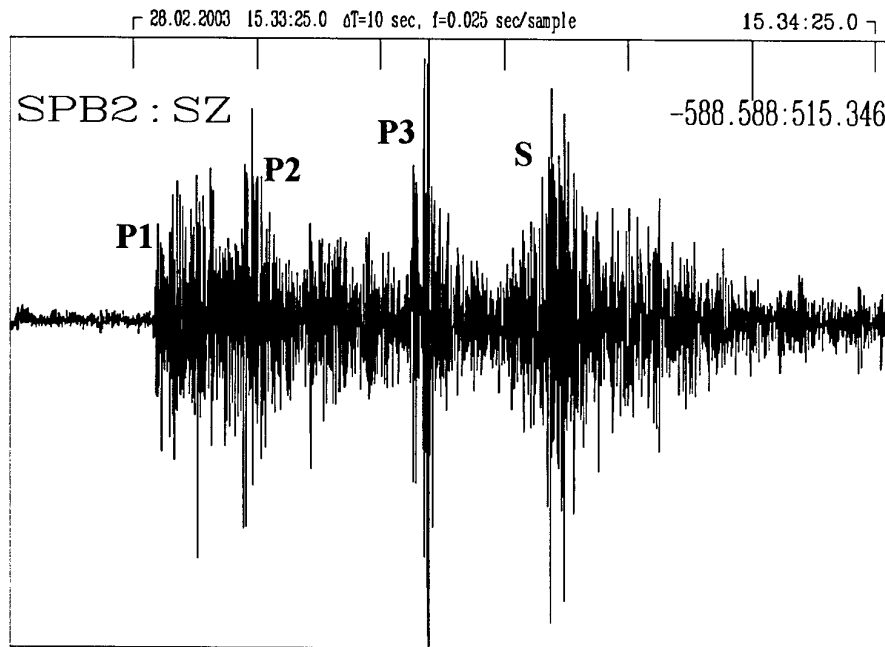
Fig. 6.3.3. *SPITS recordings of earthquake in the rift zone. At least three P-arrivals can be seen. The trace has been high-pass filtered above 4 Hz.*
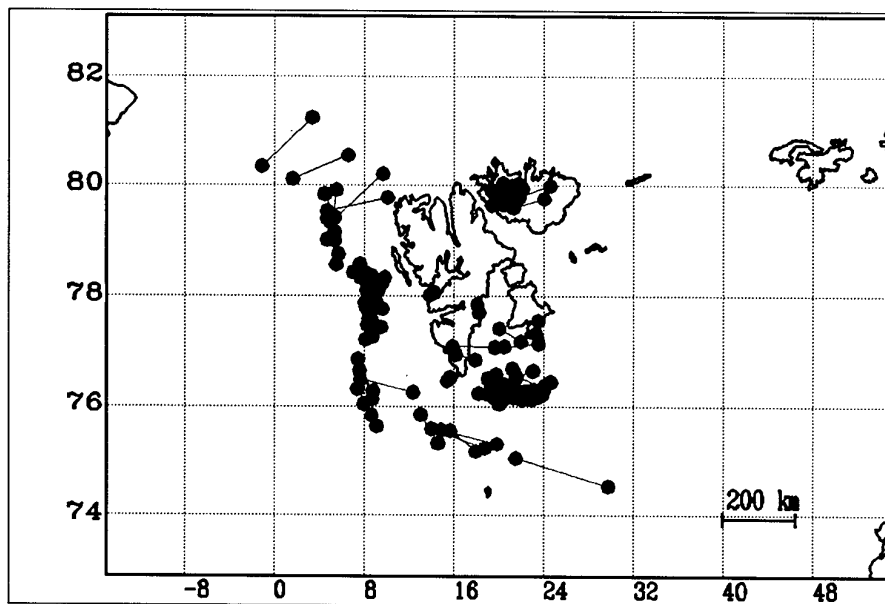
Fig. 6.3.4. *Location comparison: KRSC (red) vs. NORSAR reviewed bulletin (blue)*
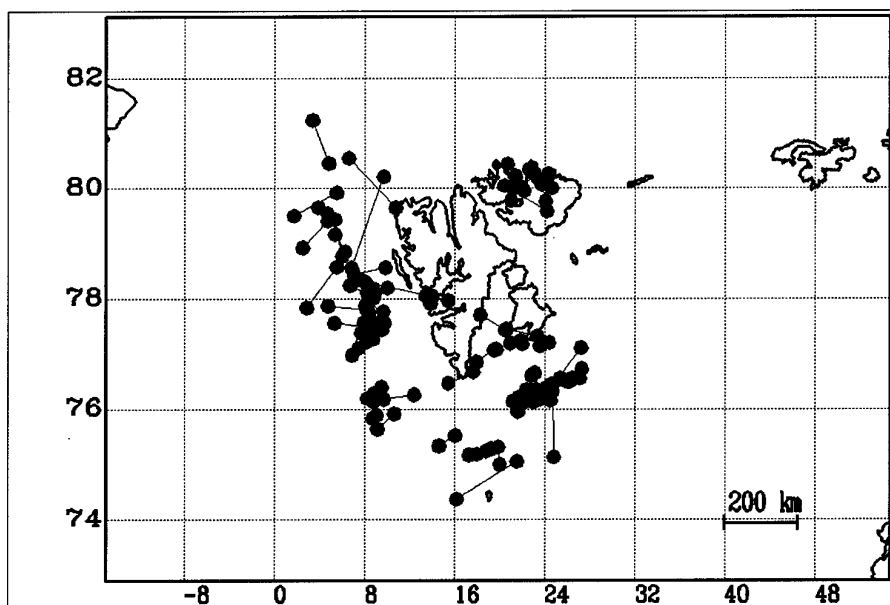
Fig. 6.3.5. *Location comparison: NORSAR automatic GBF (red) vs. NORSAR reviewed bulletin (blue)*
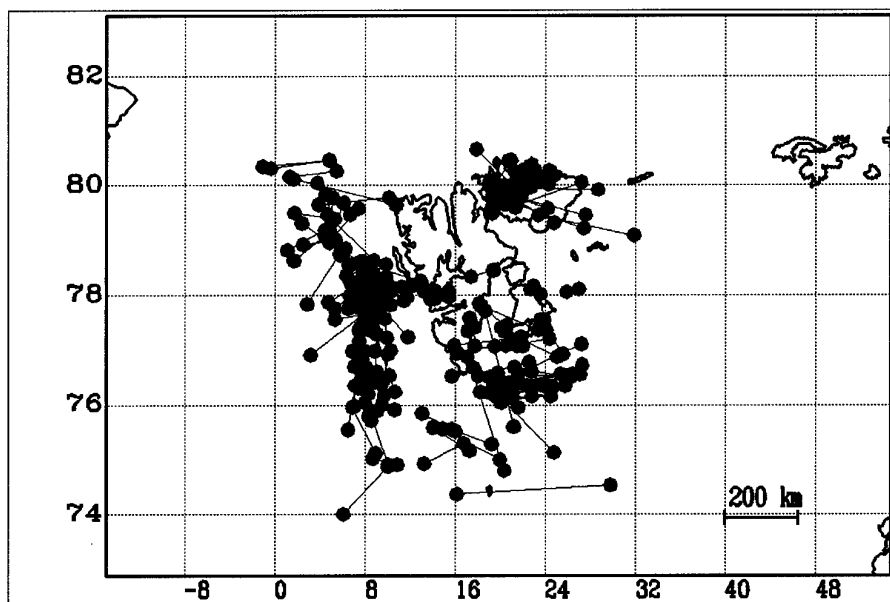
Fig. 6.3.6. *Location comparison: KRSC (red) vs. NORSAR automatic GBF (blue)*
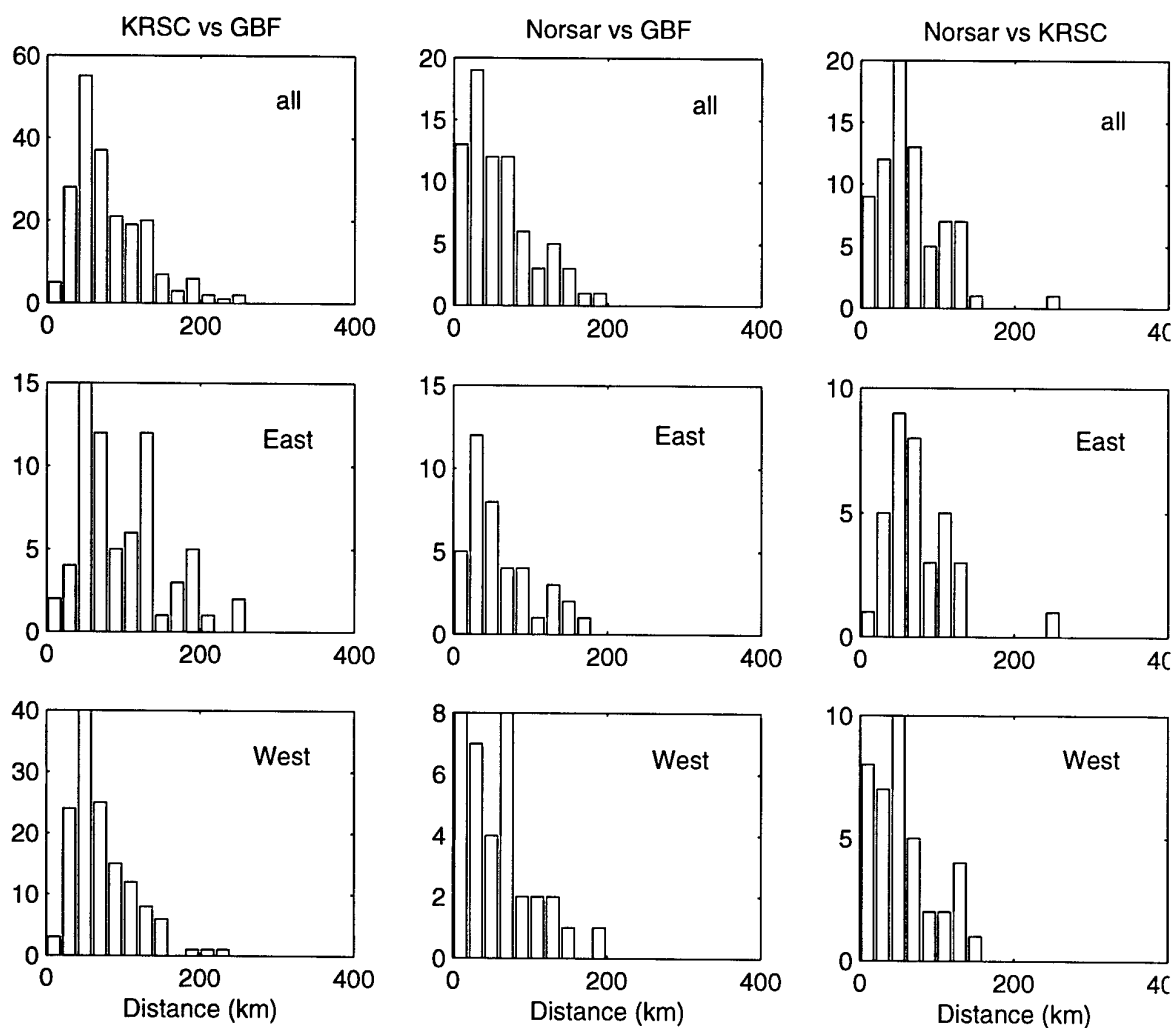
Fig. 6.3.7. *Location comparison between a) KRSC interactive location (KRSC), b) NORSAR reviewed regional bulletin (Norsar) and c) the NORSAR automatic Generalized Beamforming (GBF). The top row comprises all events, the middle row corresponds to events located by KRSC to the East of 16 degrees longitude, and the bottom row represents events to the West of this longitude.*

6.4 Ground Truth information from Khibiny mining explosions

Introduction

Through a cooperative agreement with NORSAR, Kola Regional Seismological Centre (KRSC) has for the past 10 years provided ground truth information for selected mining explosions in the Kola Peninsula. Since 2001, the project has been expanded in scope, and is currently carried out jointly with Lawrence Livermore National Laboratory, in a DOE-funded project. Under that contract, ground truth data for more than 1000 mining explosions from various mines in the Kola Peninsula (see Fig. 6.4.1) have been provided so far.

The mines in the Khibiny Massif are of particular interest in explosion source phenomenology studies. The Khibiny Massif forms a natural laboratory for examining the variations of mining explosion observations as a function of source type, since the mining explosions there are conducted in colocated underground and surface mines, with a variety of different shot geometries. In this paper we provide some examples of the type of ground truth collected, and illustrate some of the characteristic features observed from approximately colocated underground and surface explosions.

Khibiny mine explosions

Recently, seismic instrumentation has been installed inside the mines in the Khibiny Massif of the Kola Peninsula in order to provide origin times of the seismic events as well as to contribute to additional validation of the location accuracy (Ringdal et. al., 2003). These recordings supplement the ground truth information that is routinely obtained by KRSC for mining explosions in the Kola Peninsula. Our cooperative project with Lawrence Livermore National Laboratory includes the installation of additional seismometers along profiles in Norway, Finland and the Kola Peninsula, for recording over a period of at least one year. The station Ivalo (IVL) in Figure 6.4.1 is one of these temporary stations.

Some interesting results are emerging from comparing underground and surface explosions. For example, two explosions, one underground and one at the surface occurred in the neighbouring Rasvumchorr and Central mines in Khibiny on 16 November 2002. The underground explosion was a ripple-fired explosion of about 250 tons, whereas the open-pit explosion comprised four separate ripple-fired explosions, set off with about 1 second intervals, from south to north. The total charge of the four surface explosions was 430 tons.

The approximate layout of the explosions is shown in Figure 6.4.2. The surface and underground explosions were only 300 m apart, so that differences in path effects at the more distant stations can be ignored. Nevertheless, the recorded signals, e.g. at the temporary station in Ivalo, Finland at approximately 300 km distance, were remarkably different: The vertical component of these recordings is shown in Figure 6.4.3 in different filter bands. At lower frequencies (2-4 Hz), the underground explosion was stronger by a factor of 10 in amplitude, whereas above 10 Hz, the surface explosion had by far the stronger signals. A similar spectral difference between open-pit and underground explosions has been observed also in other cases.

The detailed geometry of the underground explosion is shown in Figure 6.4.4. The charges were distributed over a horizontal area approximately 100 m in diameter, and were detonated in 19 groups, with a delay of 23 ms between each group. The individual charge size of each group

is given in Table 6.4.1, where the group numbering corresponds to the numbers shown on Figure 6.4.4.

Compact explosions

A particularly interesting type of underground explosions in the Khibiny Massif is the so-called compact explosions, which typically comprise 2-3 groups of charges of about 700 kg for each group, detonated with a small delay (typically 20 ms) between each group. These explosions are intended to remove small rock masses remaining after larger explosions have been conducted. They are detonated near the end of tunnels, and sometimes several such explosions are carried out in the same tunnel. The compact explosions are the closest approximation to single, well-tamped underground explosions that are currently available in the Khibiny area.

It is interesting to compare the characteristics of such small compact explosions to the features of the large ripple-fired surface and underground shots. Figures 6.4.5 - 6.4.7 shows ARCES Pn beams for, respectively, the 257 ton underground explosion on 16 November 2002, the 430 ton surface explosion of the same day, and a 1 ton compact explosion in the Rasvumchorr mine on 20 August 2003. Using the procedure described by Kvaerna (2004), we show on each figure the ARCES Pn beam, the corresponding semblance coefficient, and the Pn beam weighted with the semblance coefficient. The frequency band used for this analysis was 4 - 8 Hz.

We note that the large underground explosion and the small compact explosion show similar features in these plots, with a clear single P-onset. In contrast, the open-pit explosion shows evidence of multiple onsets over a time interval of 3-5 seconds, corresponding to the delays in the detonations of the four explosion groups. We add, however, that even the compact explosions show significant variability when considering a number of such explosions, as documented by Harris et. al. (2003).

Video recording

The Mining Institute of the Kola Science Centre have made a video recording of the explosions on 16 November 2002. This video has been made available to us, and Figure 6.4.8 presents snapshots of the explosions. Particularly noteworthy is the formation of a "fault" or large crack in the mountainside at the same time that the underground explosion was detonated. A close-up picture of this crack is shown in one of the snapshots. Also, the video provides timing information, enabling us to verify the time delays between the four groups of surface explosions.

Such video recordings may become available for additional mining explosions, and will provide important corroborating information to the ground truth data supplied by the mining authorities.

Conclusions

The type of ground truth data already assembled for Kola Peninsula mining explosions, in addition to future more detailed information of shot configurations, is expected to contribute toward improved understanding of the nature of seismic wave generation from such sources. In particular, the compact explosions are of interest. In the ground truth data base developed until now, we have assigned each compact explosion to one of the Khibiny mines (typical diameter of one mine is 1-2 km). We will in future projects try to obtain more precise relative locations of

groups of such compact explosions, in order to study the variability of the waveform features both within groups of nearby explosions and between such groups in different tunnels.

We also plan in the future to investigate the possibilities to arrange for single, contained underground explosions in the same mines in which the compact explosions are conducted, so as to enable detailed analysis of the resulting differences in waveform characteristics between single, fully contained explosions and compact explosions.

Sergeij Kozyrev, Kola Science Center, Mining Institute
Elena Kremenetskaya, KRSC
Vladimir Asming, KRSC
Frode Ringdal
Tormod Kværna

References

Kværna, T. (2004): ARCES recordings of events from the Khibiny and Olenegorsk mines. *Semiannual Tech. Summ., 1 July - 31 December 2003*, NORSAR Sci. Rep. 1-2004, Kjeller, Norway.

Harris, D. B., F. Ringdal, E. O. Kremenetskaya, S. Mykkeltveit, J. Schweitzer, T. F. Hauk, V. E. Asming, D. W. Rock and J. P. Lewis (2003). Ground-truth Collection for Mining Explosions in Northern Fennoscandia and Russia. *"Proceedings of the 25th Seismic Research Review - Nuclear Explosion Monitoring: Building the Knowledge Base*, Los Alamos National Laboratory, *LA-UR-03-6029*, Tucson, AZ, Sept. 23-25, 2003.

Ringdal, F., T. Kværna, E. O. Kremenetskaya, V. E. Asming, S. Mykkeltveit, S. J. Gibbons and J. Schweitzer (2003). Research in Regional Seismic Monitoring. *"Proceedings of the 25th Seismic Research Review - Nuclear Explosion Monitoring: Building the Knowledge Base*, Los Alamos National Laboratory, *LA-UR-03-6029*, Tucson, AZ, Sept. 23-25, 2003.

Table 6.4.1. Distribution of charges for the underground explosion in Rasvumchorr
    mine, Khibiny on 16 November 2002. A total of 19 groups of charges were fired,
    with a delay of 23 ms between each group. The geometry of the shot is shown in
    Figure 6.4.4.

Delay #	Charge (kg)	Delay #	Charge (kg)
0	21,934	10	17,746
1	161	11	14,063
2	17,707	12	17,553
3	856	13	15,259
4	14,890	14	19,690
5	1,592	15	19,228
6	14,611	16	21,449
7	10,812	17	10,737
8	16,072	18	8,011
9	11,119		
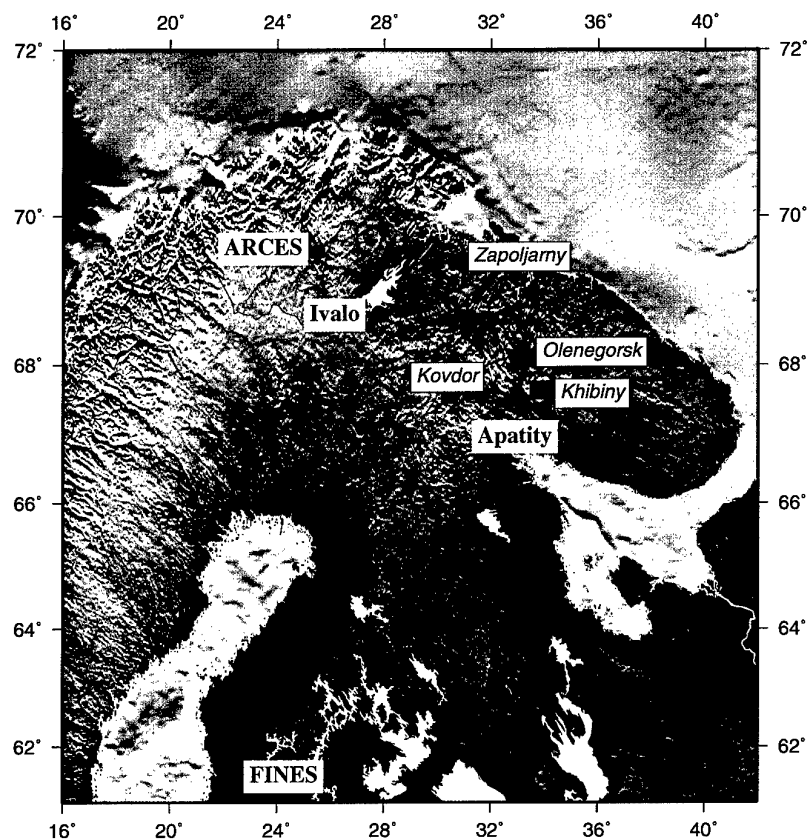
Figure 6.4.1. The map shows the main mining sites in the Kola Peninsula, marked as red squares. Some key seismic stations in this region are marked as filled (blue) circles.
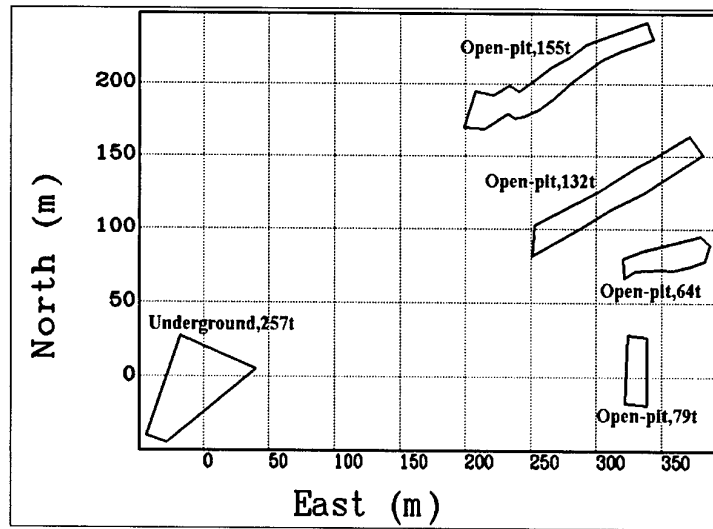
Figure 6.4.2. Schematic view of the shot configuration for the two explosions in Khibiny on 16 November 2002. Geographical coordinates of the point (0,0) are 67.6322N 33.8565E. See text for details.
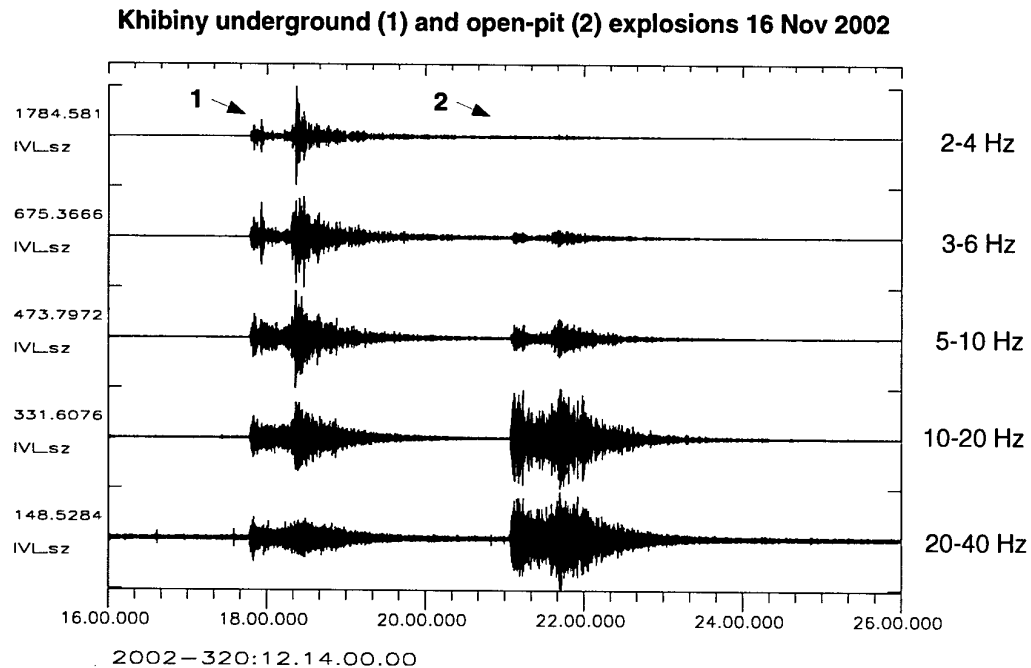
Figure 6.4.3. Recorded SPZ waveforms at station Ivalo (northern Finland) for the two explosions in Khibiny on 16 November 2002. The data have been filtered in five different frequency bands. Note the significant difference in relative size of the two events as a function of frequency.
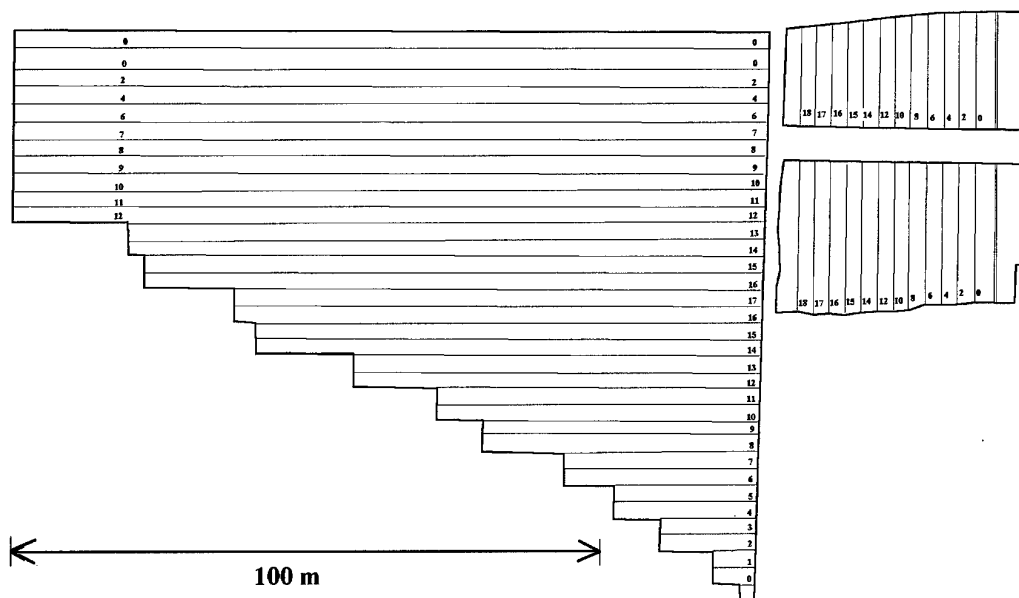
Fig. 6.4.4. Geometry of the underground mining explosion in Khibiny 16 November 2002. The charges were detonated in 19 groups (delay 23 ms between each group). The sequence is indicated by the numbers, with the charge sizes listed in Table 6.4.1. Note that the explosions begin at the outer edges (charges numbered 0), and continue towards the center.

Arcess Pn beam - Underground explosion 16 Nov 2002
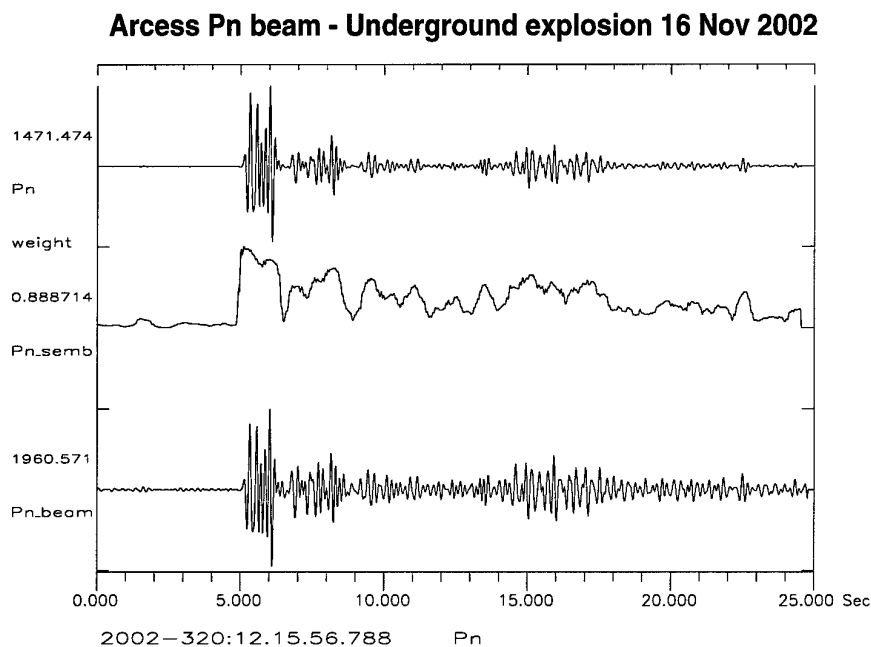
Fig. 6.4.5 ARCES Pn beam of the underground explosion on 16 Nov. 2002. See text for details.
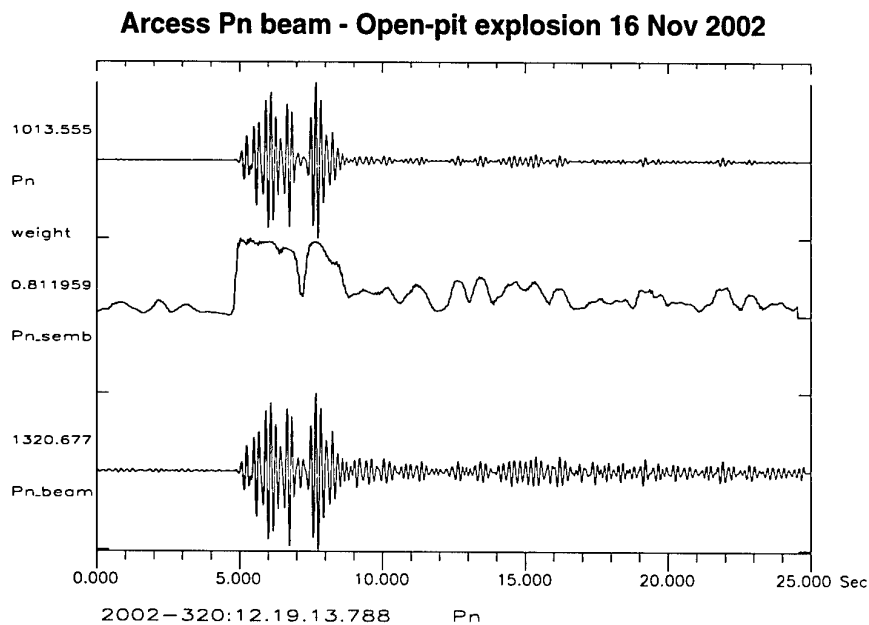
Fig. 6.4.6 ARCES Pn beam of open-pit explosion on 16 Nov. 2002. See text for details.
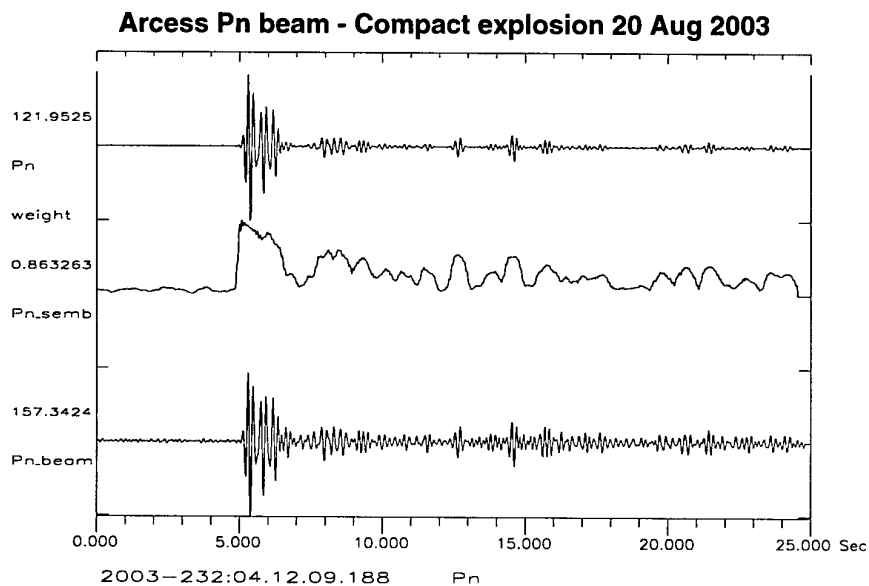
Fig. 6.4.7 ARCES Pn beam of compact explosion on 20 Aug. 2003. See text for details.

Khibiny Massif   Underground explosion
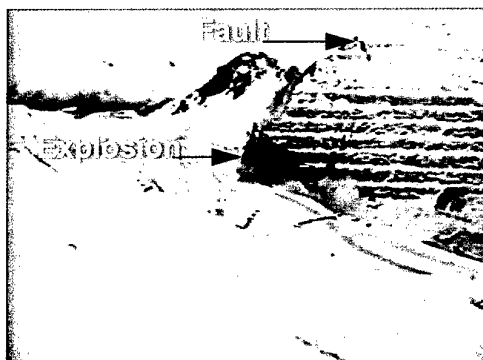
Close-in view of fault after 5 minutes   First surface explosion
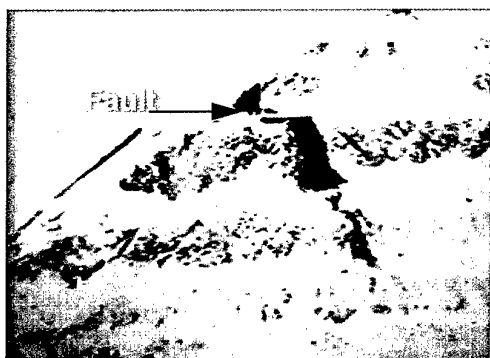
The four surface explosions (1,2,3,4)   Five seconds after first surface explosion

Fig. 6.4.8. Snapshots of video from the sequence of Khibiny explosions on 16 November 2002 Note in particular the large crack ("fault") opening up in the mountainside at the time of the first (underground) explosion.

6.5   Study of regional variations of the coda characteristics in the Barents Sea using small-aperture arrays

6.5.1   Introduction and first observations

At regional distances, coda waves arriving after deterministic phases like Pn, Pg, Sn, or Lg, are broadly attributed to seismic wave scattering phenomena associated with heterogeneities located within the crust. Therefore, the characteristics of the coda depend on the characteristics of the seismic source, but also on the properties of the medium of propagation. The analysis of phases composing the coda are then ideally suited for studying crustal structures.

Detailed analyses of coda phases can be made by using small-aperture seismic arrays. Compared with a single station, seismic arrays give the advantage of recording spatio-temporal sampling of the seismic wavefield. Therefore, array analysis not only enhances the signal-to-noise ratio (SNR) to emphasize more details in the seismograms, but it also allows the association of phase velocities and backazimuths with the coherent arrivals of the seismograms.

In this study, our objective was to obtain a better understanding of the propagation effects that affect the seismic wave field when it propagates through the Barents Sea. This work was motivated by the particular characteristics (parameters of propagation) observed for the coda of an earthquake located in northern Norway (Lat 64.68° N; Lon 22.85° E) and recorded by the ARCES array. We performed frequency-wavenumber (f-k) analysis (Kværna & Doornbos, 1986) in a moving window to analyze the waveforms of all 25 vertical components recorded by ARCES. Fig. 6.5.1 shows the results that we obtained for this particular earthquake located northern Scandinavia. The signals are band-pass filtered in the most energetic (highest SNR) frequency band (here this frequency band is 2 – 8 Hz). We used a 2 s window length to perform the wavenumber decomposition. For each time window, the most energetic peak of the wavenumber decomposition is selected and the parameters of propagation (direction and apparent velocity) are deduced from its position in the wavenumber domain. The relative power of this main peak, which is actually a coherency measure of the waveforms over the whole array, is also calculated. Fig. 6.5.1c is a map of the studied area and the black dotted line shows the source-array propagation path for this earthquake. Fig. 6.5.1a shows the signal recorded by the central sensor of the array and Fig. 6.5.1b gives the time evolution of the parameters of propagation. For each time window, we present the difference between the observed direction of propagation obtained from the wavenumber decomposition and the theoretical backazimuth. The color scale gives a measure of the apparent velocities of the different phases observed, in this case between 2.5 and 8 km/s. The size of each dot is proportional to the coherency of the wavefield calculated within each time window. The velocity scale and the coherency scale are depicted on the right hand side of the picture.

For this earthquake, the regional Pn, Pg, Sn, and Lg phases are clearly identified. The directions of propagation are very close to the one expected and exhibit a high stability for the different time windows, from the first arrival until the beginning of the Lg-coda. The seismic waves that compose the Lg-coda are clearly characterized by larger scattering from the direction of propagation. The time evolution of the apparent velocities shows that the Pn-coda is essentially composed of Pn phases, the Sn-coda of Sn phases and the Lg-coda of Lg phases. One has also to notice the high coherency of the waveforms over the whole array, not only for the deterministic phases of the seismograms, but also for the time windows used for analyzing Pn- and Sn-coda.

The time-azimuth-velocity evolution obtained for this earthquake shows that the most important scattering processes arise along the direct epicenter-array path. Lateral heterogeneities of the medium seem not to be involved in the main scattering processes. Such features of the coda have already been observed by different authors and mechanisms like multiple refractions in the crust have been proposed to explain the coda characteristics similar to those observed for this particular earthquake (Vogfjord & Langston, 1989; Dainty & Toksöz, 1990; Baumgardt, 1990).

The strong stability and coherency of the coda phases observed for this event contradicts the model of a random process, which generally is used to explain the coda, and shows that some deterministic processes of scattering are also responsible for the coda. The objective of this study is to have a better overview of the physical processes that govern the coda formation in northern Norway and adjacent areas. Therefore, we selected around 50 seismic events located in and around the Barents Sea, in order to answer specific questions:

- Can the temporal stability of the directions of propagation be observed independently from the location of the earthquakes?
- Is there a variability of the nature (P/S) of the coda phases depending on the source-array propagation path?
- How are the coda characteristics modified when the events are recorded by other arrays?

6.5.2 The data set

We selected around 50 seismic events located in and around the Barents Sea. Depending on their geographical locations, we divided the data set into 4 different groups represented in Fig. 6.5.2. The groups **G1, G2, G3,** and **G4** are composed of events located along the **Mid-Atlantic ridge**, close to **Svalbard**, close to **Novaya Zemlya** and in the **northern Fennoscandia / Kola Peninsula Region** respectively. In this study, we mainly focused on the observations made by the two arrays ARCES (Mykkeltveit *et al.*, 1990) and SPITS (Mykkeltveit *et al.*, 1992; Fyen & Ringdal, 1993) on Spitsbergen in the Svalbard Archipelago (Fig. 6.5.2).

We applied the processing as described in the first section to each event of the data set in order to retrieve the time-frequency evolutions of the parameters of propagation of the different phases of the coda. This processing is mainly divided into two steps:

- Visual check of the data quality. We used as many sensors as available (ideally, this number is 25 for **ARCESS** and 9 for **SPITS**). The signals are band pass filtered in the frequency band corresponding to the highest SNR.
- F-k decompositions using the moving time window technique for the whole signals. This step gives the time evolution of the parameters of propagation of the different seismic phases that compose the seismograms. We used a fixed length for the time window, around 2 – 3 s, depending on the central frequency of analysis, *i.e.*, the applied band-pass filter.

6.5.3   The results

Comparison of the coda characteristics recorded by ARCES for all events belonging to group G4

In order to determine if the coda characteristics of the earthquake presented in Fig. 6.5.1 are similar for all the events located in northern Norway, we compared the time-evolution of the parameters of propagation that we obtained for all the events of group G4.

The results are presented in Fig. 6.5.3. This figure represents only the energetic distribution of the directions of propagation corresponding to the different phases that compose the coda. For each event, the energy of the incoming wavefield is summed up as a function of direction of propagation and we plot the results by using a polar representation. Each circle corresponds to a different event of group G4, and the red line points to the epicenter of the event.

First of all, we see that for each event, there is a very good agreement between the expected direction of propagation and the most energetic direction of the distribution. In addition, we observe a high sharpness of the distributions around their main peak. This characteristic shows a high temporal stability of the directions of propagation of the most energetic phases that contribute to the signal. Thus, this confirms that for the group of events located in the northern Fennoscandia / Kola Peninsula Region, the coda phases result mainly from multiple scattering along the direct source-array path. Scattering due to lateral heterogeneities along the great circle paths between the sources and ARCES is very weak.

Comparison of the coda characteristics recorded by ARCES for the different event groups (G1/G2/G3/G4)

We compared the typical coda characteristics that we obtained for the events of the group G4 (see Fig. 6.5.1) with the ones obtained for the events of the groups G1, G2 and G3. One typical event of each of these groups is represented in Fig. 6.5.4. On the right hand side, we plotted the direct propagation path for each of the 3 selected events and on the left hand side, we displayed the results of the f-k analysis.

For the events of the groups G2 and G3, we observe the same characteristics as for the one of group G4 presented in Fig. 6.5.1. The direction of propagation does not change greatly with time for these two events and is close to the expected receiver to source backazimuth. The apparent velocities follow the same pattern as for the event presented in Fig. 6.5.1 (Pn phases for Pn coda and Sn phases for Sn coda). In terms of wave composition, the strongest difference between the events of the group G4, and the events of the groups G2 and G3 (or more generally with all events for which a part of the propagation path lies within the Barents Sea) is the absence of Lg phases. The Lg blockage for events located in the Barents Sea and recorded by the ARCES array has been observed and investigated by several authors (Baumgardt, 2001; Hicks *et al.*, 2004).

The characteristics of the coda are completely different for the events belonging to the group G1, *i.e.*, the ones located along the Mid-Atlantic ridge. We observe that the Pn-coda is, in this case, not longer dominated by multiple Pn phases, but by phases characterized by lower velocities. In addition, the high temporal stability of the direction of propagation is no longer present and differences close to 50° between the observed and the theoretical backazimuth can now be observed. Another interesting feature is the deviation of the main direction of propagation in the Pn- and Sn-coda. The main Pn phase propagates through the array with the expected direc-

tion, but the coda phases exhibit a slow increase of the directions of propagation to more north-
ern directions. The same pattern is observed for the S part of the seismograms. Such deviations
have been quasi-systematically observed for all the events of group G1 and this result is sum-
marized in the Fig. 6.5.5, where we represented the energetic distributions of the directions of
propagation for all the events of this group. Compared with the energetic distribution calcu-
lated for the events of the group G4 (Fig. 6.5.3), we observe a widening of the distributions
around the main peak. This means that the distributions of the direction of propagation of the
coda phases are now much more scattered around the expected bachazimuth. Fig. 6.5.5 also
shows that the main peaks of the distributions can show a systematic deviation from the
expected direction of propagation. These deviations cannot be attributed to heterogeneities
located close to the array since they are generally not observed for the events from the other
groups (Fig. 6.5.3), even for events at similar azimuths.

These results are summarized on the map represented in Fig. 6.5.6. We separate the events that
we will call *'normal events'* for which the Pn- and Sn-coda are composed of phases propagat-
ing with typical velocities values of Pn and Sn respectively, from the events called *'abnormal
events'* which do not show this pattern. The locations of the normal and abnormal events are
represented by red and black stars respectively in Fig. 6.5.6. With very few exceptions, the
abnormal events are the events of the group G1, located along the Mid-Atlantic ridge, as the
events of the groups G2, G3 and G4 exhibit a normal distribution of the coda phases. It is inter-
esting to see that for the events of the group G3, the single event which does not conform to the
normal distribution of coda phases is the nuclear explosion that took place in Novaya Zemlya
on 24 October 1990.

Comparison of the coda characteristics at ARCES and at SPITS

We the processed the waveforms recorded by the SPITS array for some of the events of our
data set (the ones with highest SNR). The processing procedure is the same as for the ARCES
array, except that the SPITS array consists of 9 vertical sensors, instead of 25 for ARCES. In
Fig. 6.5.7, the time-evolution of the parameters of propagation is shown for the same earth-
quake, for which the observation at ARCES is presented in Fig. 6.5.4b. The coda is character-
ized by even more stable parameters of propagation compared with the coda recorded by
ARCES for this event. In addition, the coherency of the wavefield over the whole array (mea-
sured by the size of the dots) is higher for the waveforms recorded by SPITS than for the ones
recorded by ARCES. To simulate a SPITS type array, the ARCES data were also processed for
only 9 sensors. The result of this test was that configuration and smaller aperture of the SPITS
array can be ruled out as reason for the observed, more coherent coda.

The more interesting events recorded by SPITS are the one located along the Mid-Atlantic
ridge. For these events, two general situations are observed: (1) no S phase is observed or (2)
when a S phase is observed, the coherency is very low or inexistent. The situation (1) is
depicted in Fig. 6.5.8a, where we present the time evolution of the parameters of propagation
for an event located along the Mid-Atlantic ridge and recorded at SPITS. For comparison, we
present also the results for an event of group G2, approximately located at the same distance
(Fig. 6.5.8b) from the array. For the event of the group G1, the time arrival of the S phase
should be around 115 s but the results of the f-k decomposition does not exhibit any S-type
energy. Instead, the velocities of propagation are very high, closer to typical Pn phases. These
features may be partly related to the radiation pattern of the seismic source, but the complex
structures located between the source and the array may also be responsible for a part of the

observed characteristics. The source mechanism of the earthquakes of group G1 should be investigated more carefully in order to find out, which of the two effects (source or propagation) is predominant.

6.5.4 Conclusion

We investigated the characteristics of the coda for a large data set recorded by ARCES and SPITS. F-k decompositions have been used to calculate the time evolution of the parameters of propagation of the different phases that compose the coda.

We show that for the arrays ARCES and SPITS, the characteristics of the coda are very similar for events located in northern Fennoscandia / Kola Peninsula region (G4), close to Novaya Zemlya (G3) and close to Spitsbergen in the Barents Sea (G2). The coda propagates mainly along the great circle paths between source and arrays. The apparent velocities are typical of Pn phases for the Pn coda and Sn phases for the Sn coda. In this case, we imply mechanisms like multiple crustal reflections to explain our observations.

The characteristics of the coda are very different for all the events of group G1, located along the Mid-Atlantic ridge. Strong differences are generally observed between the direction of propagation of the coda phases and the expected one. This shows that the scattering is no longer confined to the great circle path, but that lateral structures are also involved into multipathing and diffraction processes. In addition, compared with the events of the groups G2, G3 and G4, for which the Pn coda is mostly composed of Pn waves, the Pn coda of the events located along the Mid-Atlantic ridge are composed of energy travelling with lower apparent velocity, which is closer to typical Sn phase velocities. Such particular characteristics are observed both at ARCES and SPITS. One of the main differences between the wavefield propagation of the events of group G1, compared to the groups G2, G3 and G4 is that for the events located along the Mid-Atlantic ridge, the wavefield propagates across the western continental margin, characterized by strong topography of the Moho and a complex geometry. The continental margin is also known for many lateral heterogeneous geological features in the whole crust related with the opening of the North Atlantic (*e.g.*, Faleide, 2000). The P-to-S conversions and the backazimuth deviations that we observed for the events located along the ridge could be explained by the interactions with this large-scale structure. As further work, we plan to use the converted P-to-S travel time as well as the direction of propagation given by the array analysis in order to obtain a better characterization of the heterogeneous structures responsible for our observations.

Estelle Schissele, Institut für Geowissenschaften, Universität Potsdam, Germany
Johannes Schweitzer

References

Baumgardt, D. R. (1990). Investigation of teleseismic Lg blockage and scattering using regional arrays. Bull. Seis. Soc. Am. **80**, 2261-2281.

Baumgardt, D. R. (2001). Sedimentary basins and the blockage of Lg wave propagation in the continents. Pure Applied Geophysics **158**, 1207-1250.

Dainty, A. M. & M. N. Toksöz (1990). Array analysis of seismic scattering. Bull. Seis. Soc. Am. **80**, 2242-2260.

Faleide, J. I. (2000). Crustal structure of the Barents Sea – important constraints for regional seismic velocity and travel-time models. NORSAR Sci. Rep. **2-1999/2000**, 119-129.

Fyen, J & F. Ringdal (1993). Initial processing results for the Spitsbergen small-aperture array. NORSAR Sci. Rep. **2-92/93**, 119-131.

Hicks, E. C., T. Kværna, S. Mykkeltveit, J. Schweitzer & F. Ringdal (2004). Travel-times and attenuation relations for regional phases in the Barents Sea region. Pure appl. Geophys. **161**, 1-19.

Kværna, T. & D. J. Doornbos (1986). An integrated approach to slowness analysis with arrays and three-component stations. NORSAR Sci. Rep. **2-85/86**, 60-69.

Mykkeltveit, S., F. Ringdal, T. Kværna & R. W. Alewine (1990). Application of regional arrays in seismic verification. Bull. Seis. Soc. Am. **80**, 1777-1800.

Mykkeltveit, S., A. Dahle, J. Fyen, T. Kværna, P. W. Larsen, R. Paulsen, F. Ringdal & I. Kuzmin (1992). Extensions of the northern Europe regional array network – new small-aperture arrays at Apatity, Russia, and on the Arctic Island of Spitsbergen. NORSAR Sci. Rep. **1-92/93**, 58-71.

Vogfjord, K. S. and Langston, C. A. (1989) Multiple crustal phases from regional events recorded at NORESS. 11th Annual DARPA/AFGL Research Symposium, Proceedings, 466-473.
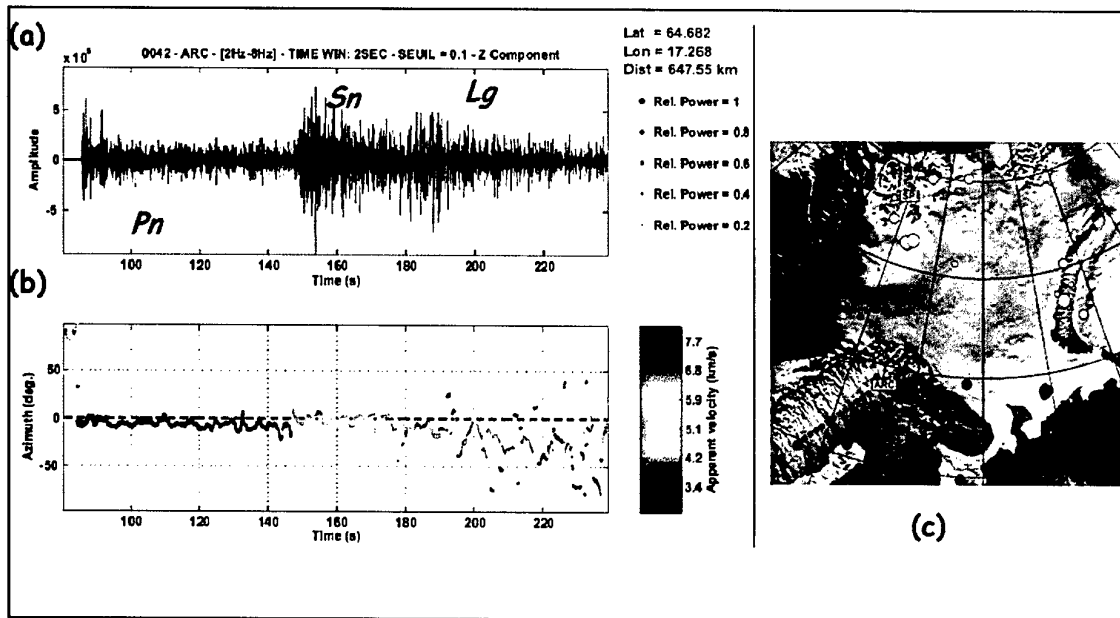
Fig. 6.5.1. (a) Signal recorded by the central sensor of the ARCES array and band-pass filtered between 2 and 8 Hz. (b) Time-evolution of the directions of propagation. The color of each dot represents the apparent velocity obtained from the wavenumber decomposition and its size is a measure of the coherency of the waveforms over the whole array (measure between 0 and 1). The scales corresponding to the coherency and the apparent velocity are given on the right side of the figure. (c) Map of the studied area. The black black line shows the propagation path for this particular event.
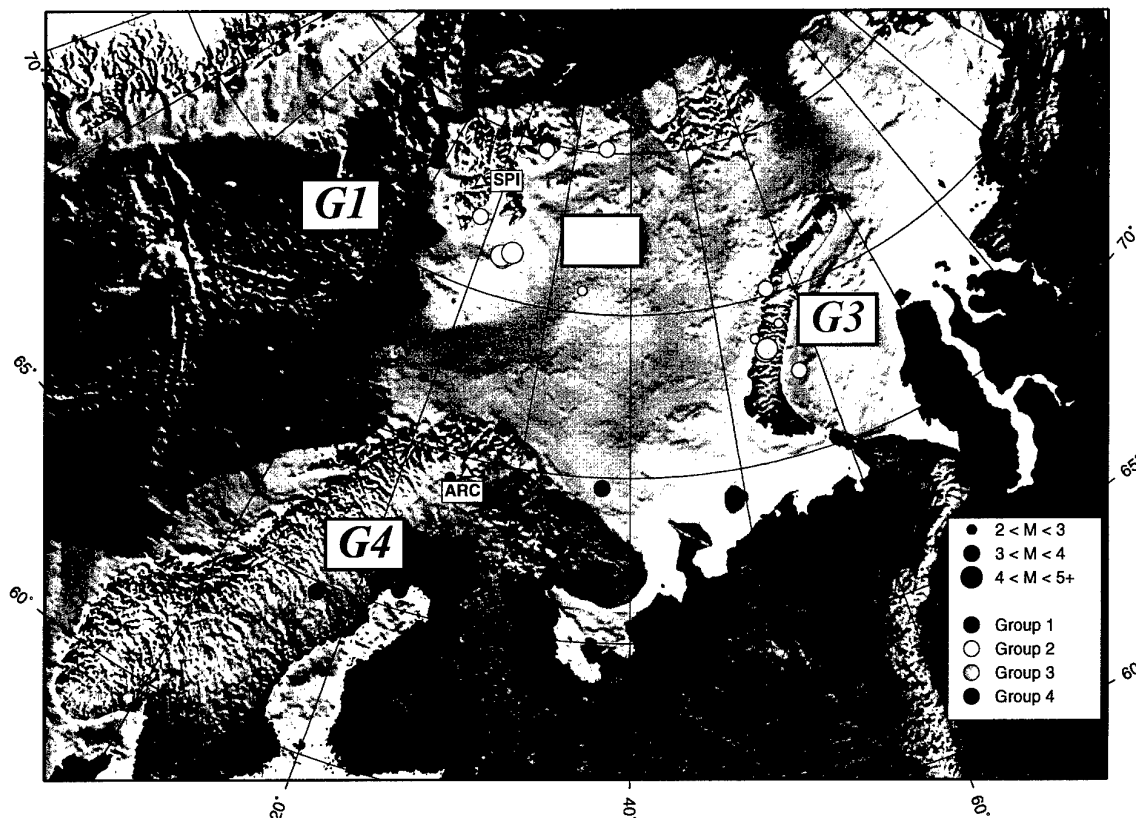
Fig. 6.5.2. *This map shows the location of the 4 groups of events (G1/G2/G3/G4) analyzed during this study. The size of each dot is proportional to the magnitude of the event.*
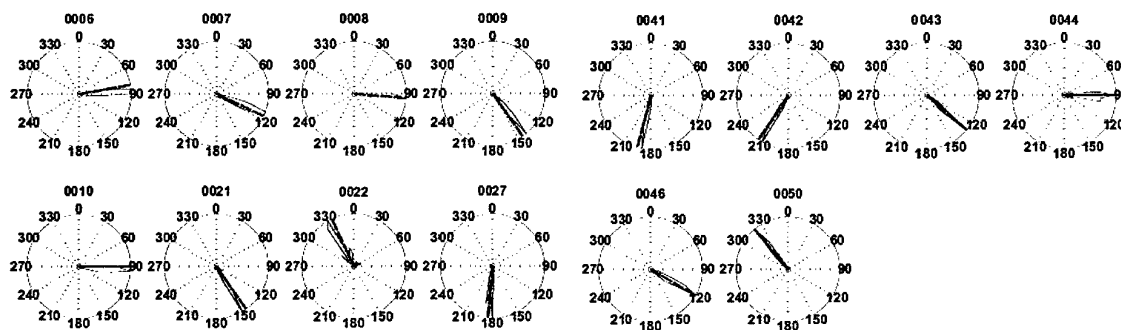
Fig. 6.5.3. *Energetic distributions of the directions of propagation for all the events of group G4 observed at ARCES.*

(a)

(b)

(c)
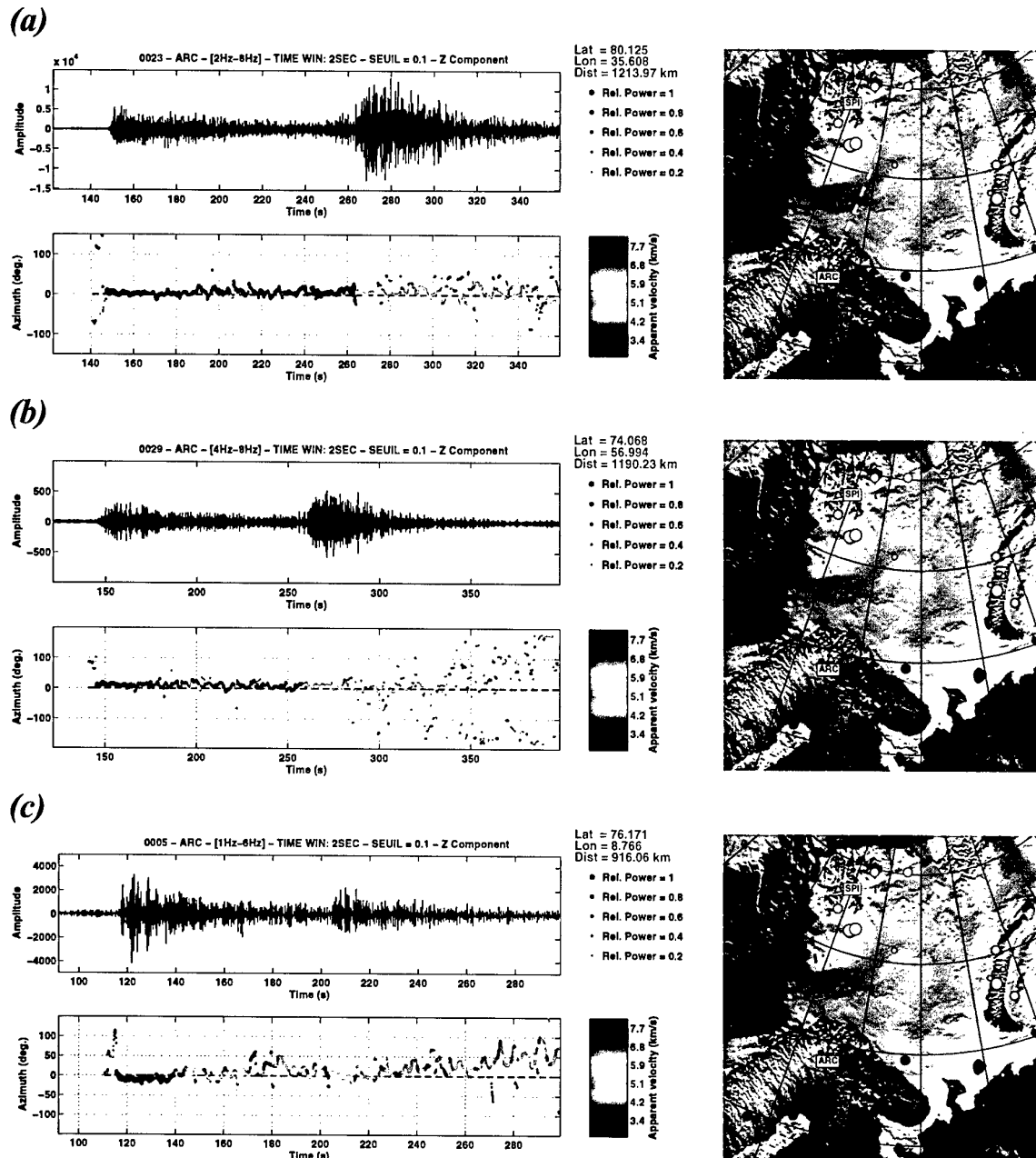
Fig. 6.5.4. *(a) Typical time evolution of the parameters of propagation for an event of group G2 observed at ARCES. (b) Idem for an event of group G3. (c) Idem for an event of group G1. On the right hand side, the propagation paths for the 3 events considered are represented.*
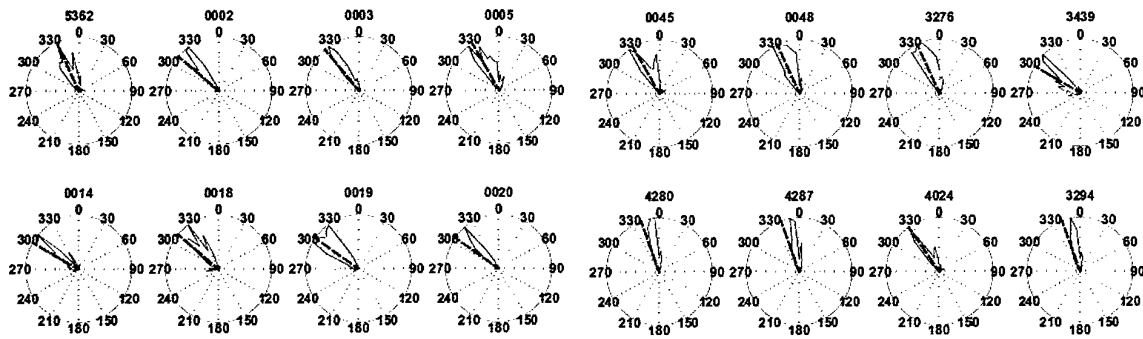
Fig. 6.5.5. *Energetic distributions of the directions of propagation for all the events of the group G1 observed at ARCES.*
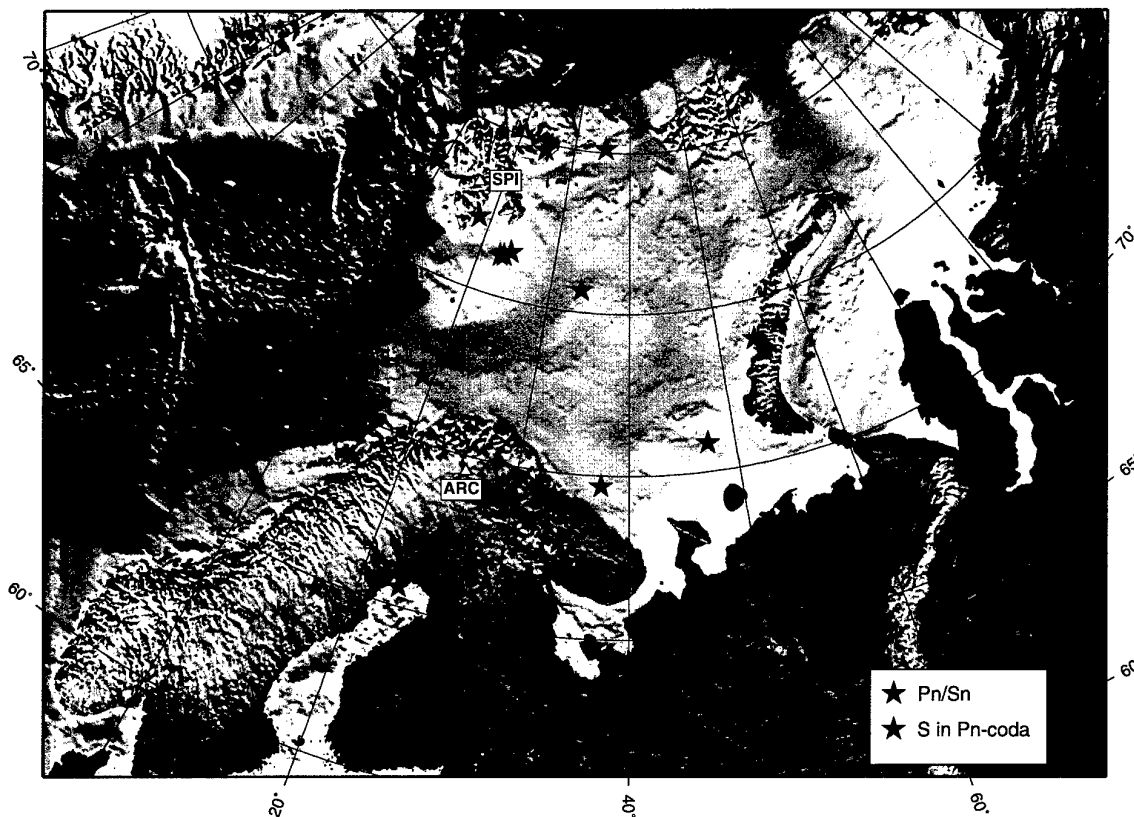
Fig. 6.5.6. *The red stars give the locations of the 'normal events' and the black stars give the locations of the 'abnormal events' (for details see text).*
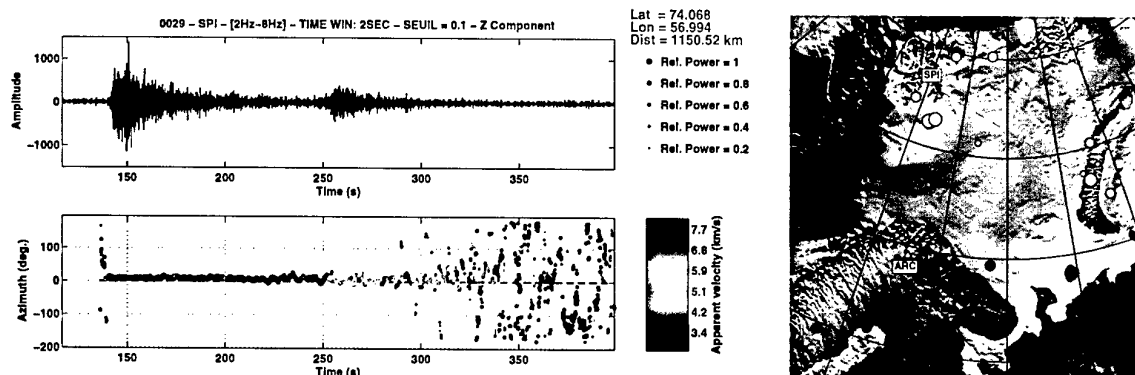
Fig. 6.5.7. *Time evolution of the parameters of propagation for an event of group G3 recorded at SPITS.*

(a)

(b)
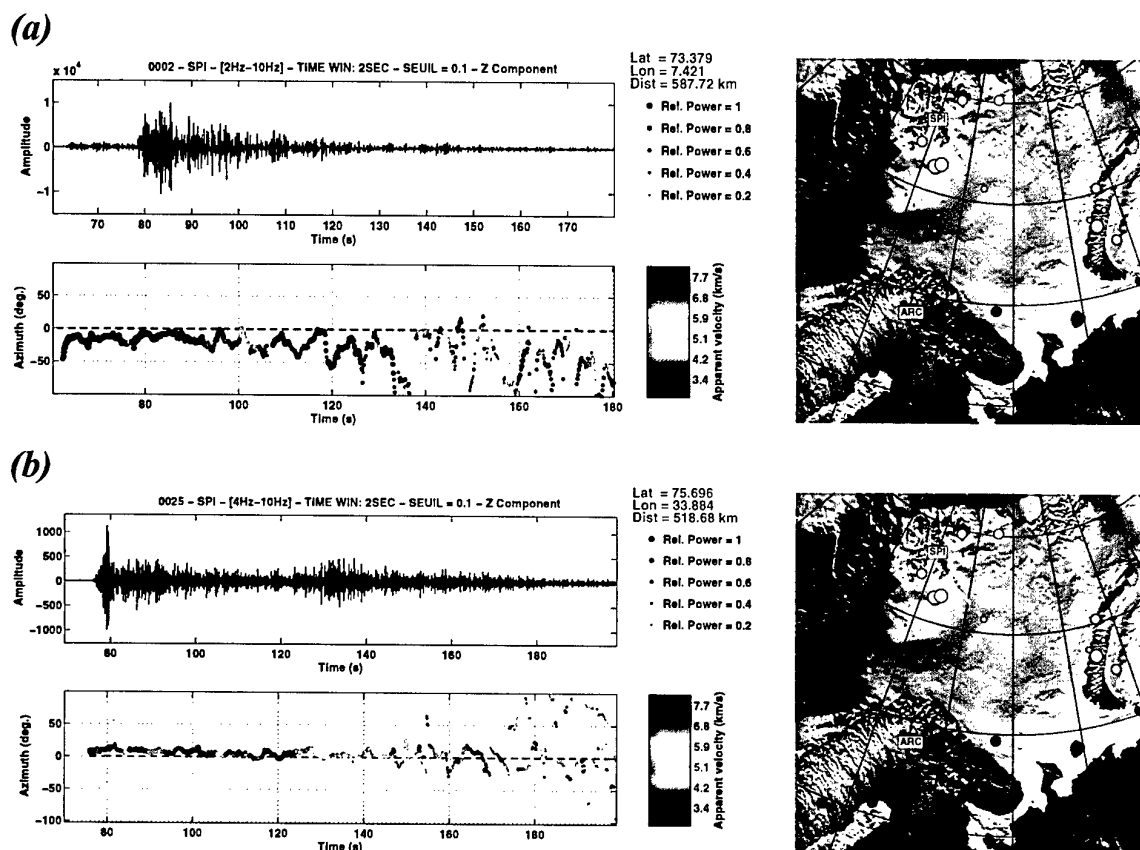
Fig. 6.5.8. *(a) Time evolution of the parameters of propagation for an event of group G1 recorded at SPITS. (b) Idem for an event of group G2.*

6.6   ARCES recordings of events from the Khibiny and Olenegorsk mines

6.6.1   Introduction

The principal objective of this project is to develop and test a new advanced, automatic approach to seismic detection/location using array processing. Our aim is to obtain significantly improved precision in location of low-magnitude events compared to current automatic approaches, combined with a low false alarm rate. We plan to develop and evaluate a prototype automatic system which uses as a basis regional array processing with fixed, carefully calibrated site-specific parameters in conjunction with improved automatic phase onset time estimation.

The first step is to study the characteristics of selected mining explosions and attempt to identify systematic features of recordings from explosions in the same mine. This paper presents some initial results from the Rasvumchorr and Central mines in the Khibiny Massif, Kola Peninsula, and the five mines in the Olenegorsk group north of the Khibiny Massif.

6.6.2   Compact underground shots from the Rasvumchorr mine in the Khibiny Massif

The initial focus of research will be to develop algorithms for processing of mining events from the northern Fennoscandian region, using the ARCES array. As shown in Figure 6.6.1, there are several active mines in this region.

Since September 2001, an extensive collection of ground truth information on mining explosions in the Kola Peninsula has been conducted on the DoE funded contract entitled "Ground-Truth Collection for Mining Explosions in Northern Fennoscandia and Russia". Our plan is to use the ground truth events for the one-year time period October 2001 - September 2002 for development and tuning of the algorithms, and to use events after September 2002 for evaluation.
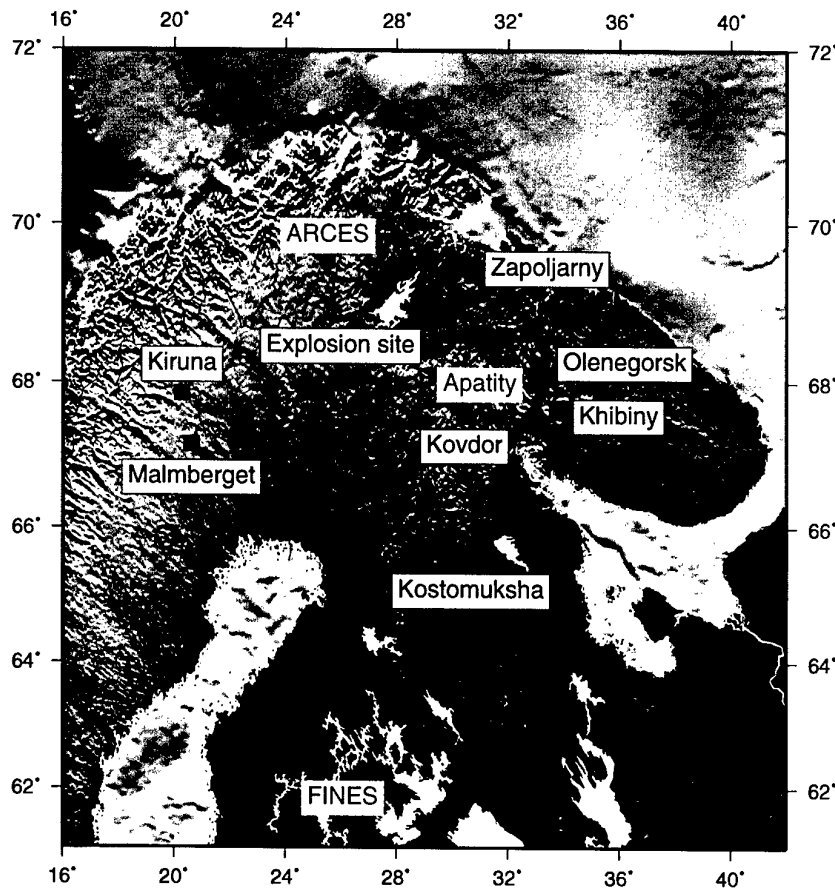
Fig. 6.6.1. *Locations of the main mining regions in NW Russia and Sweden, together with the location of a site regularly used by the Finnish military for destruction of ammunition. Also shown are the locations of the seismic arrays in the region (ARCES, Apatity and FINES).*

We have started to investigate in detail events from the Khibiny and the Olenegorsk mines (see Figure 6.6.2). Ground truth information (Harris et al., 2003) and earlier studies of mining events from this region (Gibbons and Kværna, 2002; Ringdal et al., 2003) have revealed that a wide range of source types are present at these mines. The blasts in the open-pit mines are usually large ripple-fired explosions, often detonated in several groups with some seconds delay. The regular blasts in the Khibiny Massif underground mines usually have yields between 120 and 240 tons with many delays of 20-35 milliseconds. So-called compact shots also detonated in these underground mines. The compact shots have yields between 1 and up to a few tons, having only a few delays, and provide the simplest source type available in these mines. The main purpose of the compact shots is to remove smaller parts of rocks remaining after the main underground explosion.
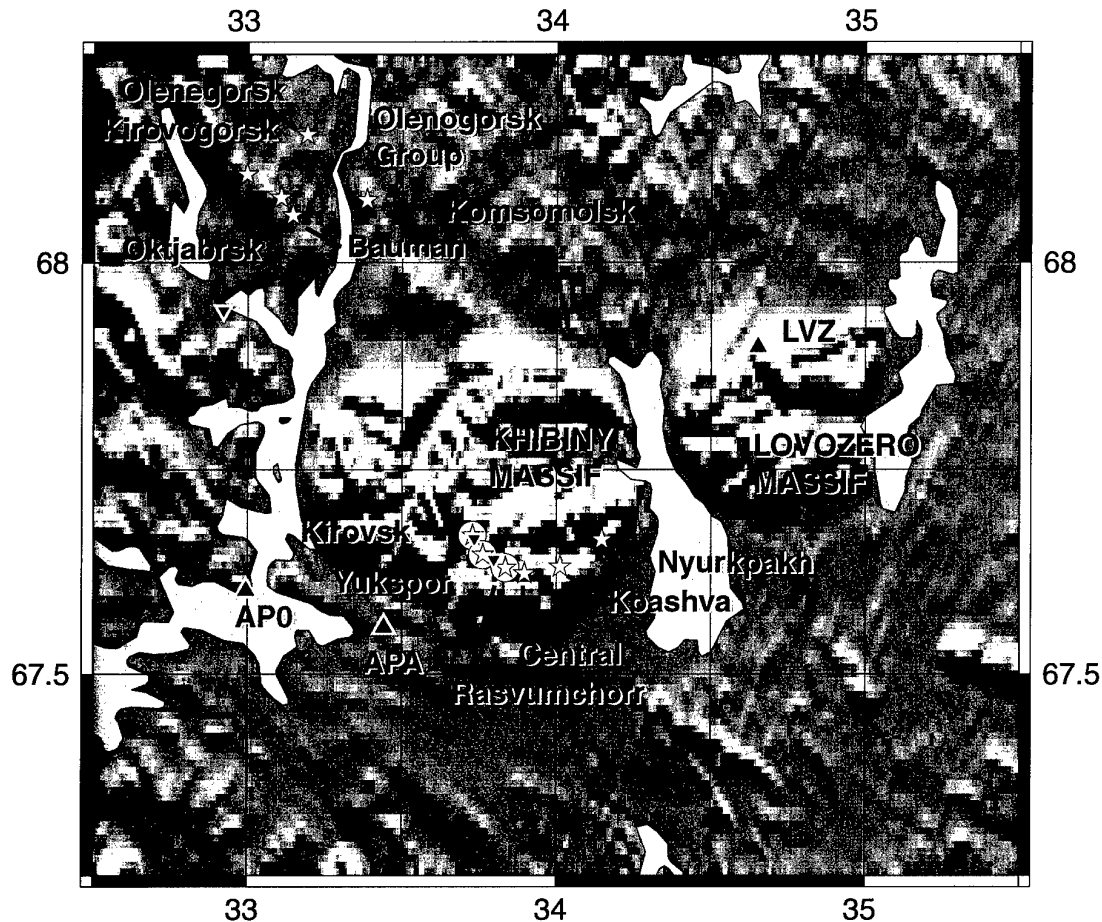
Fig. 6.6.2. *Locations of the mines (stars; circles indicate mines with both underground and surface facilities), permanent stations (triangles) and temporary stations (inverted triangles) in the vicinity of the Khibiny Massif. The five mines in the Olenegorsk group are all open-pit mines.*

In order to get an overview of typical seismograms observed at the ARCES array from explosions in the Khibiny and the Olenegorsk mines, we have taken a closer look at the compact shots from the underground Rasvumchorr mine in the Khibiny Massif. For each of the 99 events in the ground truth database (October 2001 - September 2002), we have calculated the Pn beam, the corresponding semblance coefficient, and the Pn beam weighted with the semblance coefficient. The frequency band used for this analysis was 4 - 8 Hz. The Pn beam was formed using the ARCES center instrument (A0), the C- and D-ring instruments steered with an apparent velocity of 7.5 km/s and a back-azimuth of 121.0 degrees. The semblance coefficients were calculated for 0.5 second window lengths with a 40 Hz sampling rate.

The 15 upper panels of Figure 6.6.3 show the results from semblance analysis of the first 15 events in the ground truth database. The events in the lower three panels are selected to illustrate the more complex signatures found among the ground truth events. The distance from ARCES to the center of the Rasvumchorr mine is 401 km and the back-azimuth is 118.3 degrees.

From these panels we can see that some of the events show a relatively simple source signature, whereas others have longer duration and consist of several pulses, which could be an effect of multiple seismic sources in combination with near-source scattering.
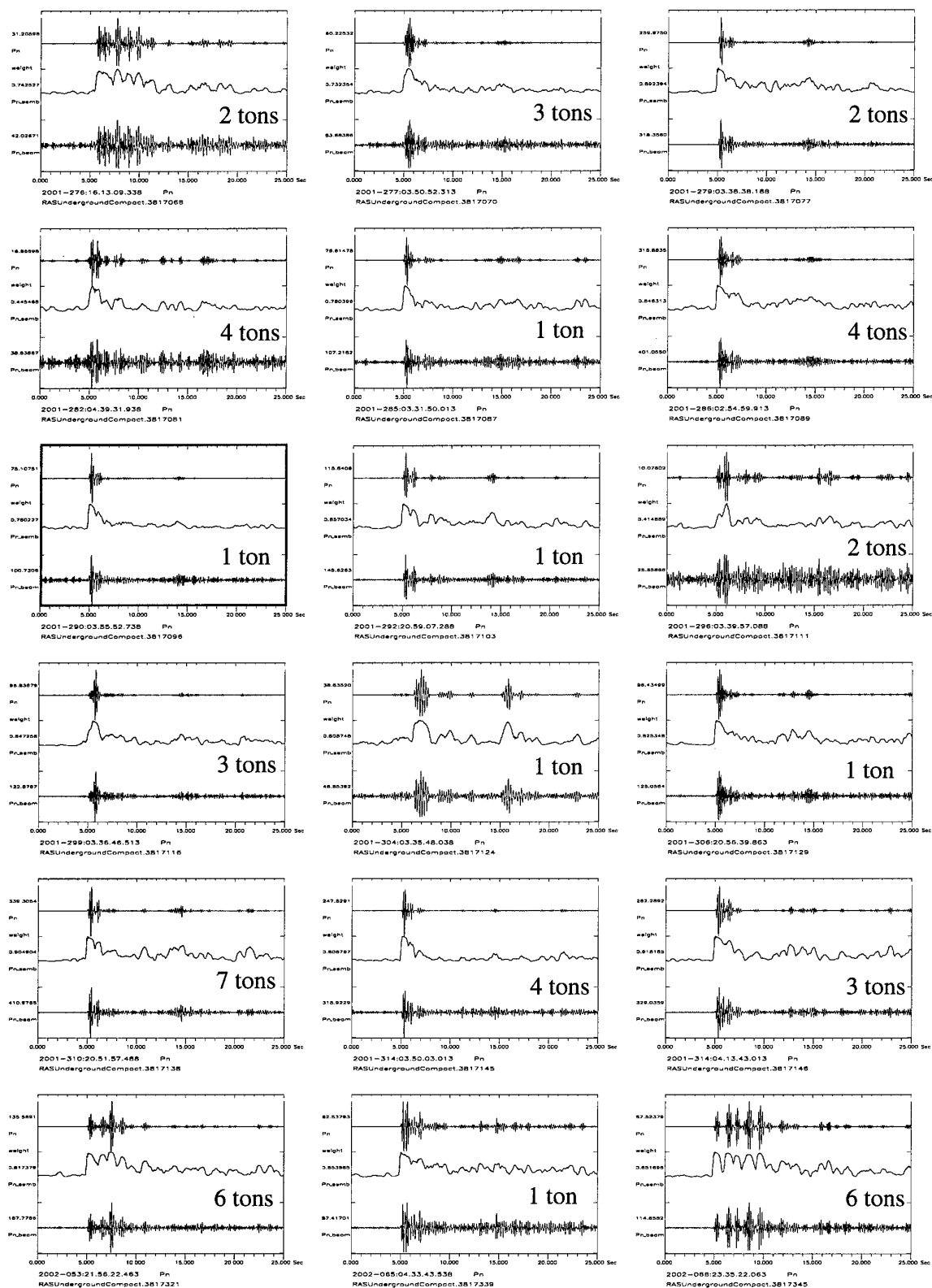
Fig. 6.6.3. *ARCES recordings of 18 compact shots in the underground Rasvumchorr mine in the Khibiny Massif. For each panel we show the 4-8 Hz Pn beam (bottom), the semblance coefficient (middle) and the Pn beam weighted with the semblance coefficient. The yields reported for each event are also given. The highlighted event, which has a relatively simple signature, is also used in Figure 6.6.4 and 6.6.5.*

For further investigating the source and propagation effects of events from the underground
Rasvumchorr mine, we have stacked the ARCES Pn semblance coefficients of the 99 events in
the ground truth database. The stacked semblance trace is shown on top of Figure 6.6.4,
together with an event having among the simplest signatures at ARCES (highlighted red in Fig-
ure 6.6.3). We note the close similarity between the stacked trace and the "simple" waveform.
In particular, the only secondary arrival on the stacked trace (arriving about 9 seconds after Pn),
corresponds to the Pg phase on the "simple" waveform. Also the Pn phases are well correlated.
For this frequency band (4-8 Hz), we can conclude that there are no other phases than Pn and
Pg, that are expected to be found within this time window for events in this mine.
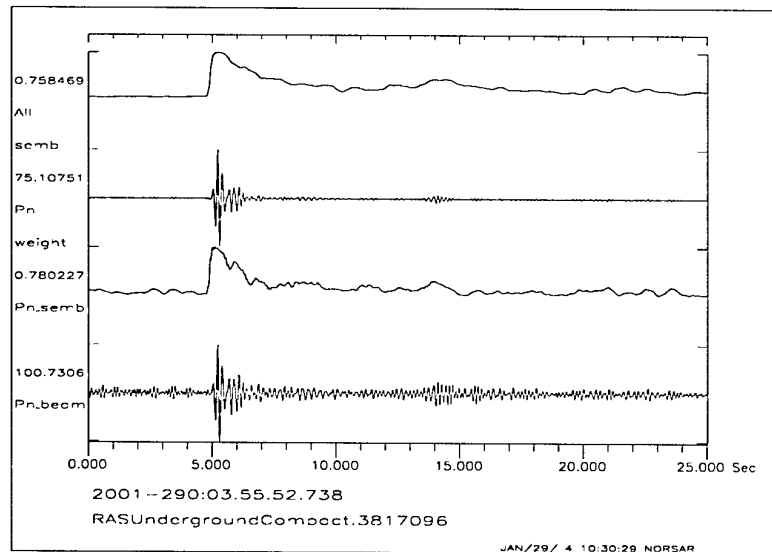
Fig. 6.6.4. *The upper trace shows the stacked ARCES Pn semblance coefficients of the 99 ground truth
events of compact underground shots from the Rasvumchorr mine in the Khibiny Massif. For
comparison, the three lower traces show the result from semblance analysis of an event having
a simple signature at ARCES (highlighted red in Figure 6.6.3).*

Vespagram analysis can be efficiently used to find coherent signals arriving at a seismic array.
Figure 6.6.5 show vespagrams in the 4-8 Hz and 2-4 Hz frequency bands for the compact shot
displayed in Figure 4. For the 4-8 Hz band we can clearly observe the Pn phase arriving at
about 20 seconds, a couple of coherent pulses in the P coda, some coherent Sn energy arriving
at about 63 seconds, and some additional signals in the Lg wavetrain arriving at about 75 sec-
onds.

In the 2-4 Hz band the phases Pn, Pg (arriving at about 29 seconds), Sn and Lg can be seen
more clearly. The arrival time of these phase are in accordance with the theoretical arrivals of
the so-called 'barey' crustal and upper mantle model (Schweitzer and Kennett, 2002).

Based on the overview gained from semblance analysis and visual inspection of ARCES data
of 99 compact shots from the underground Rasvumchorr mine, we have found that the vast
majority of these events are characterized by a single strong Pn pulse. For these events, it
should be possible to detect and characterize the Pn, Pg, Sn and Lg phases at ARCES automat-
ically.

However, for about 25% of the events, there are multiple pulses in the Pn-Pg time window, indicating separate explosions with time delays ranging from 1 and up to several seconds. Consequently, automatic processing of these events will be a more difficult task.
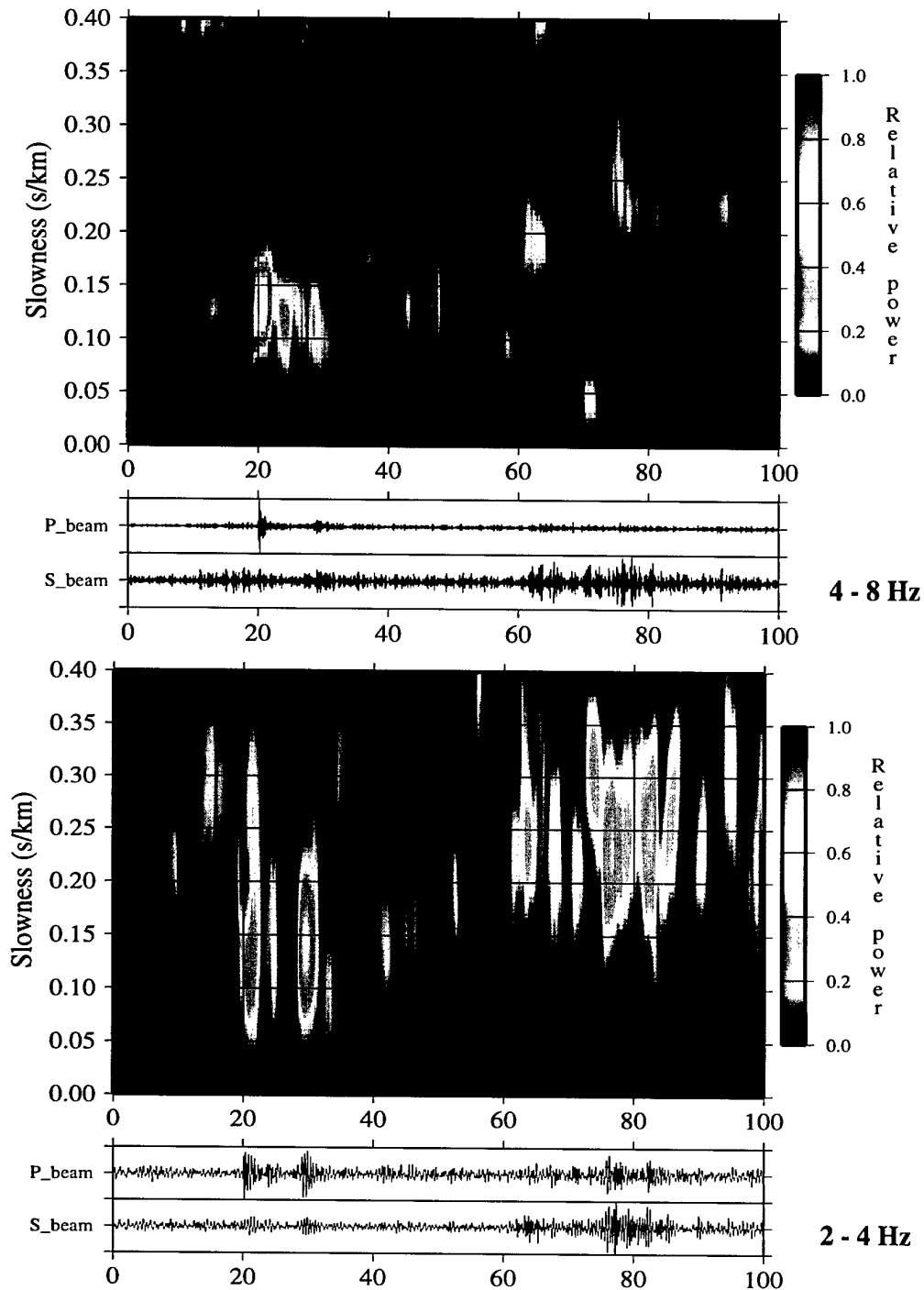
Fig. 6.6.5. The upper panel shows a 4-8 Hz ARCES vespagram of the Rasvumchorr compact shot shown in Figure 6.6.4. The slowness space is scanned at a back-azimuth of 120 degrees, using a window length of 2 seconds sampled at 0.1 second steps. The ARCES center instrument (A0), the C- and D-ring instruments are used in the calculations. The P beam shown below the vespagram is steered with an apparent velocity of 7.5 km/s, and 4.3 km/s is used for the S beam. The lower panel show similar plots for the 2-4 Hz frequency band.

6.6.3   Comparisons of ARCES recordings from different mines

We have also made similar semblance calculations for all ground truth events from the Khibiny Central mine (open-pit), as well as for the five open-pit mines in the Olenegorsk group. Panels with such plots are shown in Appendix A-F. In cases when more than 18 ground truth events are available, we show the first 18 events in the database.

The Khibiny Central mine is located very close to the underground Rasvumchorr mine (within 1-3 km), but visual inspection of the semblance plots (Appendix A) indicate quite complex wavetrains at ARCES as compared with the wavetrains from the compact underground shots at the Rasvumchorr mine (see Figure 6.6.3). From visual inspection of the semblance plots we found that more than half of the 48 ground truth Central mine events are multiple explosions with up to several seconds delay between each shot. However, by stacking of the semblance traces from the Central mine events, the random structure caused by differences in the shooting practice is averaged out, and we are left with the common properties for these events. The stacked semblance trace is shown in the upper panel of Figure 6.6.6, where we find that except for the first few seconds after Pn, the curve closely resembles the corresponding curve for the Rasvumchorr events.

The distance from ARCES to the Olenegorsk mines range between 341 and 350 km, spanning the back-azimuth range between 112.8 and 114.5 degrees. These mines are located 50-60 km closer to ARCES than the Khibiny mines. For the Olenegorsk mines (see Appendix B-F) the ARCES waveforms appear even more complex than for the Central mine events, and will be a real challenge for any automatic processing procedure. But again, by stacking of the semblance traces for each mine, the random structure caused by differences in the shooting practice is averaged out. The stacked semblance traces for these mines are shown in the lower five panels of Figure 6.6.6.
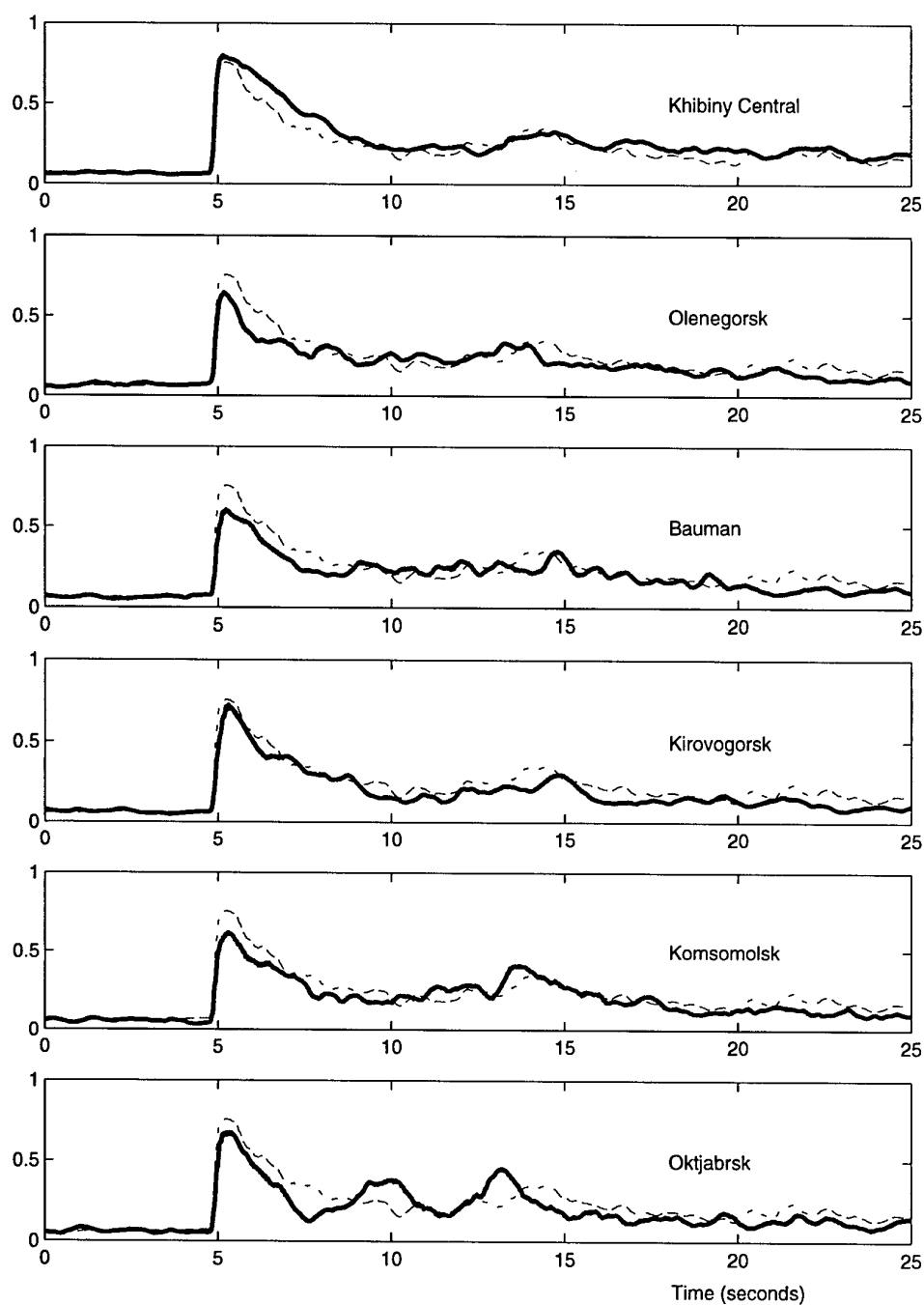
Fig. 6.6.6. *The blue curves show the stacked ARCES Pn semblance coefficients in the 4-8 Hz frequency band for the ground truth events in the Khibiny Central mine (upper trace), and for the mines in the Olenegorsk group (the lower five traces). The dashed red curve shows the stacked semblance coefficients for the compact underground shots in the Rasvumchorr mine.*

References

Harris, D. B., F. Ringdal, E. O. Kremenetskaya, S. Mykkeltveit, J. Schweitzer, T. F. Hauk, V. E. Asming, D. W. Rock and J. P. Lewis (2003). Ground-truth Collection for Mining Explosions in Northern Fennoscandia and Russia. "*Proceedings of the 25th Seismic Research Review - Nuclear Explosion Monitoring: Building the Knowledge Base*, Los Alamos National Laboratory, *LA-UR-03-6029*, Tucson, AZ, Sept. 23-25, 2003.

Gibbons and Kværna, 2002. Analysis and Processing of Events from the Kovdor Mine, NW Russia, NORSAR Contribution No. 793.

Ringdal, F., T. Kværna, E. O. Kremenetskaya, V. E. Asming, S. Mykkeltveit, S. J. Gibbons and J. Schweitzer (2003). Research in Regional Seismic Monitoring. "*Proceedings of the 25th Seismic Research Review - Nuclear Explosion Monitoring: Building the Knowledge Base*, Los Alamos National Laboratory, *LA-UR-03-6029*, Tucson, AZ, Sept. 23-25, 2003.

Schweitzer, J. and B.L.N. Kennett (2002). Comparison of Location Procedures - the Kara Sea event 16 August 1997. *Semiannual Technical Summary, 1July - 31 December 2001*, NORSAR Sci. Rep. No. 2-2001/2002.

T. Kværna

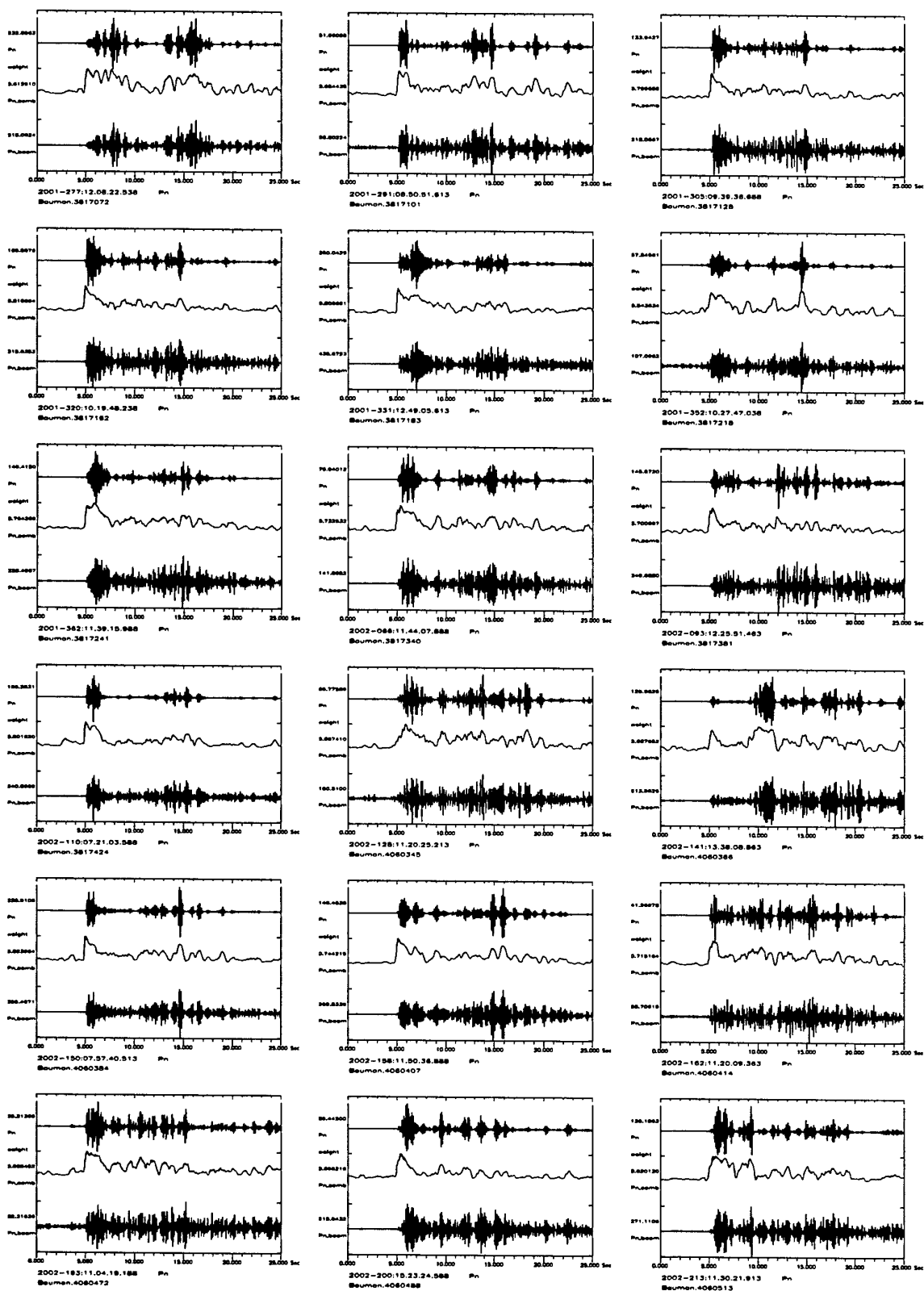# Appendix A, Semblance analysis of events from the Khibiny Central Mine (4-8 Hz)
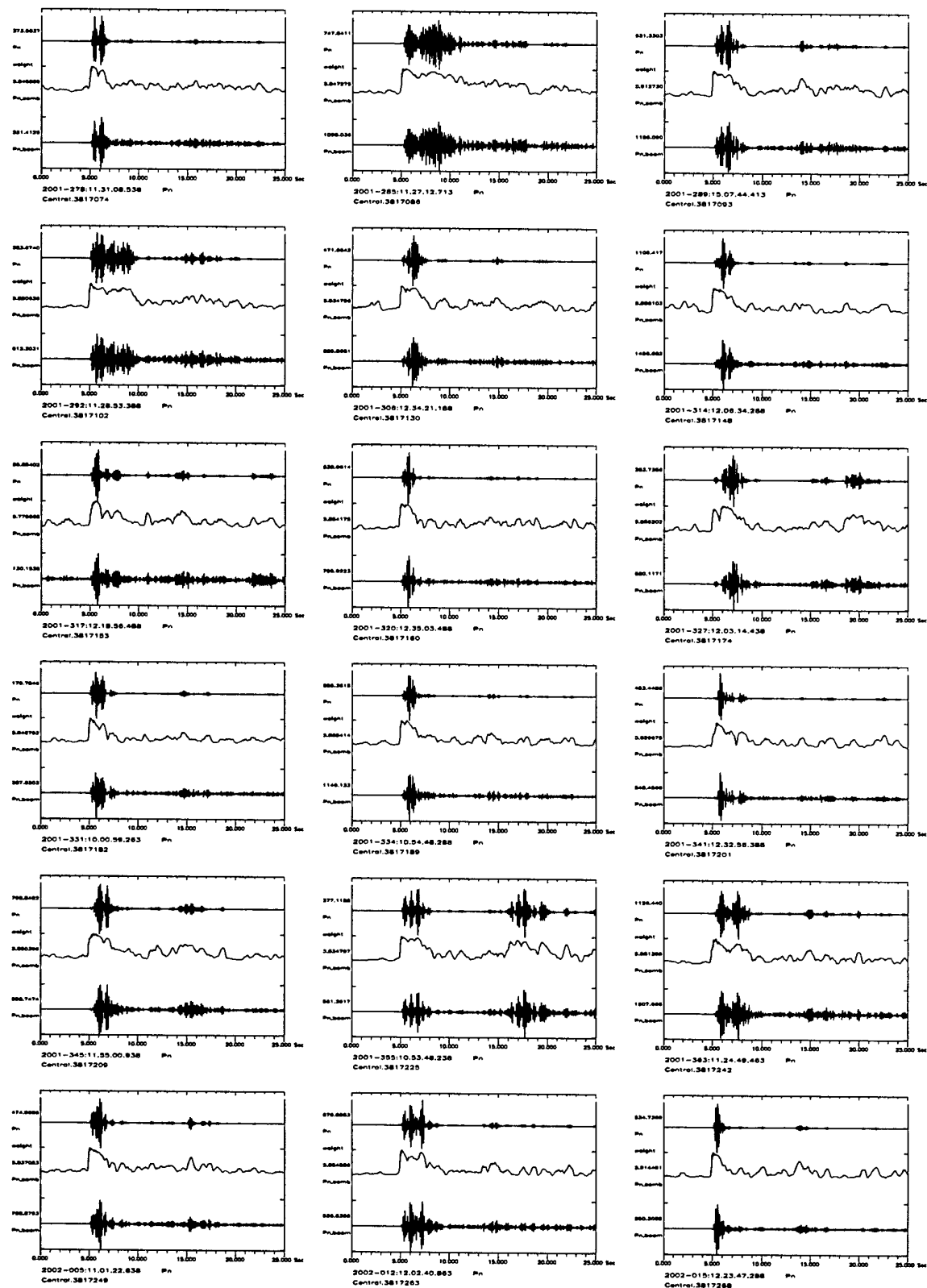
Appendix A. *ARCES recordings of 18 explosions in the Central open-pit mine in the Khibiny Massif. For each panel we show the Pn beam (bottom), the semblance coefficient (middle) and the Pn beam weighted with the semblance coefficient.*

Appendix B, Semblance analysis of events from the Olenegorsk Mine (4-8 Hz)
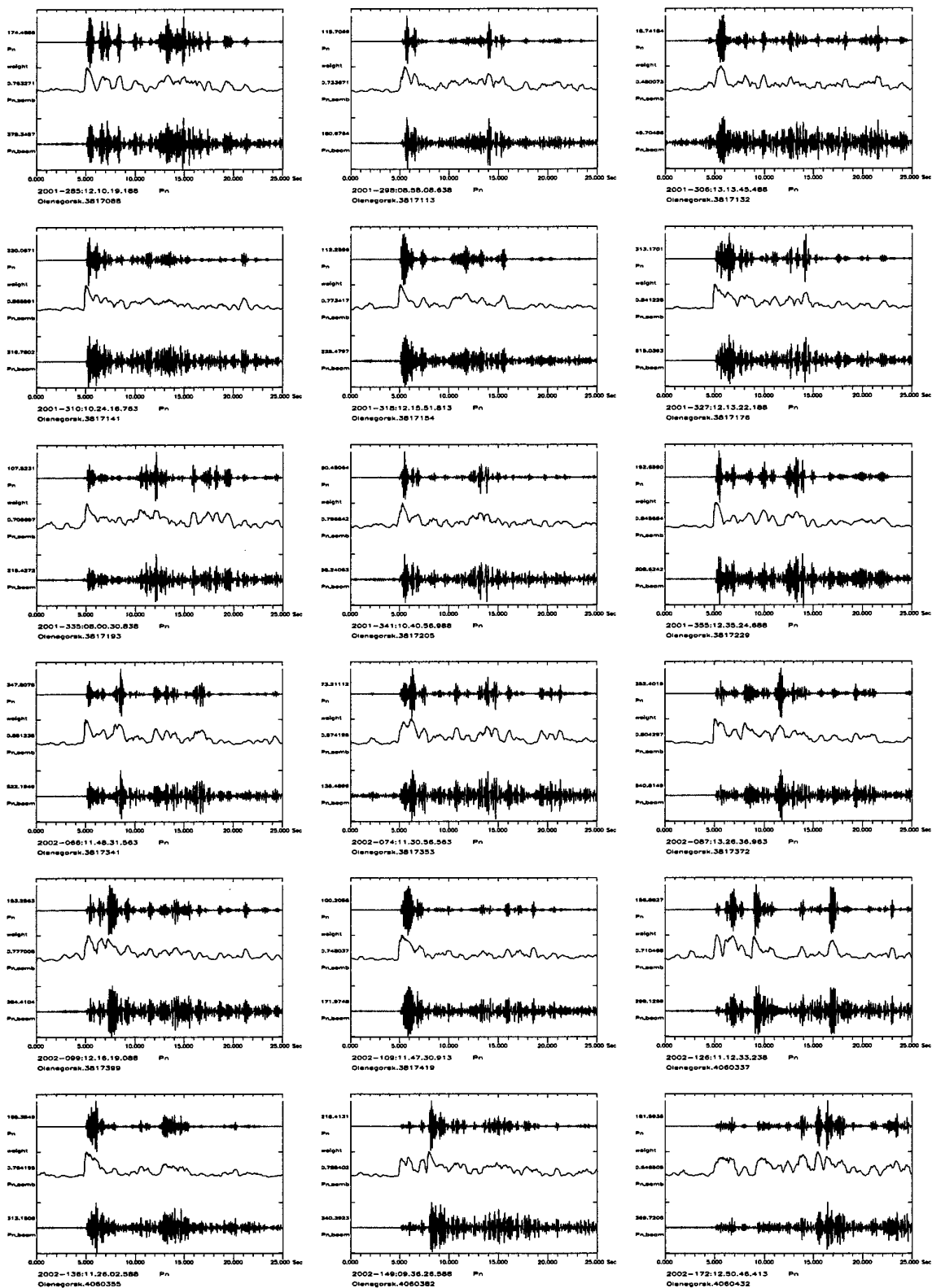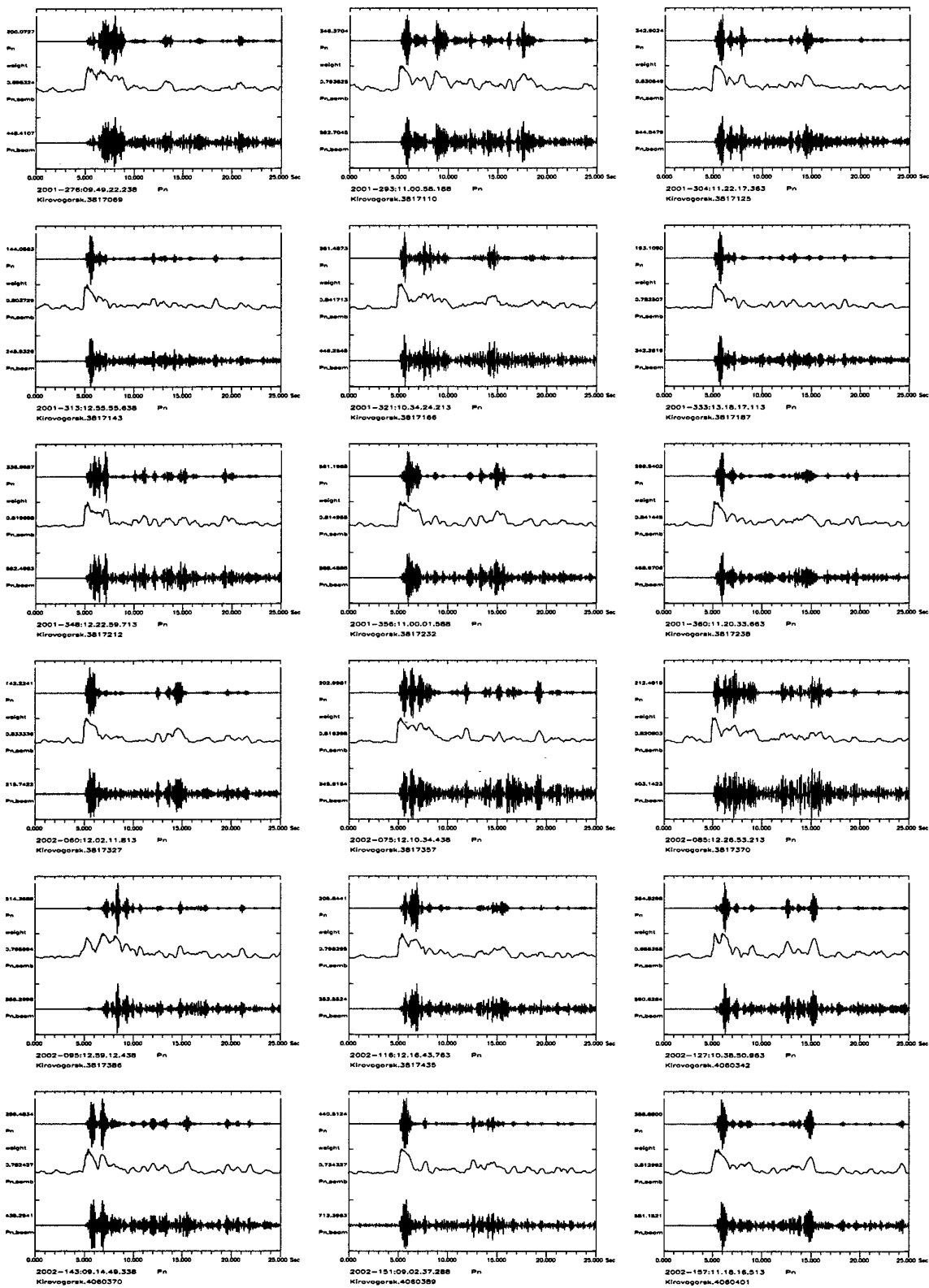

Appendix B. *ARCES recordings of 18 explosions in the Olenegorsk open-pit mine. For each panel we show the Pn beam (bottom), the semblance coefficient (middle) and the Pn beam weighted with the semblance coefficient.*

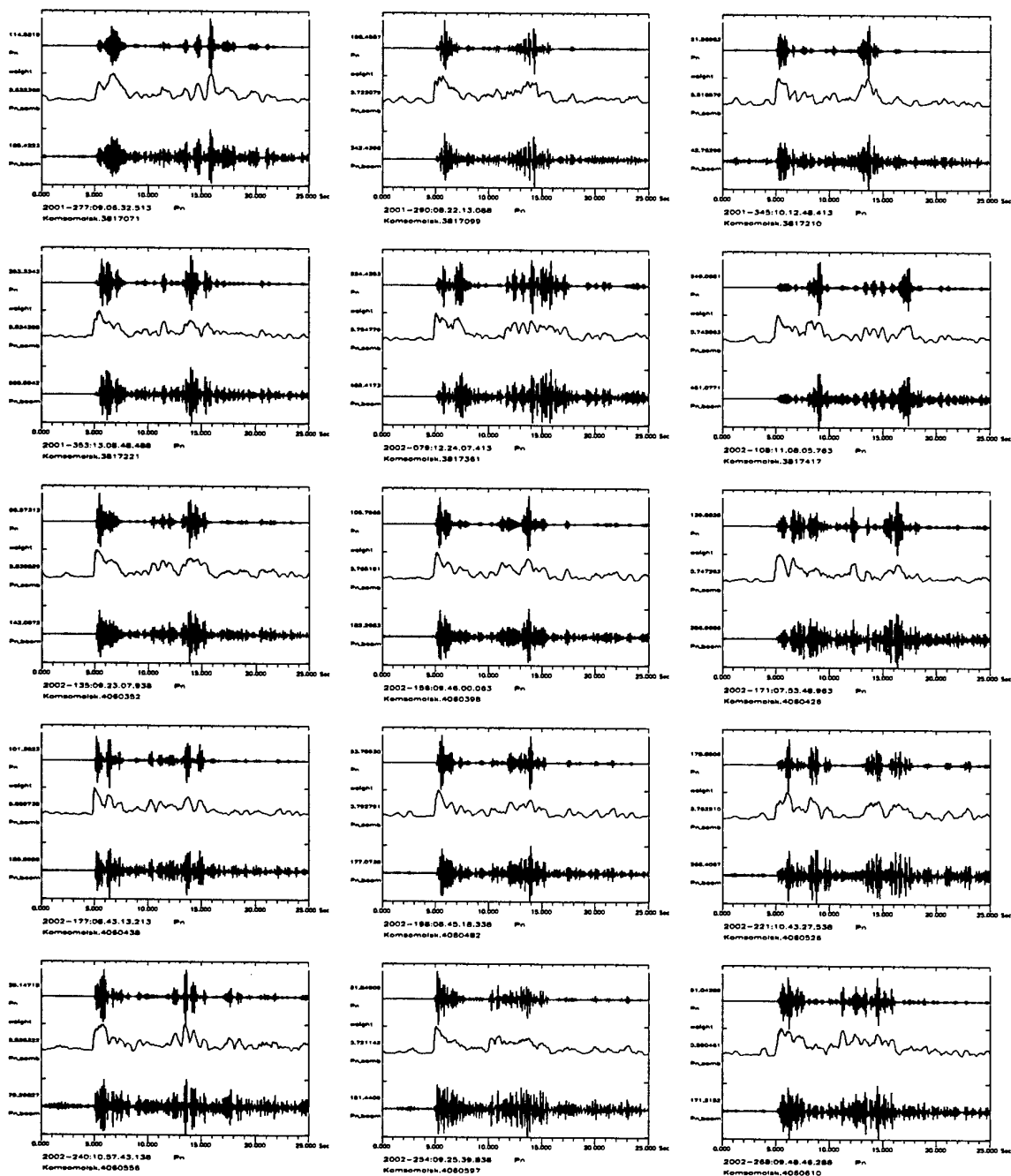# Appendix C, Semblance analysis of events from the Bauman Mine (4-8 Hz)

Appendix C. *ARCES recordings of 18 explosions in the Bauman open-pit mine. For each panel we show the Pn beam (bottom), the semblance coefficient (middle) and the Pn beam weighted with the semblance coefficient.*

# Appendix D, Semblance analysis of events from the Kirovogorsk Mine (4-8 Hz)

Appendix D. *ARCES recordings of 18 explosions in the Kirovogorsk open-pit mine. For each panel we show the Pn beam (bottom), the semblance coefficient (middle) and the Pn beam weighted with the semblance coefficient.*

Appendix E. *ARCES recordings of 15 explosions in the Komsomolsk open-pit mine. For each panel we show the Pn beam (bottom), the semblance coefficient (middle) and the Pn beam weighted with the semblance coefficient.*

Appendix F, Semblance analysis of events from the Oktjabrsk Mine (4-8 Hz)
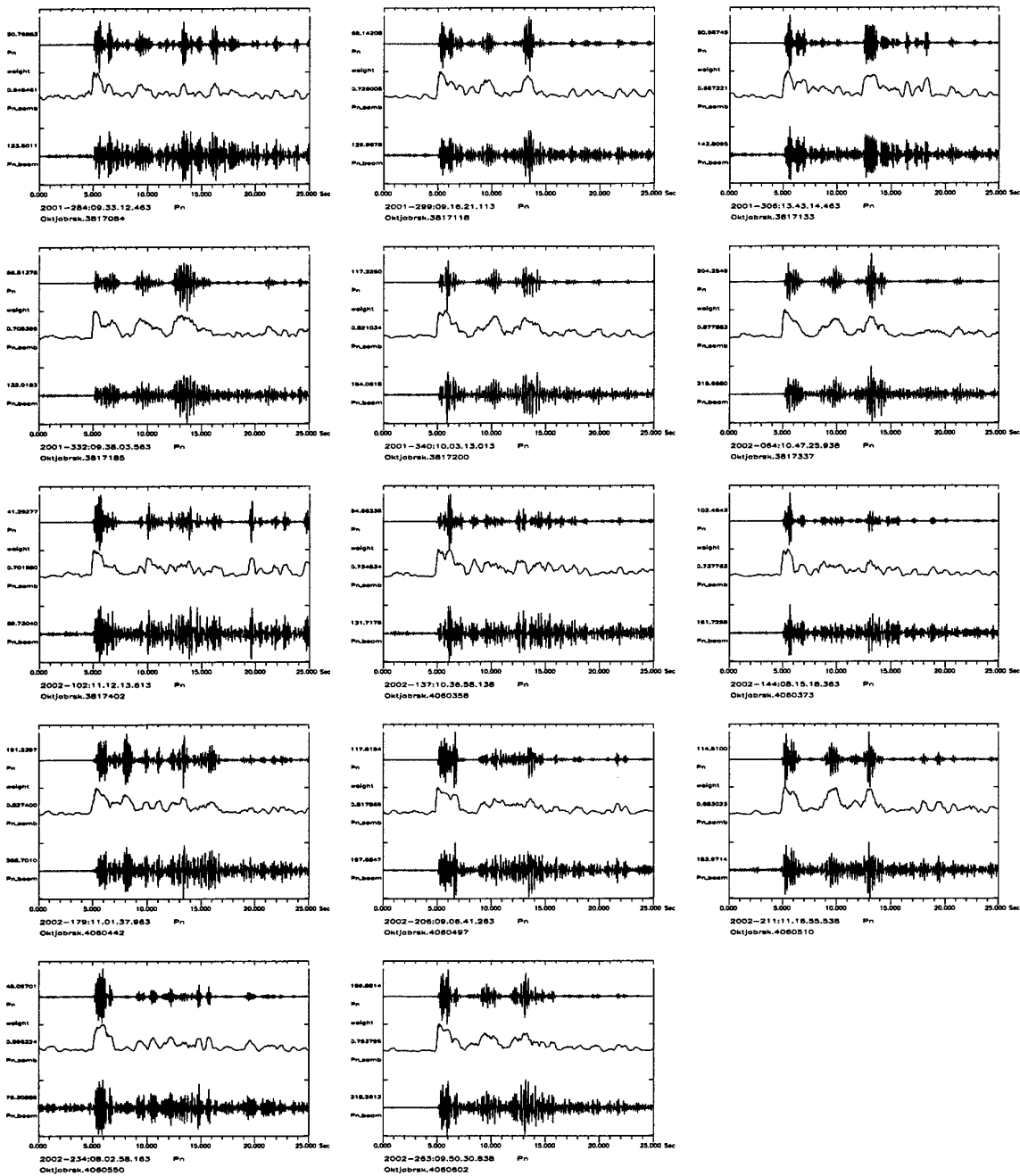
Appendix F. *ARCES recordings of 14 explosions in the Oktjabrsk open-pit mine. For each panel we show the Pn beam (bottom), the semblance coefficient (middle) and the Pn beam weighted with the semblance coefficient.*